

Synthesis and Biological Investigation of Organometallic 3,4-Diarylalkenyne and 1,1,2-Triarylalkene Derivatives as Potential New Leads in Tumor Therapy

Dissertation zur Erlangung des akademischen Grades
des Doktors der Naturwissenschaften (Dr. rer. nat.)

eingereicht im Fachbereich Biologie, Chemie, Pharmazie
der Freien Universität Berlin

vorgelegt von

ELENA MAZZANTI

aus Cento (Fe) Italien

2012

Die vorliegende Arbeit wurde von September 2006 bis September 2012 unter der Leitung von Prof. Dr. Ronald Gust (Institut für Pharmazie, Freie Universität Berlin) angefertigt.

1. Gutachter: Prof. Dr. Ronald Gust
 2. Gutachter: Prof Dr. Gerhard Wolber
- Disputation am 30.05.2013

Dedicated to my daughter Sara, to my husband Robert Gromotka and
to my parents Olga and Angelo Mazzanti

Acknowledgements

This work was developed in the Institut für Pharmazie of the Freien Universität Berlin, under the supervision of Prof. Dr. Ronald Gust, whom I would like to offer my gratitude for inspiration and for giving me the opportunity to work in his team.

I would like to express my deepest gratitude to Dr. Anja Schäfer, Dr. Maria Proetto and Dr. Margarethe Urban for their help and support during the writing of this dissertation and also for becoming good friends of mine.

I would also like to thank Michael Gromotka for editing, my sister Zoriana and Jules Spier, for reading, even though they never really understood what I was writing.

Furthermore I would like to thank all my colleagues and all the technical and academic staff for their help and for the nice atmosphere during these years. Especially Dr. Ewelina Fogelström, Thomas Rudolf, Nora Reitner, Maxi Wenzel, Dr. Sandra Alscher, Dr. Sandra Maieranz, Silke Bergemann, Dr. Magnus Krüger, Maha Hammoud, Dr. Ana Maria Scutaru, Dr. Annegret Hille, Andrey Molchanov, Murat Üstünel, Anja Wellner and Kerstin Bensdorf. I would like to thank also Frau Veronique vom Bauer for her cordiality and for leading me through the jungle of bureaucracy. I've had a lot of fun spending the past years with this team.

Finally I give a special thanks to my husband Robert for being supportive and patient during my years in the lab and on the Laptop and my daughter Sara for being the "positive energy" in my life and supporting me in all my endeavors. Thank you for keeping me sane.

And of course I would like to show my gratitude to my parents, my brother and parents-in-law for their unconditional presence. This thesis would not have been possible without the support of all my family and my friends.

Abstract

In this work synthesis, structural characterization and biological evaluation of the activity of organometallic compounds were conducted. Starting from the idea to tether a metal cluster to estrogen receptor ligands, thereby achieving a targeting of the ER and combining estrogenic/antiestrogenic and cytotoxic properties. Furthermore, the choice of the metal enables us to expand their applications on other biological targets.

Two series of compounds, analogues of diethylstilbestrol (3,4-diarylalkenyne) and analogues of tamoxifen (1,1,2-triarylethylene) were investigated (Fig.1).

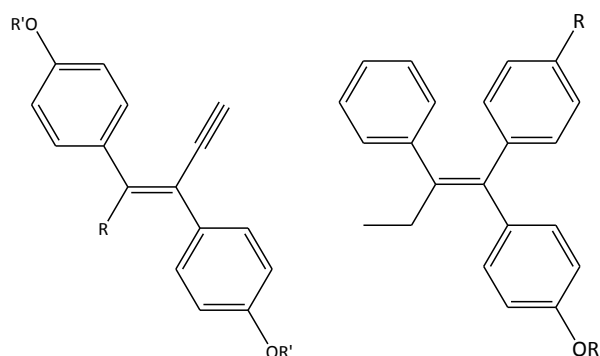


Figure 1. Chemical structures of lead compounds of the 3,4-diarylalkenyne (left) and 1,1,2-triarylethylene (right) series.

Their scaffolds were obtained in three main steps, followed by addition of an appropriate metal cluster. Since the compounds can adopt a (*Z*-) or (*E*-) configuration, they were characterized by $^1\text{H-NMR}$ spectroscopy, especially with $^1\text{H-NMR}$ NOE experiments. The presence of the metal was detected by EI or ESI mass spectroscopy experiments. The cytotoxicity was investigated on hormone-dependent MCF-7 cells and hormone-independent MDA-MB-231 cells. The cobalt complexes of the 3,4-diarylalkenyne series showed strong antiproliferative properties (IC_{50} values less than $5\ \mu\text{M}$) on both cell lines and were tested in a time- and concentration-dependent cytotoxicity assay. However, these compounds did not show any estrogenic potency on $\text{ER}\alpha$ and $\text{ER}\beta$ in an established luciferase assay, and no structure-activity relationship has been found.

The 1,1,2-triarylalkene compounds described in the second series are analogues of tamoxifen, in which the key^a amino side-chain has been replaced by a lipophilic and stable organometallic entity. On the one hand, the introduction of a cobalt cluster to the structure *via* triple bond led to molecules which display estrogenic properties, but also a loss of antiproliferative activity.

On the other hand, the compounds were successfully labeled by a double bond exchange with Zeise's salt, which has been identified as a COX enzymes inhibitor in this group. The Zeise's complexes present high inhibition activity. The high COX inhibition and the lack of ability to antagonize the effects of estradiol (E2) made an antiestrogenic mode of action unlikely.

Investigations to gain insight into the enzyme inhibitory properties as well as an enlarged structure activity relationship should be conducted in the future and will give us the opportunity to explain the mode of action more precisely.

^a It is deemed essential for the anti-estrogenic activity.

Zusammenfassung

In der vorliegenden Arbeit wurden verschiedene Organometallverbindungen synthetisiert, chemisch charakterisiert und auf ihre pharmakologischen Eigenschaften untersucht. Ausgehend von der Idee, durch die Verbindung einer metallorganischen Gruppe mit einem Estrogenrezeptorliganden ein sogenanntes *drug targeting* zu erreichen, sollten Verbindungen mit sowohl cytotoxischen als auch estrogenen oder antiestrogenen Eigenschaften erhalten werden. Zusätzlich sollte durch die Verwendung unterschiedlicher Metalle untersucht werden, ob auch eine Aktivität an anderen biologischen Zielstrukturen erreicht werden kann.

Im Rahmen dieser Arbeit wurden zwei verschiedene Verbindungsklassen untersucht, zum einen Analoga von Diethylstilbestrol (3,4-Diarylalkenone) und zum anderen Analoga von Tamoxifen (1,1,2-Triarylethylene) (Abb. 1).

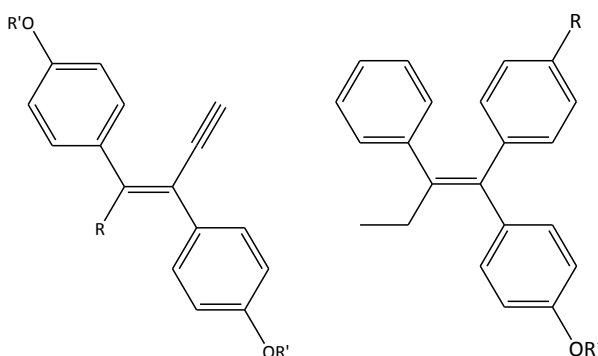


Abbildung 1. Strukturformeln der Leitstrukturen der 3,4-Diarylalkenone (links) und 1,1,2-Triarylethylene (rechts) Serie.

In drei Syntheseschritten wurde jeweils zunächst die Grundstruktur erhalten und im darauffolgenden vierten Schritt die metallorganische Gruppe eingeführt. Die auf diesem Weg synthetisierten Verbindungen in (Z)- oder (E)-Konfiguration wurden durch $^1\text{H-NMR}$ NOE Untersuchungen charakterisiert. Das erfolgreiche Einführen der Metallgruppe wurde durch EI oder ESI Massenspektrometrie bestätigt.

Die Cytotoxizität der synthetisierten Verbindungen wurde sowohl an hormonabhängigen MCF-7 als auch an hormonunabhängigen MDA-MB-231 Zellen untersucht. Die Cobaltkomplexe der 3,4-Diarylalkenone zeigten dabei in beiden verwendeten Zell-Linien starke antiproliferative Effekte (IC_{50} Werte unterhalb von $5 \mu\text{M}$) und wurden daher zusätzlich in einem zeit- und konzentrationsabhängigen

Cytotoxizitätstest untersucht. Die Verbindungen zeigten jedoch weder an ER α noch an ER β estrogene Effekte. Für diese Verbindungen konnten keine Struktur-Wirkungsbeziehungen abgeleitet werden.

Bei der zweiten untersuchten Strukturklasse, den 1,1,2-Triarylalkenen, wurde die basische Seitenkette^b durch eine lipophile stabile organometallische Gruppe substituiert. Diese Funktionalisierung führte zu Verbindungen mit estrogenen Eigenschaften, allerdings unter Verlust der antiproliferativen Aktivität.

Desweiteren wurden die Verbindungen erfolgreich mit dem Zeisesalz substituiert, welches in dieser Arbeitsgruppe bereits als COX-Inhibitor identifiziert werden konnte. Die Zeisesalz-Komplexe der im Rahmen dieser Arbeit synthetisierten Verbindungen zeigten ausgezeichnete COX-Inhibierung, welche in Verbindung mit der fehlenden antiestrogenen Wirkung einen cytotoxischen Effekt über das Estrogenrezeptorsystem als sehr unwahrscheinlich erscheinen lassen.

Die Frage, ob die Verbindungen über die COX-Hemmung cytotoxisch wirken, sollte Gegenstand einer größeren Struktur-Wirkungsstudie sein. Durch diese Untersuchungen kann auch eine eventuelle Tumorselektivität näher erforscht werden.

^b Diese wird als unerlässlich für die antiestrogene Wirkung angesehen

Table of Contents

1	Introduction.....	2
1.1	Cancer and Causes.....	2
1.2	Breast Cancer	2
1.3	Treatments	4
1.4	The Role of Estrogen Receptors in Breast Cancer	5
1.5	Structure and Gene Transcription.....	7
1.6	ER Ligands.....	9
1.7	Metal Complexes as Anticancer Drugs	13
	1.7.1 Cobalt Compounds	14
	1.7.2 Alkyne Hexacarbonyl Dicobalt Complexes	15
	1.7.3 Zeise' s Salt	18
2	Objectives of the Research Project.....	22
2.1	Background	22
2.2	Aim of the Thesis.....	24
3	Synthesis	26
3.1	Overview of the Synthesized Compounds	26
3.2	Overview of the Synthetic Pathway of the 3,4-Diarylalkenyne Cobalt Complexes	29
	3.2.1 Synthesis of 4-Methoxyphenylacetyl Chloride	30
	3.2.2 Friedel-Crafts Acylation	30
	3.2.3 Deoxybenzoin 's Alkylation.....	31
	3.2.4 Synthesis of the 3,4-Diarylalkenyne Derivatives	32
	3.2.5 Cleavage of Trimethylsilyl Group.....	34
	3.2.6 Cleavage of the Methoxy Groups	34
	3.2.7 Silyl Ethers as Protecting Groups.....	37
	3.2.8 Synthesis and Chemistry of Hexacarbonyl Dicobalt Complexes	41
3.3	Overview on the Preparation of the 1,1,2-Triarylalkene Compounds.....	44
	3.3.1 Preparation of 1-(4-Methoxyphenyl)-2-phenylethanone.....	45
	3.3.2 Alkylation of the Ethanone.....	45
	3.3.3 Grignard Reaction	46

3.3.4	Ether Cleavage.....	48
3.3.5	O-Alkylation.....	49
3.3.6	Preparation of the Alkyne Hexacarbonyl Dicobalt Complexes	50
3.3.7	Synthesis of Zeise' s Complexes	51
4	Proton NMR and Mass Spectrometry Analyses	54
4.1	3,4-Diarylalkenyne Ligands.....	54
4.1.1	3,4-Diarylalkenyne Complexes with Dicobaltoctacarbonyl	57
4.2	1,1,2-Triarylalkene Ligands.....	58
4.2.1	Hydroxyl Triphenylalkene Ligands.....	59
4.2.2	Triphenylalkene Complexes with Zeise's Salt.....	61
5	Pharmacological Evaluation.....	65
5.1	Cell Lines Used.....	65
5.1.1	MCF-7 (hormone dependent cancer cell line).....	65
5.1.2	MDA-MB-231 (hormone independent cancer cell line).....	65
5.1.3	MCF-7-2a and U2-OS/ α , β	66
5.2	<i>In-vitro</i> Chemosensitivity Assay	66
5.2.1	Growth Inhibitory Effects on MCF-7 and MDA-MB-231 cells.....	68
5.2.2	Determination of the Antiproliferative Activity.....	69
5.2.2.1	3,4-Diarylalkenyne Derivatives.....	69
5.2.2.2	1,1,2-Triarylalkene Derivatives.....	74
5.3	Luciferase Assay System.....	76
5.3.1	Estrogenic Activity	77
5.3.2	Antiestrogenic Activity	77
5.3.2.1	3,4-Diarylalkenyne Derivatives.....	78
5.3.2.2	1,1,2-Triarylalkene Derivatives.....	78
5.4	Binding to COX-1 and COX-2	81
5.4.1	Cyclooxygenase Isoenzymes	81
5.4.2	COX Inhibitory Assay System.....	82
5.4.2.1	1,1,2-Triarylalkenes Zeise' s Complexes.....	83

6	Conclusions	86
7	Experimental section.....	92
7.1	Synthesis and Structural Analysis.....	92
7.1.1	General Considerations.....	92
7.1.1.1	Solvents and Chemicals	92
7.1.1.2	Thin-Layer Chromatography (TLC) and Column Chromatography	92
7.1.1.3	Melting Points.....	92
7.1.1.4	Nuclear Magnetic Resonance.....	92
7.1.1.5	Mass Spectrometry.....	93
7.1.1.6	Elemental Analysis	93
7.1.2	Synthetic Procedures and Analytical Data.....	93
7.1.2.1	Synthesis of the Acid Chloride	93
7.1.2.2	General Method to Synthesize the Ethanone.....	94
7.1.2.3	Alkylation of the Ethanone -General Method-	95
7.1.2.4	Introduction of the Alkyne Unit.....	97
7.1.2.5	Cleavage of the Trimethylsilyl Group	100
7.1.2.6	General Method for the Preparation of Cobalt-Alkyne Complexes	102
7.1.2.7	Grignard reaction.....	108
7.1.2.8	Ether Cleavage with BBr ₃	109
7.1.2.9	O-Alkylierung.....	110
8	Pharmacological Part.....	113
8.1	Cell Lines	113
8.2	Cell Culture Conditions.....	113
8.2.1	Growth Conditions.....	113
8.2.2	Determination of Cell Concentration.....	114
8.3	In-Vitro Chemosensitivity Assays.....	114
8.3.1	Cell Seeding.....	114
8.3.2	Addition of the Substances.....	114
8.3.3	Cell Fixation	116
8.3.4	Cell Staining and Evaluation.....	117
8.4	Luciferase Assay: Estrogenic and Antiestrogenic Activity	117

8.4.1	MCF-7-2a and U2-OS Cells -Cultivation and Transfection-	117
8.4.2	Addition of the Substances	118
8.4.2.1	Dilution from Stock Solutions	118
8.4.2.2	Transfer of the Diluted Solutions to the Microtiter Test Plates	118
8.4.2.3	Cells Lysis and Luciferase Activity	119
8.5	COX Inhibitory Activity	119
8.5.1	COX Inhibitor Screening Assay	120
8.5.1.1	Procedure of the COX-Inhibitor Screening Assay	120
8.5.1.2	Plate Set Up	120
8.5.2	PGE2-Assay.....	121
8.6	Materials and Reactants	122
8.6.1	Instrumentation.....	122
8.6.2	Used Materials	123
8.6.3	Reactants and Solutions.....	123

9 Appendix: Time- and concentration-dependent cytotoxicity diagrams 126

9.1	MCF-7	126
9.2	MDA-MB-231	129

Curriculum Vitae..... 132

1 Introduction

1 Introduction

1.1 Cancer and Causes

Cancer is a major public health problem in many parts of the world, which affects countries at various level of development. It can be defined as a group of diseases which can attack any part of the body, characterized by uncontrolled growth and spread of abnormal cells (metastasis). It can form an encapsulated benign tumor, leading to invasion and destruction of adjacent tissues. On the other hand, non-encapsulated malignant tumors grow rapidly, and can spread to various regions of the body and metastasize¹. Metastasis is a secondary growth though originating from the original primary tumor and it is responsible for 90% of cancer deaths. In Germany each year approximately 210,000 people die of cancer. Determining the cause of cancer is complex, and in some cases even impossible, because most cancers have multiple possible origins². Of course there are certain factors which increase the chances for a person to develop cancer, these are:

- Physical risk factors -ultraviolet (uv) radiation, ionizing radiation
- Biological risk factors -viruses, bacteria, certain hormones
- Genetic -family history of cancer
- Behavioural risk factor –alcohol, poor diet, lack of physical activity or being overweight
- Environmental risk factor –tobacco, etc.
- Chemicals

The specific treatment of a cancer depends on its location, stage, type of cancer as well as the general state of the patients' health (performance status). The most common treatment options include surgery, radiotherapy and chemotherapy³.

1.2 Breast Cancer

Among females breast cancer is the most frequent form of cancer and leading cause of cancer mortality (see Fig. 1.1), with approximately one out of ten being

affected over their lifetime⁴. Although very seldom, also men can suffer from breast cancer.

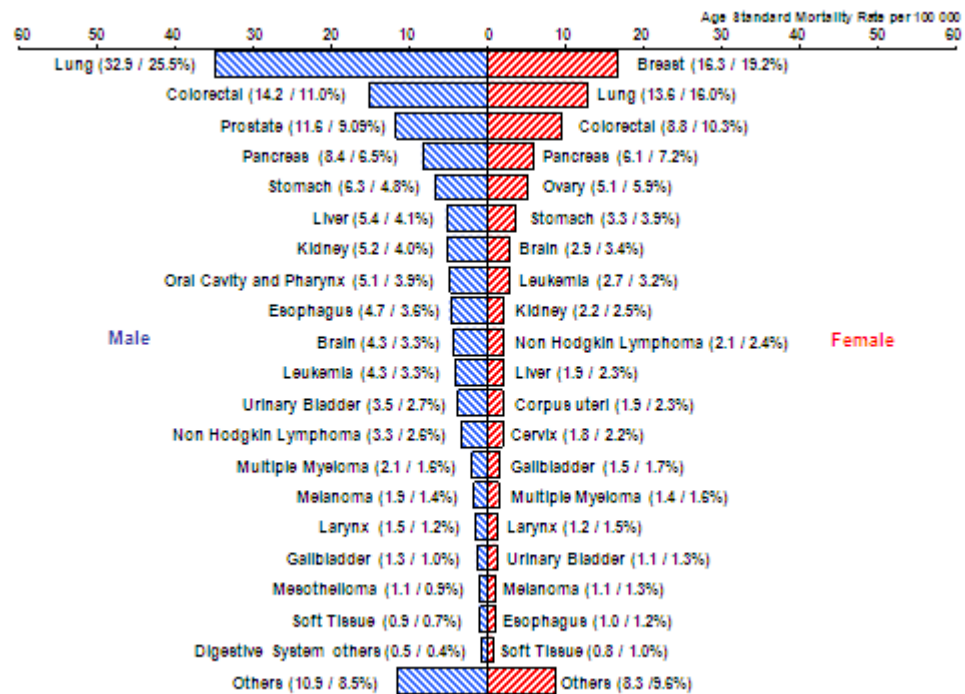


Figure 1.1. The 20 most frequent causes of cancer deaths in Germany 2010⁵.

Annually, more than 1.1 million women are diagnosed with breast cancer globally, causing approximately 410,000 deaths⁶. After increasing over the past 30 years, since 1990s female breast cancer incidence rates decreased in many developed countries by an average of 2.0% per year. This decrease may reflect the utilization of the slight drop in mammography, a screening program, as well as the reduction in the use of estrogen combined with progestin in the menopausal hormone therapy (MHT, known as hormone replacement therapy), which increased the risk of coronary heart disease and breast cancer⁷.

Breast cancer is frequently hormone-dependent, which means that hormones stimulate the cancer cells to grow. Otherwise the growth of the cancer cells can be down regulated by the anti-hormones, substances that inhibit or prevent the effects of a hormone. The relation between ovarian function and breast cancer progression was recognized more than a century ago. The identification of estrogenic hormones produced by the ovary provides the basis for the development of a hormone therapy as a possible adjuvant treatment on breast cancer as

well as with metastases⁸. Depending on the presence or absence of the estrogen receptor in the cells, breast cancer is often treated by endocrine therapy (tamoxifen) or chemotherapy, respectively.

1.3 Treatments

The treatment of the majority of cases of breast cancer involves the combination of surgical excision, chemotherapy, radiotherapy and, in some cases, hormone or biological therapies⁷.

- Surgery means the removing of the main tumor from the breast and the lymph nodes. Some surgical procedures are followed by radiation therapy, which uses high-energy radiation (X-rays or gamma-rays) to kill remaining cancer cells by damaging their DNA.
- Radiation can affect normal cells surrounding the cancer cells, causing the skin to become red, itchy or both. However, the side effects should be temporary for the normal healthy cells, unlike to the cancer cells, and the treatment does not involve drugs. Furthermore, it affects only the cells in the area being treated.
- Biological therapy uses the body's immune system to fight cancer.
- Chemotherapy uses drugs to destroy cancer cells. In estrogen receptor ER-negative breast cancer, a combination of drugs (Fig. 1.2) is used to killed cancer cells which could not be removed by other means. The molecules used are cytotoxic, considering that they affect mainly fast-dividing cells of the body, such as blood cells and the cells lining the mouth, stomach, and intestines. This produce side-effects including hair loss, fatigue, nausea, depression of the immune sytem and nerve damage.

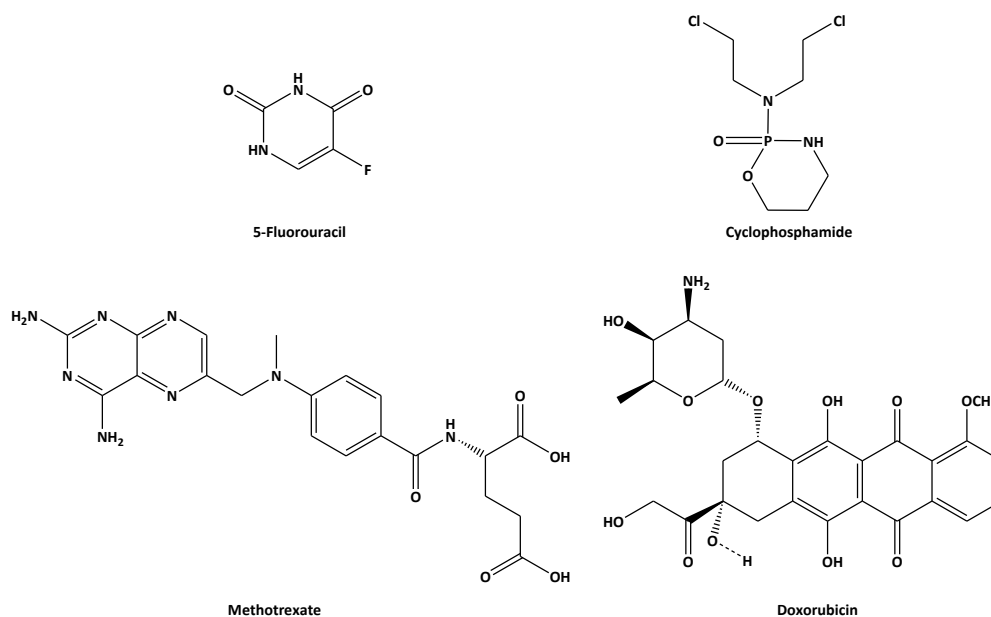


Figure 1.2. Examples for compounds used in chemotherapy in ER-negative breast cancer.

On the contrary for ER-positive breast cancers used a hormone therapy, with antiestrogens^{9,10} or with aromatase inhibitors¹¹, which appears more safer.

1.4 The Role of Estrogen Receptors in Breast Cancer

In earlier studies, in which the ER was purified from tumors, it was suggested that breast cancer patients with ER-positive tumors might be more likely to respond to endocrine treatments than those with ER-negative tumors¹². The therapeutic targets ERs (ER α and ER β) are ligand-inducible transcription factors, which belong to the nuclear receptor super family and act as a dimeric species. ER α was the first estrogen receptor cloned and it was isolated from MCF-7 human breast cancer cells in the late 1980s^{13,14}. Ten years later, a second receptor (ER β) was cloned first from a rat prostate¹⁵. Afterwards the human ER β (hER β) was characterized and cloned¹⁶.

Both receptors have different distributions patterns, including breast, urogenital tract, the central nervous system, the cardiovascular system¹⁷, the liver¹⁸ and the bones¹⁹ (Fig. 1.3). Their influence to the target gene activity in the variety of responsive tissue is mediated by binding to the cognate estrogen response

elements (EREs) on the DNA²⁰. The abundance and distribution of the receptors will, in part, determine whether a ligand will have a particular effect.

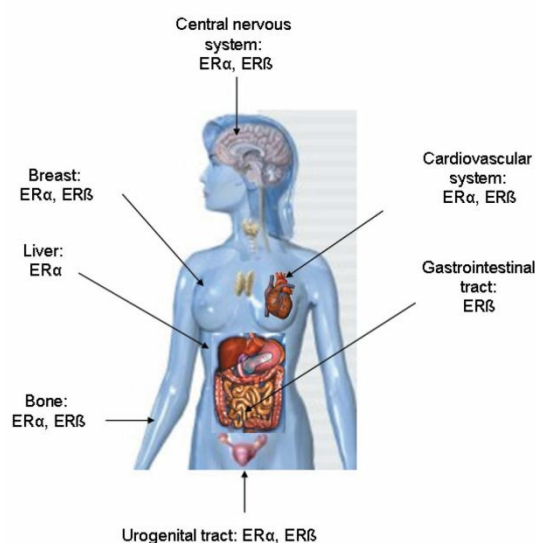


Figure 1.3. Overall distribution of ERα and ERβ in the human body adapted from Gust²¹.

To apply subtype-specific drugs for therapeutic use accordingly it is necessary to know where the affected tissues are located and the relative amounts of ERα and ERβ. In brief when normal breast tissues become tumorigenic, the amount of ERα increases whereas the amount of ERβ decreases²². Because estrogen is a growth stimulus through ERα, the use of ERα-specific antagonists to block this interaction or aromatase (which converts testosterone to estradiol) inhibitors may be ideal in clinical settings as anticancer agents. Furthermore, ERβ appears to play a protective role against the development of breast cancer. To support this hypothesis, an ER-negative breast cancer cell line (MDA-MB-231) was modified by genetic engineering to express functional ERα and ERβ. The result was that cells with ERα have the same rate of proliferation as naive cells in the absence of estrogens; on the contrary ERβ is able to inhibit the proliferation in a ligand-independent pathway and is also able to activate the transcription of synthetic as well as natural endogenous promoters in a ligand-dependent manner. These results suggested that ERβ could effectively act as an inhibitor of breast cancer development²³. Another explanation is that the presence of ERβ could simply antagonize the growth stimulatory effects mediated by ERα. This is suggested by a study in which ERβ inhibited the agonistic activity of the ERα-

tamoxifen complex. Further studies are required to explain the exact interaction between ER α and ER β in cell growth control²⁴.

1.5 Structure and Gene Transcription

ER α and ER β , which are encoded by two different genes²⁵, have similar (but not identical) structure²⁶. The ER α consists of 595 amino acids and is located on chromosome 6 (molecular weight = 66 kDa)²⁷. Whereas the ER β , composed by 530 amino acid residues is positioned on chromosome 14 (molecular weight = 59 kDa)²⁸. The sequence of both ERs has a multi-domain structure consisting of six functional regions, from the N-terminal A/B domain to the C-terminal F domain, which shows various degrees of sequence conservation (Fig. 1.4). The A/B domain has an 18% sequence identity between ER α and ER β which is not well conserved. It contains the activation function 1 (AF-1) that contributes to the transcriptional activity of the ER²⁹. In the C domain, the most highly conserved region, the DNA-binding domain (DBD) is located.

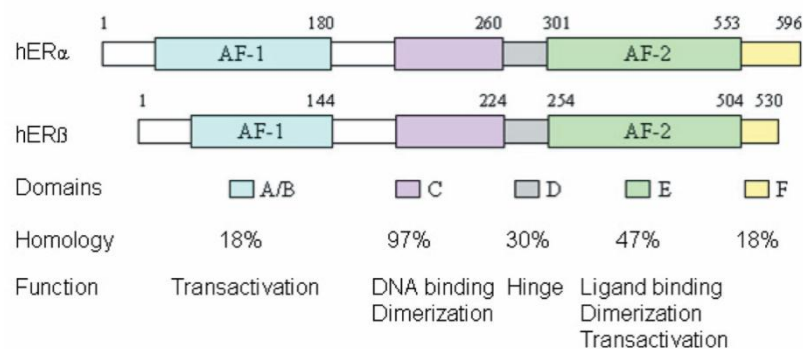


Figure 1.4. Domain-structure representation of human ER α and ER β isoforms³⁰

This allows both receptors to bind to similar target sites, due to the fact that they share of the same response element. The hinge D domain can be considered as a linker peptide between the DBD and the LBD. It has a role in receptor dimerization and in binding to chaperone heat-shock proteins (Hsp). Finally the E/F region presents a homology of only 47%³¹. This region encompasses the ligand binding domain (LBD) of the receptors, that harbor a co-regulator binding surface, the dimerization domain, a co-activator and the hormone-inducible activation function 2 (AF-2). AF-1 and AF-2 are independently autonomous in their regions but they

can activate transcription also synergistically in a promoter- and cell-specific manner.

The ER is a ligand-activated transcription factor, which means that ER becomes activated upon binding to a ligand. In the “classical” way (see Fig. 1.5) of nuclear-initiated estrogen signaling, this process involves the dissociation from proteins chaperones (such as heat-shock proteins 90 and 70), and a conformational change with consequently dimerization of the ER to either homodimers (ER α / ER α and ER β / ER β) or heterodimers (ER α / ER β)³². The dimer complex is translocated to the nucleus of the target cells and can bind to the estrogen response elements (ERE) resulting in gene transcription. To promote the start of the transcription, the interaction between ER and ERE recruits the cooperation of co-regulators^(c) in the TATA-box^(d) and RNA-polymerase II.

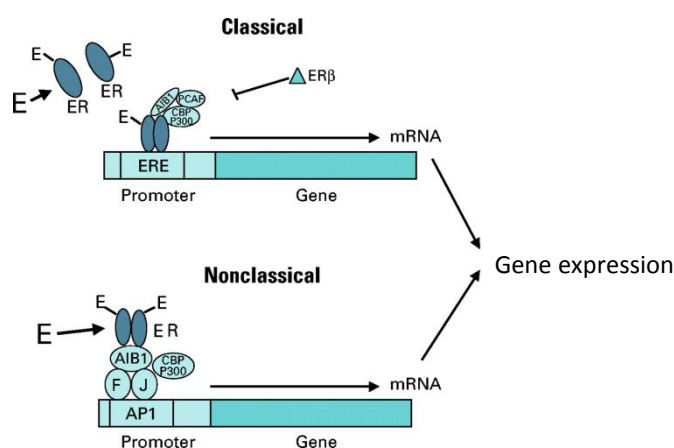


Figure 1.5. Above: Classical transcriptional regulation- AIB1, CBP/P300, PCAF are co-activator proteins. ER β may antagonize the activity of ER α . Upstairs: Non-classical gene regulation: downregulation of gene expression by estrogen results from the recruitment of co-repressors to specific promoters²⁵.

In the “non-classical” transcriptional regulation (Fig. 1.5), the ERs can modulate gene expression at alternative promoter sites on DNA sequences such as specificity protein 1 (SP-1), activator protein 1 (AP-1) and upstream stimulatory factor sites, as well as other poorly defined non-ERE sites³³. Under this condition, ER is tethered to the specific promoter complex by its interaction with other DNA-bound transcription factors or with other co-activator proteins (it does not

^(c) Co-regulators can be divided into co-activators, which facilitate ER transcription, and co-repressor, that promote transcriptional repression.

^(d) TATA-box is the core promoted sequence, located 25 base pairs upstream of the transcription site

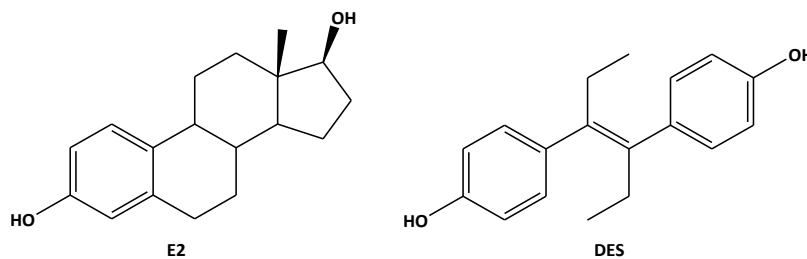
function as the major transcription factor). Consequently ERs can themselves function as co-activator proteins by stabilizing the DNA binding of the transcription factor complex or by recruiting other co-activators to these complexes. The transcription of several genes, important in growth factor signal transduction pathways, is regulated in this way^{27,34}.

1.6 ER Ligands

Estrogens play often a role in the growth and development of hormone dependent breast cancers. Therefore their use in clinical settings can be a logical approach for the treatment of the hormone dependent breast cancer.

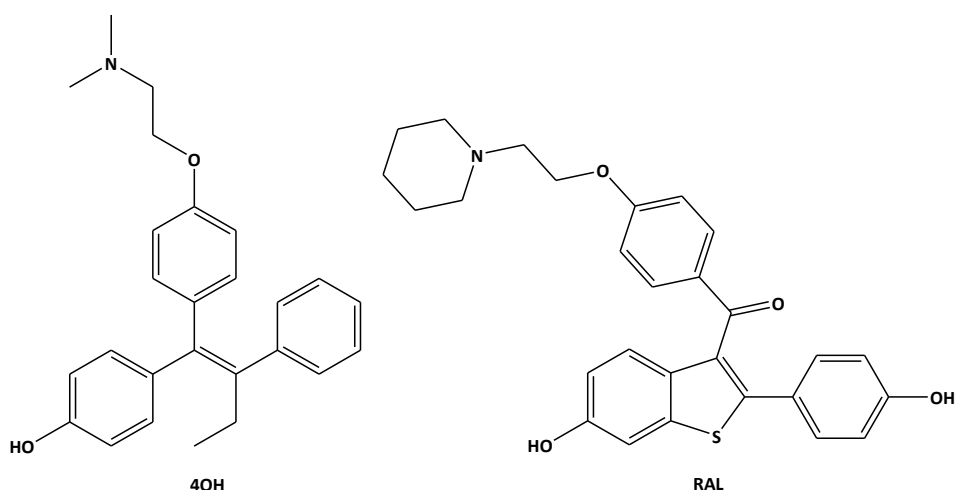
The hormonal compounds can be categorized into three major pharmacological classes:

Agonist



- The most potent and dominant estrogen in humans is 17β-estradiol (**E2**), which plays a prominent role in mediating the maturation, proliferation, differentiation, apoptosis, inflammation, metabolism, homeostasis, brain function and influences the growth and development of breast cancer³⁵.
- Besides from E2, there are many other synthetic estrogens, e.g. diethylstilbestrol (**DES**), a synthetic non-steroidal estrogen which was widely used between the 1940s and the 1970s to prevent spontaneous abortion in women³⁶. Now it is used as estrogen-replacement therapy for estrogen deficiency states as well as in the treatment of advanced breast cancer in postmenopausal women.

Selective estrogen receptor modulators

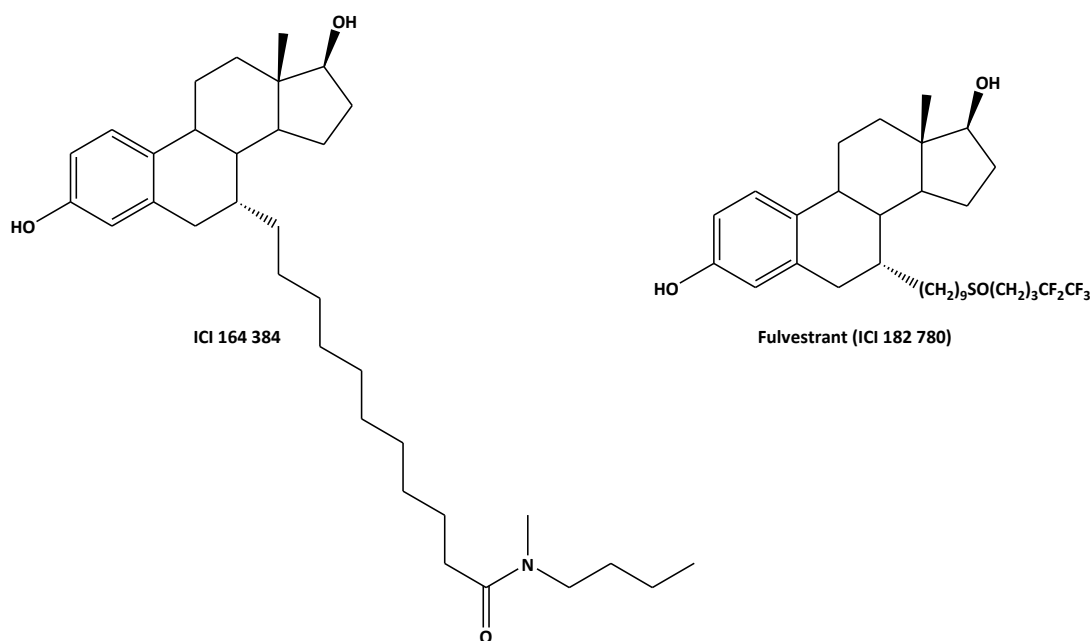


- Tamoxifen (TAM) is a selective estrogen modulator (SERM) widely used in the therapy for all stages of breast cancer in pre- and post-menopausal woman. It presents anti-estrogenic property, that are related to compete with E2 for binding sites in target tissues like breast tissue, but it also functions as an agonist in some tissues including the bone, uterus, liver, and the cardiovascular system. TAM acts as a prodrug and is metabolized in vivo into 4-hydroxytamoxifen (4OH), its active metabolite. The dimethylaminoethoxy side chain interaction with Asp351 of the binding site of the ER is held responsible for the observed antiestrogenic effect of 4OH. Because of this selectivity, up to now, tamoxifen has been used as standard therapy in adjuvant hormone treatment on breast cancer. However, about half of patients with advanced ER-positive disease immediately fail to respond to tamoxifen and in the responding patients the disease ultimately progresses to a resistant phenotype. The possible causes for intrinsic and acquired resistance have been attributed to the pharmacology of tamoxifen, alterations in the structure and function of the ER, the interactions with the tumor environment and genetic alterations in the tumor cells³⁷.
- Raloxifene (RAL) is an estrogen antagonist in the breast and uterine tissues, but functions as an estrogen in the bone and cardiovascular

system. In vitro RAL is an inhibitor of cultured breast cancer cells and possesses antitumor activity in vivo³⁰.

Antagonist

- ICI 164 384, ICI 182 780 (Fulvestrant) may perhaps prove to be more effective than tamoxifen in treating hormone-responsive breast cancer. This pure antiestrogen blocks ER nuclear localization, since it induces a protein synthesis-dependent clustering of ER in the cytoplasm. It seemed that the long hydrophobic side-chain of these antiestrogens is responsible for the disruption of the ER protein structure. Besides the increasing risks of osteoporosis and coronary heart disease, these molecules presented particular problems of bioavailability, since they are highly hydrophobic, and of the route of administration, thus excluding oral administration.



To develop selective compounds it is necessary to consider the structure of the LBD, in fact upon binding different ligands, ER can adopt multiple conformations³⁸ resulting in expression of different genes-different physiological functions.

The LBD is a globular and flexible domain, which contains 11 α -helices (H1, H3-H12) organized in a three layered sandwich structure with H4, H5, H6, H8, and H9 flanked on one side by H1 and H3, and on the other side by H7, H10, and H11³⁹. After hormone binding, the ligand pocket is closed on one side by an

antiparallel β -sheet and on the other side by H12, which is known to be directly involved in the transactivation function AF-2 by mutagenesis studies⁴⁰, for which several “agonist” or “antagonist” conformations have been evidenced.⁴¹

The LBDs pockets of ER α and ER β is very similar. However, the two sub-pockets seem to have somewhat different size and flexibility, and this seems to be a critical distinction that is useful in the development of subtype-selective ligands. In general, ER β selective ligands seem to be smaller and more polar than ER α -selective ligands⁴².

The crystal analyses of **4OH**-ER α LBD and **DES**-ER α LBD complexes (Fig. 1.6) show that **4OH** is bound within the same pocket that recognizes **DES**.

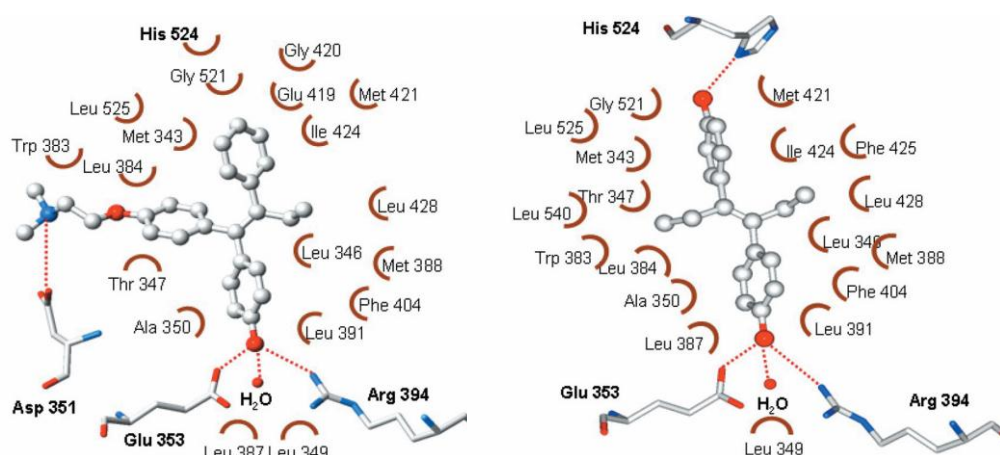


Figure 1.6. The interaction of OHT (left) and DES (right) with critical amino acids in the ER α LBD⁴³.

Next to the hydrogen bonds of its hydroxyl groups with Glu353, Arg394 and water, **4OH** stretches its side chain (a flexible dimethylaminoethyl group) between H3 and H6. This position is stabilized by van der Waals contacts with Thr347, Ala350, Trp383 and by a salt bridge between the dimethylamino group of the side chain and the β -carboxylate of Asp351. Further studies demonstrated that the dimethylaminoethyl side chain of 4-hydroxytamoxifen protrudes and displaces H12.

DES builds H-bridges to Glu353, Arg394, and His524 as well as a water molecule and van der Waals contacts to aliphatic residues of amino acids in the LBD. A phenolic hydroxyl group at para-position of the phenyl ring appeared to be essential for its estrogenic activity.

1.7 Metal Complexes as Anticancer Drugs

Usually, metals are often considered as toxic for living systems and the idea of using inorganic chemicals to treat cancer was rather uncommon. However, many metal-based proteins (e.g. cytochrome oxidase enzymes) or metals containing molecules (e.g. cobalt bearing Vitamin B₁₂) are required in biological process. Historically, metals and metal complexes have played a key role in the development of pharmacy and modern chemotherapy. In 1965 Rosenberg and co-workers⁴⁴ accidentally found the anti-tumoral properties of cisplatin and since this discovery there has been a growing interest in the field of metal complex-based chemotherapy.

Cisplatin has become one of the most effective antineoplastic agents in clinical use, and since up to now it still remains the most used agent against testicular cancer. Several other platinum complexes such as carboplatin and oxaliplatin (Fig. 1.7) are used in the treatment of a variety of tumors. Their clinical use is, however, severely limited by dose-limiting side-effects⁴⁵ (such as neuro-, hepato- and nephrotoxicity) and by acquired resistance.

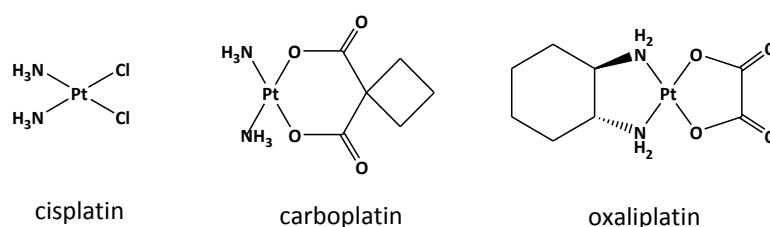


Figure 1.7. Structures of platinum complexes.

These limitations in platinum-based anti-cancer therapy have stimulated increased research efforts in the development of alternative strategies based on different metals and aiming to different target.

The pool of these agents comprises classical inorganic compounds, complexes with ionic organic ligands but also increasingly organometallic species⁴⁶. Organometallic compounds (containing transition metals, such as Co, Cu, Fe, Ga, Ge, Mo, Pt, Sn, Rh, Ru and V), which are defined as metal complexes are emerging as promising anticancer drug candidates, since they present anti-

proliferative (*in vitro*) and anti-neoplastic (*in vivo*) activities⁴⁷. They offer mechanism of drug action, which cannot be realized by organic agents. Furthermore, they are kinetic stable, usually uncharged, and relative lipophilic and their metal atom is in a low oxidation state⁴⁸. The possibility of many different coordination geometries enables the synthesis of compounds with stereochemistry that are quite unique and not obtainable in the group of pure organic compounds⁴⁹. The determining factors for the biological activity of the metal complexes are the type of ligands and the oxidation state of the metal, which also dictates a particular coordination geometry⁵⁰.

Hence, promising non-platinum metal complexes with proven anti-proliferative activity have been developed and some of them have already been evaluated in early-phase clinical trials research⁴⁴.

1.7.1 Cobalt Compounds

Among the new non-platinum metal anticancer drugs, cobalt complexes have attracted much attention as anticancer agents.

Cobalt is an essential trace element in humans, exhibiting many useful biological functions. It is required in the active center of coenzymes, the so called cobalamins (especially Vitamin B12 which regulates indirectly the synthesis of DNA). Moreover, there are at least eight cobalt-dependent proteins.

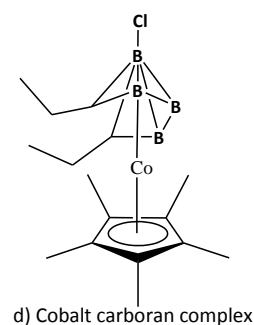
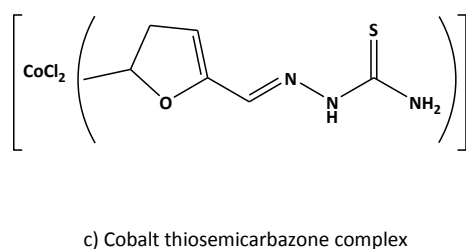
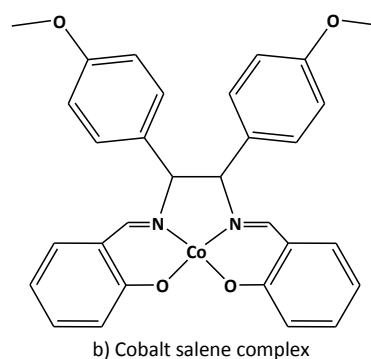
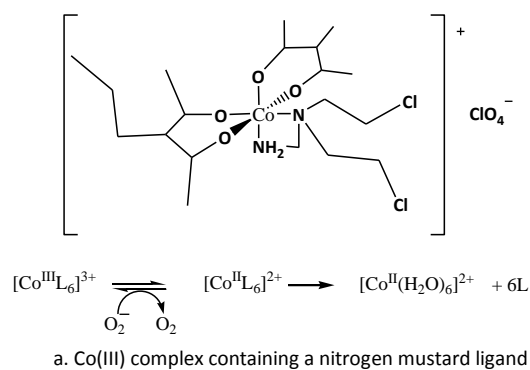


Figure 1.8. Structures of several cobalt complexes.

The interest in cobalt(III) complexes of bidentate mustards (Fig. 1.8-a.) has arisen since the first reported studies on the biological activity of cobalt complexes in 1952⁵¹. Ware and co-workers followed a new approach, which is based on the fact that many tumor tissues exhibit a hypoxic environment and develop resistance to chemotherapeutic agents. Cobalt(III) complexes might be reduced under hypoxic conditions to Co(II) species, followed by loss of a neutral ligand (L) and can be used as prodrug that release the cytotoxic compound after bioreductive activation, exclusively in tumor cells. In particular nitrogen mustards ligands coordinated to Co(III) showed hypoxic selectivity against repair-proficient tumor cells⁵².

Other important examples include Co(III)-based prodrugs which can release potent cytotoxins under activation by ionizing radiation^{53,54}. The slightly acidic pH of tumor cells can also be used for activation of Co(III) species based on the generation of free radicals leading to DNA fragmentation. Cobalt salene complexes (Fig. 1.8-b.) represent a Schiff base species active as anti-tumor agents. The cytotoxicity of these agents depended on the configuration of the bridging -CH and on the kind of the substituents in the aromatic rings on the ethylenediamine bridge. The change from *d,l* to *meso* configuration reduced the growth inhibitory properties of the complexes, which were equipotent to cisplatin. While hydroxyl substitution in place of methoxy derivatives led to inactive compounds, as explained by cellular uptake studies. The oxidative damage of DNA seems unlikely as a mode of action for this class of compounds⁵⁵.

In following studies Hall and co-workers examined cobalt thiosemicarbazone (Fig. 1.8-c.) and cobalt carborane complexes (Fig. 1.8-d.) and showed them to be antitumor active^{56,57}. These compounds showed higher activity in leukemia and lymphoma cell lines ($ED_{50} < 1 \mu\text{g/ml}$) than in tissues derived from human solid tumors. The mechanism involved inhibition of DNA synthesis, but DNA itself is not the target⁵⁸.

1.7.2 Alkyne Hexacarbonyl Dicobalt Complexes

In our research group this field was expanded including hexacarbonyl dicobalt complexes with alkyne ligands^{59,60}.

These complexes derived from the reaction of dicobalt octacarbonyl with an appropriate alkyne. In synthetic chemistry, they are useful intermediates in the Nicholas reaction and the Pauson-Khand reaction⁶¹ (see Fig. 1.9)

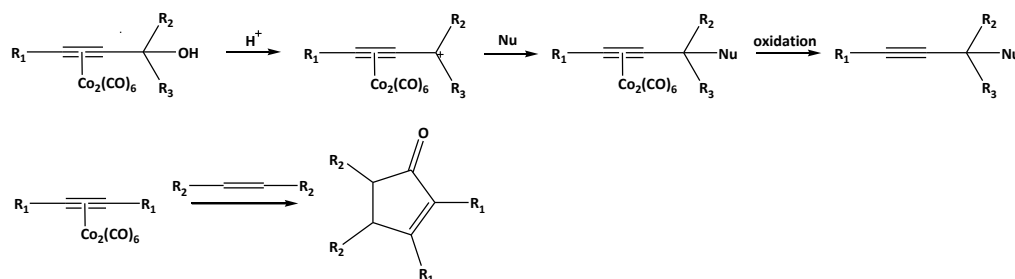


Figure 1.9. Nicholas reaction (above) and Pauson-Khand reaction (below)

In particular in the Nicholas reaction the Co₂(CO)₆ moiety has been used to stabilize carbocationic charge generated at the α -carbon to the alkyne moiety, prior to treatment with a variety of nucleophiles⁶². In the Pauson-Khand reaction the Co₂(CO)₆ unit enables the synthesis of cyclopentanone rings by cyclization of an alkene, an alkyne and a carbon monoxide (a [2 + 2 + 1] cycloaddition).

Also in the field of medicinal chemistry cobalt-alkyne complexes have gained importance as labeling agents and a new class of cytostatic⁵⁹. The cell growth inhibitory properties of these compounds were reported for the first time by Hyama et al., which noted activity against murine leukemia cells⁶³. A successive study conducted by Jung and co-workers described a series of alkyne hexacarbonyl dicobalt derivatives with strong antiproliferative activity towards various cancer cell lines⁶⁴. These properties led to more intensive efforts in the investigations of cobalt alkyne compounds as antitumor agents. A complex of the propargylic ester of acetylsalicylic acid ligand (Co-ASS, see Fig. 1.10) was the most active compound and emerged as a lead compound for the investigated series.

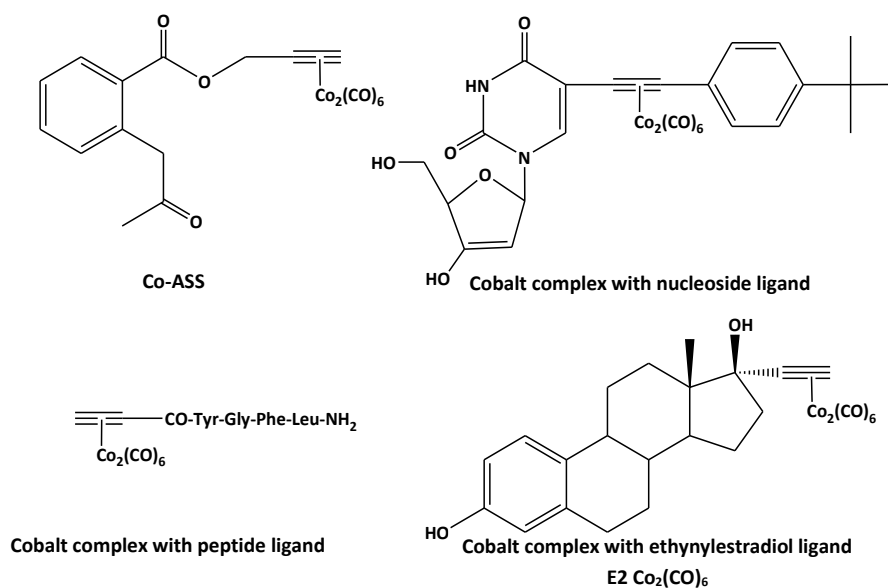


Figure 1.10. Hexacarbonyl dicobalt complexes

Following studies on compounds based on the lead drug Co-ASS indicated the high cytotoxic activity in breast cancer cell lines, but less activity against leukemia and lymphoma cell lines. It was found that marginal structural modifications of Co-ASS (e.g. introduction of a methyl group on the terminal end of the alkyne group or a change of the position of the acetoxy group on the aromatic ring) led to significantly decreased antiproliferative effects. The results obtained about inactive complexes were used to deduce that alkyne hexacarbonyl dicobalt complexes are not necessarily cytotoxic and the activity is strongly dependent on the alkyne ligand structure⁶⁵. The pharmacological properties of acetylsalicylic acid, which belongs to the class of nonsteroidal anti-inflammatory drugs (NSAIDs), have to be considered in the search for the mode of action. Co-ASS triggers its pharmacological effects and is able to inhibit isolated enzymes cyclooxygenase-1 (COX-1) and COX-2. Based on its good stability, it could be concluded that the active species was indeed the intact organometallic complex.

Cellular uptake of these complexes was shown to be dependent upon lipophilicity, establishing a passive transport mechanism through cellular membranes. However, lipophilicity did not correlate with cytotoxicity, hence cellular accumulation does not account for the cytotoxicity of the complexes⁶⁴.

Beside the benzoic acid derivatives, other alkyne ligand structures have been incorporated into alkyne hexacarbonyl dicobalt complexes and investigated for biological activity, namely nucleosides⁶⁶, peptide derivatives⁶⁷ and complexes with hormonally active ligands^{68, 69} (Fig. 1.10). On the basis of the chemical struc-

tures of these compounds, it is very likely that different biological structures are targeted, and that the COX system could not be confirmed to be involved in the mode of action of these derivatives. One might deduce that the $\text{Co}_2(\text{CO})_6$ moiety modifies the interaction with those biomolecules⁴⁶

Hence, estradiol (E2) was derived with a 17α -alkynyl substituent to coordinate with $\text{Co}_2(\text{CO})_6$ giving the **E2- $\text{Co}_2(\text{CO})_6$** complex⁷⁰ (see Fig 1.10). This compound was originally developed as a marker of the estrogen receptor (ER). The most striking finding was that this derivative bind irreversibly to the ER, despite its voluminous $\text{Co}_2(\text{CO})_6$ moiety and cause its partial inactivation, as a consequence of a covalent bond of the cobalt-alkyne complex⁷¹. These results suggested that for complexes with hormone-derived ligands the hormonal activity and the receptor binding were retained.

Besides the function as potential cytostatics, hexacarbonyl dicobalt complexes offer interesting opportunities for medicinal and bioorganometallic chemical research. The mode of action of most of these complexes is not yet understood and still under investigation. The derivatization of biologically active ligands or drugs as metal carbonyl complexes might represent the major drug development strategy for these agents.

1.7.3 Zeise' s Salt

The next advancement in combination of modern organometallic synthesis with biochemical studies could be Zeise' s salt $\text{K}[\text{PtCl}_3(\text{C}_2\text{H}_4)]$. This platinum-ethylene complex was one of the first organometallic compounds already reported in 1831 by William Christopher Zeise. However, since up to now the fields about its possible biological properties still remain unknown. The discovery took place exploring the reaction of ethyl alcohol with platinum tetrachloride (PtCl_4). Interestingly, by dissolving PtCl_4 in 10 parts by weight of ethyl alcohol and successive volume concentration by gentle heating to one-sixth of the original volume, a brown solution remained, usually containing some black powder. The evaporation of the concentrate gave a brown residue which contained yellow and black particles. By heating more strongly, this residue swelled, giving off an inflammable gas and gaseous HCl and eventually inflamed, leaving behind platinum sponge⁷². Initial,

chemists did not imagine what the molecular structure of this grand molecule was. It was not until recently that it was determined to be a square planar complex where the ethylene molecule coordinated to the platinum (the bond of the ethylene is coordinated) (Fig. 1.11).

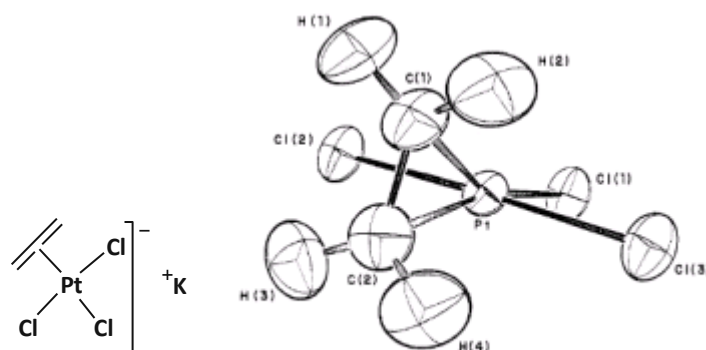


Figure 1.11. Molecular geometry of the Zeise anion, $[(C_2H_4)-PtCl_3]^{-}$ ⁷³

The mode of coordination of an olefin to a transition metal is described by the Dewar-Chatt-Duncanson model and the bond between the metal and olefin is stabilized by the contribution of $d\pi-p\pi^*$ back donation⁷⁴. In this model the olefin acts as a 2-electron ligand, which donates electron density into a metal d-orbital. The metal donates electrons back. Both these effects tend to reduce the C-C bond order, leading to an elongated C-C distance and a lowering of its vibrational frequency.

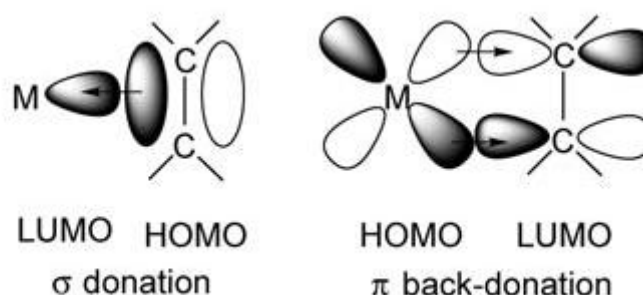


Figure 1.12. Description of the metal-alkene bond according to the Dewar-Chatt-Duncanson model⁷⁵.

These findings gave the background for further investigations in organometallic chemistry. Furthermore, platinum-olefin complexes with cytotoxic proper-

ties on HeLa tumor cells have been reported⁷⁶. More efforts in research to gain a deep insight into possible cellular targets and the molecular details of target interactions of Zeise' s salt are requested.

2 Objectives of the Research Project

2 Objectives of the Research Project

2.1 Background

Despite the success of cisplatin and its derivatives as chemotherapeutic agents, these compounds still present some limitations (described in chapter 1.7). In addition, breast cancer is not sensitive to platinum agents. This generated the impetus for the search for alternative anticancer agents.

Hexacarbonyl dicobalt complexes, which display cytotoxic effects in various tumor cell lines, especially in human breast cancer cells, stimulated our interest in the development of novel organometallic drugs, combining the properties of cobalt cluster with the pharmacological profile of hormone receptor ligands. Affinities of the cobalt-based compounds for the ER were already observed by Vessières and co-workers, who developed derivatives of estradiol (E2)⁷⁰. Thus, the incorporation of $\text{Co}_2(\text{CO})_6$ into the scaffold of an ER-affin molecule can be expected to enhance its biological properties.

Diethylstilbestrol and tamoxifen are well known drugs for the therapy of hormone dependent tumors. Tamoxifen is the most common chemotherapeutic agent used to treat patients with ER-positive breast cancer. Unfortunately, some breast cancer cells become resistant during the therapy. Several analogues were synthesized and investigated in term of their antitumor effect.

The idea to synthesize molecules with a strong antiproliferative effect as a step towards the discovery of antiestrogens with improved cytotoxic properties, was appealing. In this context, we focused our interest on the creation of organometallic complexes.

Diethylstilbestrol Derivatives Series

A series of diethylstilbestrol derivatives, in which one of the ethyl groups has been replaced by a ferrocenyl substituent, was described by Tan and co-workers⁷⁷ (see Fig. 2.1). Cytotoxicity studies of these complexes on hormone-independent breast cancer cell line MDA-MB-231 underline their potency. Two of the tested compounds, which were found to be most cytotoxic, were able to oxidize to quinone species *via* the ferrocene group. This result suggested that the

oxidative activation could be the key to the biological activity of these types of molecules.

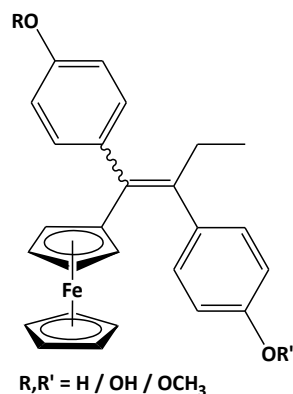


Figure 2.1. Chemical structure of ferrocene derivative of diethylstilbestrol.

Tamoxifen Derivatives Series

In analogy to the strategy used for diethylstilbestrol, tamoxifen has been systematically modified over the past years, including the incorporation of a metal fragment into its structure (see Fig 2.2). A series of ferrocenyl derivatives of hydroxytamoxifen was synthesized *via* a Mc-Murry coupling route by Jaouen and co-workers⁷⁸. These compounds display a new therapeutic spectrum consisting of anti-estrogenicity and cytotoxicity.

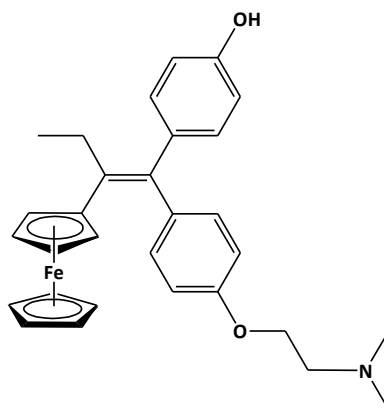


Figure 2.2. Chemical structure of ferrocene derivative of hydroxytamoxifen.

In other studies, Graham and co-workers⁷⁹ observed that the replacement of the aminoalkoxy group by non-basic groups leads to compounds which are more active than tamoxifen.

Further possible targets for the design of drugs in cancer chemotherapy are the cyclooxygenase enzymes COX-1 and COX-2, as demonstrated in earlier

studies⁸⁰. In our group, it was discovered that Zeise's salt can inhibit COX-1 and COX-2. This interesting result lead us to the synthesis of Zeise's compounds. The aim was to demonstrate that depending on the metal used, the organometallic compound could have different modes of action, even though the scaffold remains the same.

2.2 Aim of the Thesis

In the present work synthetic routes were investigated to obtain cobalt complexes of modified diethylstilbestrol (3,4-diarylalkenyne) and tamoxifen (1,1,2-triarylethylene). These complexes were considered to be new agents for the treatment of breast cancer. Due to the fact that the modulation of the ER by tamoxifen depends on its basic aminoalkoxy group different attempts were made to alter this key side chain, mostly leading to less active compounds. In case the basic nitrogen in the side chain is modified in such way that it cannot form hydrogen bonds, antiestrogenic action was reduced. In contrast, in case the side chain is exchanged with a carboxylic acid group or with another non basic group, activity was increased. Thus, we wanted to explore the estrogen activity of non basic metal complexes compared to the activity of compounds which contain basic side chain. To our knowledge, previous to this work, the cobalt unit has not been incorporated into an antiestrogenic entity. Hence, we devised a *drug targeting* strategy using a vehicle (the antiestrogenic compound) to introduce a potentially cytotoxic substance (the cobalt complex) into estrogen-responsive tumors.

Besides the synthesis and structural characterization of the different complexes the research objectives also included pharmacological evaluation of all target compounds for cytotoxic activity as well as for estrogenic or antiestrogenic effects using an established luciferase assay.

Finally, we investigated the inhibing effect of Zeise's complexes on isolated COX-1 and COX-2 enzymes using ELISA.

3 Synthesis

3 Synthesis

3.1 Overview of the Synthesized Compounds

Two series of metal complexes have been synthesized. The first series are hexacarbonyl dicobalt ($\text{Co}_2(\text{CO})_6$) complexes of (*E-Z*)-3,4-bis(4-methoxyphenyl)alken-1-yne called 3,4-diarylalkenyne derivatives hereafter (Fig. 3.1). The second series are hexacarbonyl dicobalt and Zeise (PtCl_3) complexes of the structures depicted in Fig. 3.2 termed 1,1,2-triarylalkene compounds in this work.

The 3,4-diarylalkenyne derivatives (see Fig. 3.1) can adopt a (*Z*-) or (*E*-) configuration depending on the substitution pattern of the ethylene bridge.

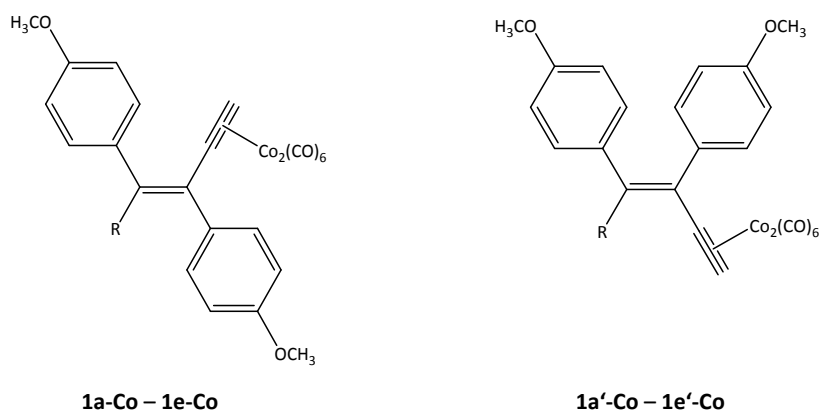


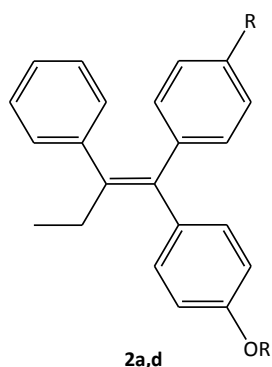
Figure 3.1. Chemical structure of the *Z* (left) and *E* (right) derivatives.

The synthesized 3,4-diarylalkenyne compounds with their substitution pattern and configuration are presented in Table 3.1.

Table 3.1. Substitution pattern of the 3,4-diarylalkenyne hexacarbonyl dicobalt complexes.

Ligand	R	Configuration ^e	Complex
F1a	CH ₃	<i>Z</i>	1a-Co
	CH ₃	<i>E</i>	1a'-Co
F1b	C ₂ H ₅	<i>Z</i>	1b-Co
	C ₂ H ₅	<i>E</i>	1b'-Co
F1c	C ₃ H ₇	<i>Z</i>	1c-Co
	C ₃ H ₇	<i>E</i>	1c'-Co
F1d	CH(CH ₃) ₂	<i>Z</i>	1d-Co
	CH(CH ₃) ₂	<i>E</i>	1d'-Co
F1e	C ₄ H ₉	<i>Z</i>	1e-Co
	C ₄ H ₉	<i>E</i>	1e'-Co

The 1,1,2-triarylalkenes compounds (Fig. 3.2) can exist as (*E*)- or (*Z*)-isomers, in respect to the relative positions of the two substituted phenyl groups at one carbon of the double bond.

**Figure 3.2.** Chemical structure of the 1,1,2-triarylalkene derivatives.

^e Upon the coordination of the ligand with cobalt the priority of the substituents at the double bond in the complex change. However to simplify the (*E*)- and (*Z*)- configurations were attributed by referring the position of substituents in the ligand. - To assign the (*E*)- and (*Z*)- configurations we have referred to the configuration of the ligands.

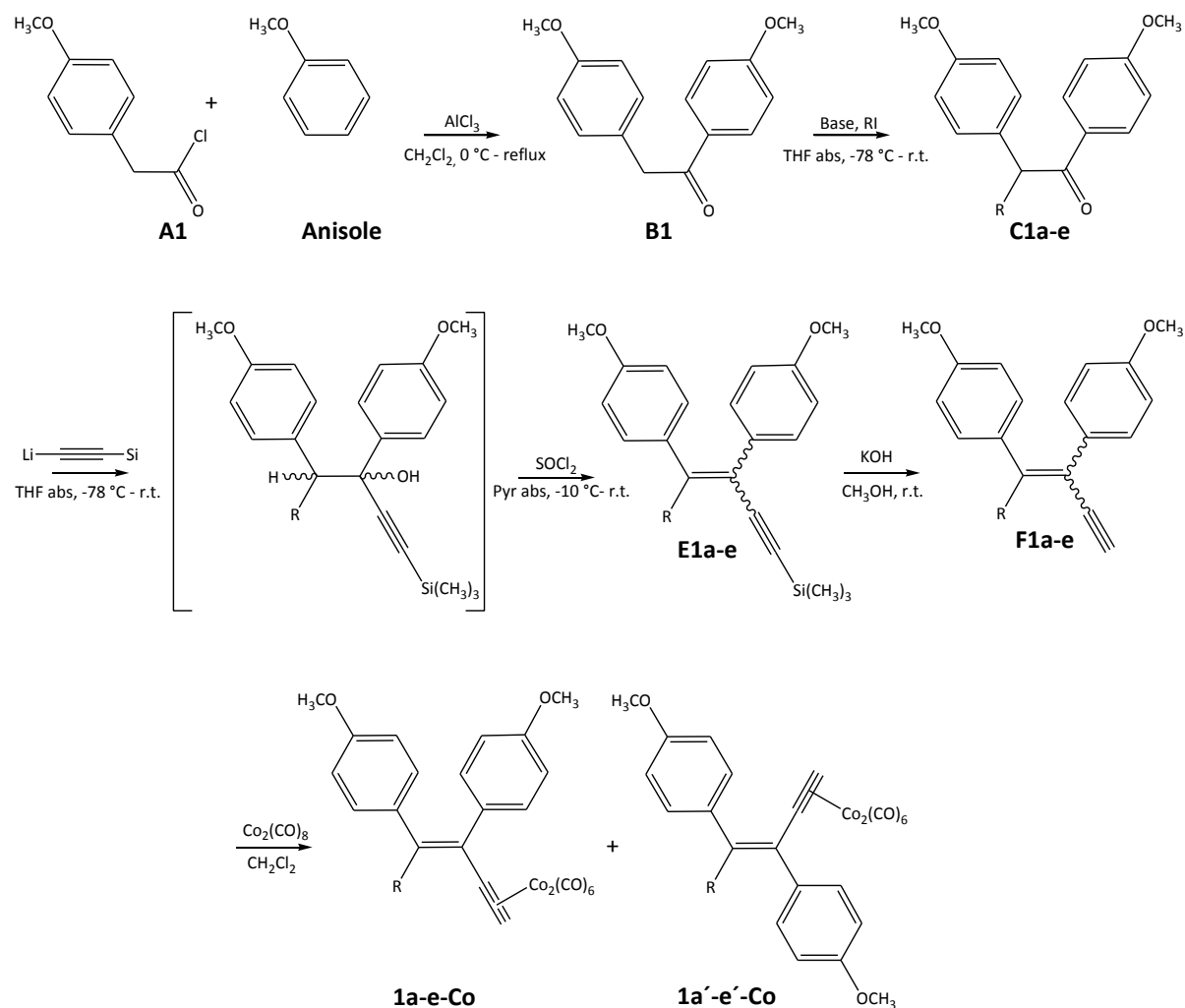
The synthesized 1,1,2-triarylalkene compounds **2a-d** with their substitution pattern and configuration are presented in Table 3.2.

Table 3.2. Substitution pattern of the 1,1,2-triarylalkene compounds.

Ligand	R	R'	Configuration	Complex
2a	H	-CH ₂ -C≡CH	Z	2a-Co
2b	-OCH ₂ -C≡CH	-CH ₂ -C≡CH		2b-Co
2c	H	-CH ₂ -CH=CH ₂	Z	2c-PtCl₃
2d	-OCH ₂ -CH=CH ₂	-CH ₂ -CH=CH ₂		2d-PtCl₃

3.2 Overview of the Synthetic Pathway of the 3,4-diarylalkenyne Hexacarbonyl Dicobalt Complexes

Synthesis of the 3,4-diarylalkenyne hexacarbonyl dicobalt complexes is described in Scheme 1.



Scheme 1.

3.2.1 Synthesis of 4-Methoxyphenylacetyl Chloride

The 4-methoxyphenylacetyl chloride (**A1**) was synthesized *in situ* starting from the corresponding 4-methoxyphenylacetic acid (see Fig. 3.3).

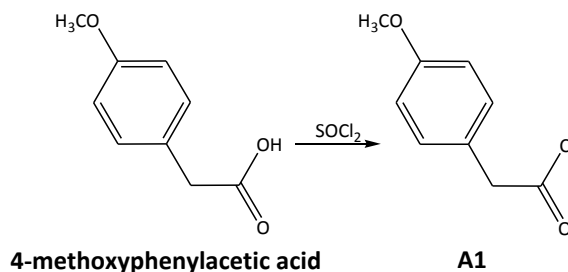


Figure 3.3. Synthesis of the 4-methoxyphenylacetyl chloride.

Thionyl chloride was slowly added and the mixture was carefully heated to prevent side reactions, such as elimination or polymerization. After approximately 1 hour, when no more gas production was observed, excess of SOCl₂ was removed by vacuum distillation. Because of the high reactivity, the crude product was directly used for the next reaction without further purification.

3.2.2 Friedel-Crafts Acylation

The desoxybenzoin (**B1**) was obtained by Friedel-Crafts acylation⁸¹ using 4-methoxyphenylacetyl chloride (**A1**) and anisole⁸² (see Fig. 3.4).

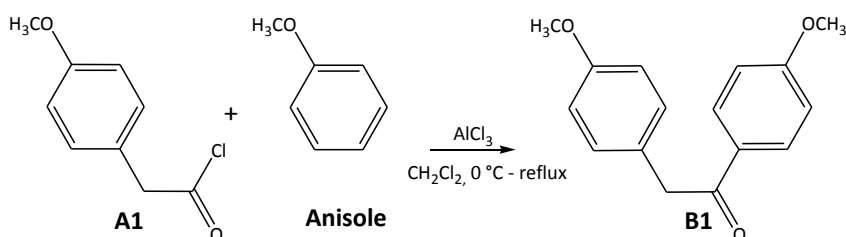


Figure 3.4. Synthesis of 1,2-bis(4-methoxyphenyl)ethanone (**B1**).

To activate the electrophilic attack on the aromatic ring, the Lewis acid aluminium chloride (AlCl₃) was used as catalyst in excess. The anisole was dissolved in dry dichloromethane with AlCl₃ and cooled at 0 °C in an ice-bath. Afterwards the 2-arylacetyl chloride was slowly dropped to generate a complex with AlCl₃ in equilibrium with its dissociated ions: the AlCl₄⁻ anion and the acylium cat-

ion as the active electrophilic species. The anisole acts as a nucleophile, attacking the electrophile with a pair of its π -electrons.

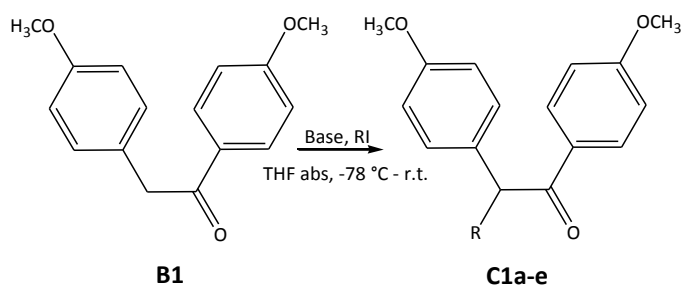
The OCH_3 group is an *ortho/para* director because intermediate carbocations that result from electrophilic attack *ortho* or *para* to the OCH_3 group can assume four resonance contributors, one of which has a complete octet on every atom.

Under thermodynamic control it was possible to direct the attack at low temperature exclusively in *para* position. The mixture was heated to reflux for 30 min and was successively stirred at room temperature for 1 hour, followed by addition of chopped ice and HCl 1 M in order to destroy the complex with AlCl_3 . Polyacylation does not occur, because the acyl group deactivates the ring to further attacks.

The crude product was purified by crystallization with ethanol/diethyl ether to afford the pure product as colorless crystalline solids in high yields.

3.2.3 Deoxybenzoin 's Alkylation

In a second step the deoxybenzoin (**B1**) was alkylated with different alkyl halides (see Fig. 3.5):



Compound	C1a	C1b	C1c	C1d	C1e
R	CH_3	CH_2CH_3	$\text{CH}_2\text{CH}_2\text{CH}_3$	$\text{CH}(\text{CH}_3)_2$	$\text{CH}_2\text{CH}_2\text{CH}_2\text{CH}_3$
Yield (%)	100	98	85	57	67

Figure 3.5. Alkylation of the deoxybenzoin (**B1**).

Different bases were screened for this reaction. Potassium bis(trimethylsilyl)amide (KHMDs) gave better results than potassium tertbutoxide.

Because of the electron-withdrawing effect of the carbonyl group, the protons bound to the α carbon in the deoxybenzoin were acidic and could be easily released under basic conditions.

KHMDs is a strong base as a result of its anionic N stabilized with K^+ . Its effects is accentuated by the (+I)-effect from the methyl groups, which are also responsible for its activity only as base (Fig. 3.6).

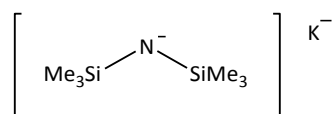
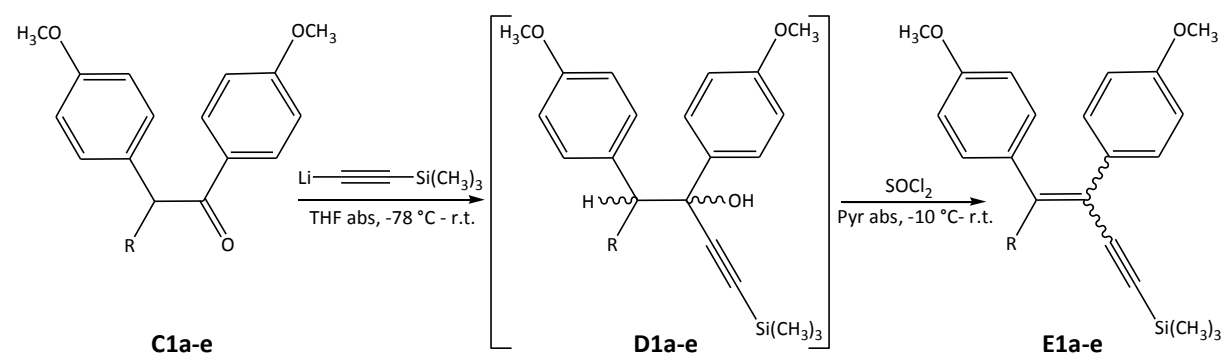


Figure 3.6. Structure of potassium bis(trimethylsilyl)amide or (KHMDs).

The reaction proceeded under argon adding 1.2 equivalents of KHMDs to a solution of **B1** in dry THF, previously cooled to -78°C . It was necessary to use aprotic solvents so that solvent deprotonation does not compete with enolate formation⁸³. The deoxybenzoin **B1** gave a carbanion and could attack an electrophile to form the corresponding derivative. The reaction mixture was stirred at -78°C for 1 hour. After then the corresponding alkyl halide dissolved in dry THF was added dropwise through a septum. The reaction, which became a suspension during the addition, was stirred at room temperature overnight. After the reaction ended, water was added and the layers were separated. The aqueous phase was washed with ethyl acetate and the combined organic fractions were extracted with distilled water and brine. The organic extracts were dried over Na_2SO_4 , filtered through a fritted funnel and the filtrate was evaporated to dryness to obtain a colorless oil. The crude product was purified by column chromatography on silica gel with diethyl ether/ligroin. The structures of **C1a,e** were confirmed by $^1\text{H-NMR}$ and mass spectrometry.

3.2.4 Synthesis of the 3,4-Diarylalkenyne Derivatives

The preparation of the diarylalkenyne derivatives **E1a-e** from the 2-alkyldeoxybenzoins **C1a-e** was performed in three steps⁸⁴ as shown in Fig. 3.7.



Compound	E1a	E1b	E1c	E1d	E1e
R	CH ₃	CH ₂ CH ₃	CH ₂ CH ₂ CH ₃	CH(CH ₃) ₂	CH ₂ CH ₂ CH ₂ CH ₃
Yield (%)	56	57	33	66	84

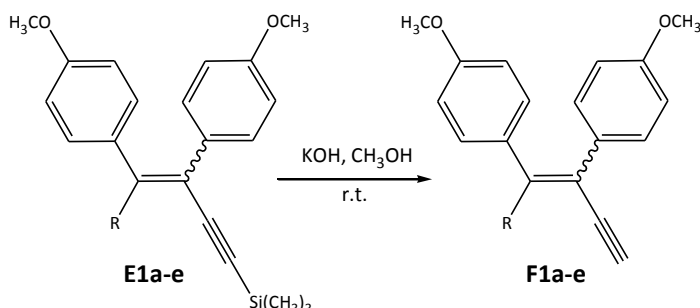
Figure 3.7. Nucleophilic addition get to 2-alkyl-deoxybenzoins.

In the first step the acetylene had to be activated as nucleophile in order to be able to attack the carbonyl function in a procedure called “Favorskii reaction”. The metal acetylide could be generated *in situ*. The acetylene is mildly acidic (pK_a = 25) and its treatment with a strong bases such hydroxide or an alkoxide gives the corresponding metal acetylides. The other acetylenic hydrogen was protected by the bulk of a silane. Trialkylsilyl acetylenes are often used as a convenient reagent to introduce an acetylene unit because they tend to be easily handled liquids or solids as opposed to gaseous acetylene⁸⁵. Lithium(trimethylsilyl)acetylide solution as a stable “free flowing liquid” is also be commercially available.

Lithium(trimethylsilyl)acetylide solution 0.5 M in THF was cooled to -78° C and then reacted with the ketone (**C1a-e**) (S_Ni reaction) which was dissolved in dry THF yielding a tertiary alcohol. In the second step the tertiary alcohol was immediately converted to the *E/Z*-alkene **E1a-e** using thionyl chloride in dry pyridine and dry diethyl ether at 0° C. Note that under these conditions the elimination reaction was favored (then nucleophilic substitution) and the selectivity *Z* versus *E* was 6:1. It was not possible to separate the residual *E*- isomer by column chromatography or crystallization. The structures of **E1a-e** were confirmed by ¹H-NMR and mass spectrometry.

3.2.5 Cleavage of Trimethylsilyl Group

The trimethylsilyl group could be easily removed by a variety of synthetic methods⁴.



Compound	F1a	F1b	F1c	F1d	F1e
R	CH ₃	CH ₂ CH ₃	CH ₂ CH ₂ CH ₃	CH(CH ₃) ₂	CH ₂ CH ₂ CH ₂ CH ₃
Yield (%)	91	100	100	100	100

Figure 3.8. Elimination of the alkyne's protective group.

In the synthesis we chose, the mixture of isomers **E1a-e** was dissolved in dry MeOH and cooled at 0° C. KOH, in a pellet formulation, was added in stoichiometric amount and the reaction mixture was stirred at room temperature for 24 hours. Under these basic conditions, the more electron-deficient silylalkyne can be cleaved faster. The ¹H-NMR and mass spectrometry analyses confirmed the structures.

3.2.6 Cleavage of the Methoxy Groups

To obtain molecules that combine possible ER activity and cytotoxic properties, different methods for cleavage the methoxy group were explored. In order to cleave an aryl methyl ether to obtain an aryl alcohol (Fig. 3.9), a large number of reagents can be used (BBr₃, EtSH, etc.).

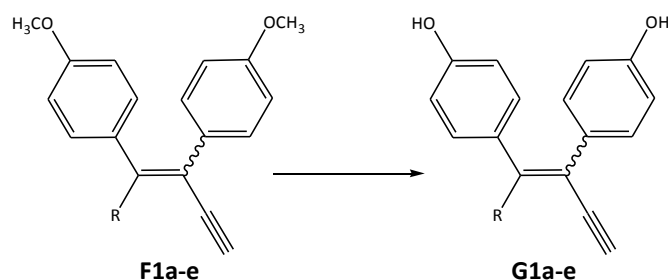


Figure 3.9. Attempted ether cleavage of **F1a-e** derivatives.

Boron tribromide is regarded as one of the preferred ether cleavages molecules: in addition to its high efficiency, it requires mild conditions (e.g. low temperatures) and it cleaves without affecting a large number of functional groups, including double bonds⁸⁶. For these reasons we decided to use it as first choice for our attempts.

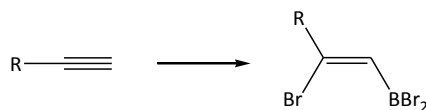
The methoxy-substituted molecule was dissolved in dry dichloromethane and cooled to -78°C . BBr_3 was carefully added *via* a syringe under argon atmosphere and the reaction mixture was stirred at room temperature for approximately 2 hours. The reaction was monitored by thin layer chromatography (TLC). The mixture of products was hydrolyzed three times with dry methanol, dried by rotatory evaporation and purified by column chromatography on silica gel with dichloromethane/methanol as eluant. TLC products spots were very close or overlapping so that they were difficult to separate. At last the variety of isolated substances were analyzed by $^1\text{H-NMR}$ and mass spectrometry, but the desired products **G1a-e** were not present in the reaction mixture.

Various attempts were made to dealkylate the methyl ether by respectively changing the experimental conditions such as the number of the equivalent and the time of reaction (see Table. 3.3), but none of these reaction conditions was successful.

Table 3.3 Different parameters used for the experiments with BBr₃.

Equivalent of BBr ₃	Reaction time (h)	Temperature (° C)	Yield (%)
1.2	2	0	Complex mixture
1.2	2	-20	Complex mixture
1.2	1	-78	Complex mixture
1	1	-78	Complex mixture
0.8	1	-78	Complex mixture
0.8	0.5	-78	Complex mixture

We assume the problem arises from the reactivity of triple bonds towards boron tribromide⁸⁷. As a matter of fact, either boron tribromide or the late-formed hydrobromide react with a bond to give the compound depicted in Fig. 3.10.

**Figure 3.10.** Addition of BBr₃ was found to proceed in a Markovnikov manner to afford *cis* alkenes.

As the attempts to prepare **G1a-e** were unsuccessful, other possibilities to cleave the ether were investigated, and a second try with ethanethiol was made.

The compound **F1a** was dissolved in dichloromethane under argon atmosphere. After cooling to 0° C with an ice-bath, AlCl₃ and ethanethiol were successively added. After stirring at 0° C for 30 min and an additional 30 min at room temperature, the reaction was stopped with chopped ice and a 5% NaHCO₃ solution, extracted with CH₂Cl₂ and purified by column chromatography. Unfortunately, by analyzing ¹H-NMR and mass spectra, we deduced that the starting material was still polymerized in the reaction. However, the seemingly trivial demethylation turned out to be troublesome. Despite attempts with various demethylation reagents, we found it impossible to cleave the methyl group without destroying the diphenylalkyne moiety.

We were drawn to the idea of using trimethylsilyl iodide (TMSI) by the work of Jung and co-workers⁸⁸, who showed in 1977 that methyl ethers also react with trimethylsilyl iodide to generate mixtures of alkyl iodide and trimethylsilyl ethers which can be easily converted into the alcohol upon simple hydrolysis.

One main drawback of the use of it is its inherent instability towards moisture and light. However this reagent is more selective than BBr_3 ⁸⁹. It does not affect triple bonds and it could be synthesized in two steps from trimethylsilyl chloride or it is commercially available.

A straightforward mechanism for this process is described in Fig. 3.11:

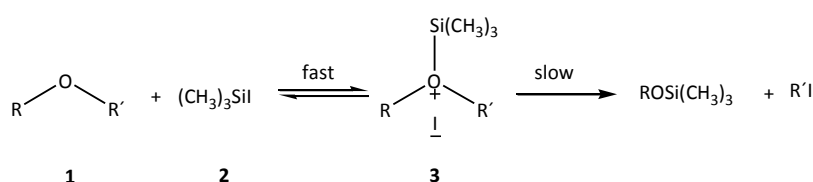


Figure 3.11. The ether **1** reacts with trimethylsilyl iodide **2** in a fast and reversible step to produce the silylated oxonium iodide **3** which then reacts to the products in a slow, irreversible process by either an $\text{S}_{\text{N}}2$ mechanism or $\text{S}_{\text{N}}1$ ($\text{S}_{\text{N}}\text{i}$) mechanism.

We started the reaction by dissolving **F1a** in CDCl_3 in a NMR tube with a tightly sealed cap under nitrogen. To this solution containing 1 equivalent of the ether was added 1.3 equivalent of trimethylsilyl iodide *via* dry syringe. The reaction was stirred at room temperature and monitored by $^1\text{H-NMR}$ analysis every 2 hours. After 72 hours, the signal of the methoxy group in the $^1\text{H-NMR}$ remained unchanged, indicating that no reaction occurred.

To achieve our aim we decided to turn to another protecting group for the *para*-hydroxy function, because of the instability of triple bond under acidic conditions or high temperatures and the difficulty to cleave the methylether under mild conditions (without affecting the triple bond).

3.2.7 Silyl Ethers as Protecting Groups

Silyl ethers are frequently used to protect alcohol functions. Because of their reactivity, both formation and cleavage can be easily modulated and they do not require extreme conditions. At first we tried using a trimethylsilyl group (TMS)

which combines stability under a wide range of conditions with susceptibility to easy removal by a highly specific reagent.

We started from the **C1a-e** derivatives, described above in Fig. 3.5, which were subsequently demethylated by refluxing it for 18 hours in pyridine-HCl (see Fig. 3.13). Finally the reaction was stopped with distilled water and extracted with ethyl acetate. No purification was needed. The structures were confirmed by $^1\text{H-NMR}$ and mass spectrometry.

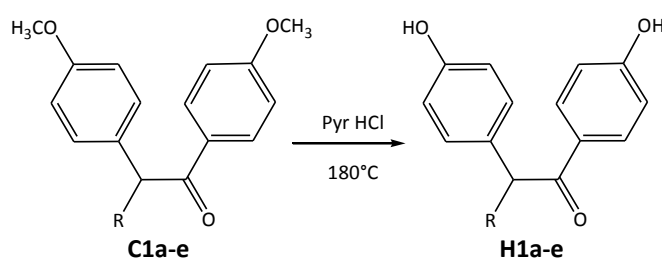


Figure 3.12. Demethylation of the **C1a-e** compounds.

The alcohols **H1a-e** were now re-protected⁹⁰ using 1,1,1,3,3,3-Hexamethyldisilazane (HMDS) and a catalytic amount of silica supported perchloric acid as a recyclable solid Brønsted acid catalyst. HMDS is a stable and cheap reagent for trimethylsilylation of hydrogen-labile substrates, which is commercially available. On the one hand the handling of this reagent is easy but on the other hand it requires the use of a catalyst for its activation as a result to its low silylation power. A variety of catalyst can be used, for instance iodine, lithium perchlorate, $\text{Al}(\text{HSO}_4)_3$, etc. However all of these reagents are either too sensitive or expensive. Because of this, we preferred the use of silica supported perchloric acid, which provides high selectivity, low cost and simplicity in handling. This heterogeneous catalyst was prepared adding HClO_4 (1.8 g, 12.5 mmol, as a 70% aq solution) to a suspension of SiO_2 (230-400 mesh, 23.7 g) in dry Et_2O (70 mL). The mixture was concentrated and the residue was heated at 100° C for 72 hours in vacuo to generate $\text{HClO}_4\text{-SiO}_2$ as a free-flowing powder⁹¹.

The trimethylsilylation of the hydroxyl groups was easily carried out by adding the catalyst (0.05 g, equal to 0.025 mmol of H^+) to a stirred solution of the compounds **H1a-e** (1 mmol) in *n*-hexane and HMDS (1.7 mmol) (Fig. 3.13). The mixture was stirred at room temperature for only 4 min and after the completion of the reaction, monitored by TLC (*n*-hexane/ EtOAc , 9:1) the mixture was diluted

with *n*-hexane and filtered through a short pad of silica gel. Then, the pad column was washed with *n*-hexane (2 times 10 mL). The resulting solution was evaporated under reduced pressure giving the pure product, characterized by $^1\text{H-NMR}$ and mass spectrometry as well.

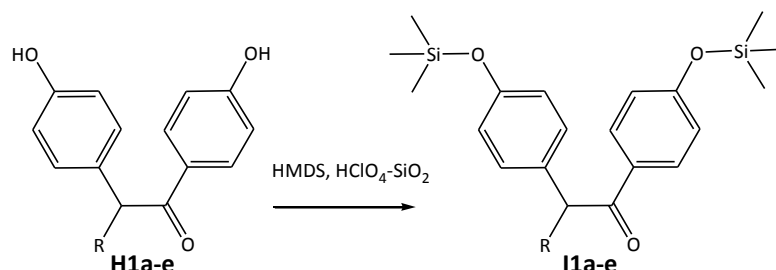


Figure 3.13. Trimethylsilylation of **H1a-e** compounds.

In the next step the compounds **I1a-e** reacted first with lithium(trimethylsilyl)acetylide 0.5 M in THF, as illustrated in Fig. 3.7, and was directly dehydrated *in situ* by SOCl_2 in diethyl ether/pyridine. The crude products were purified by column chromatography (diethyl ether/ligroin) and identified through $^1\text{H-NMR}$ and mass spectrometry. From the analyses emerged that lithium(trimethylsilyl)acetylide did not react with the carbonyl function but with the protective group TMS to give the following compounds (Fig. 3.14):

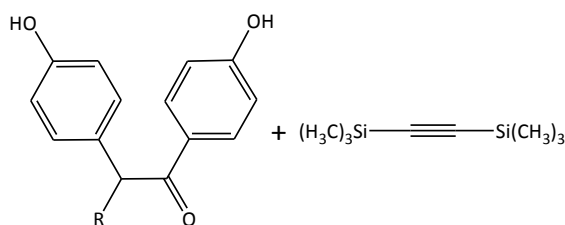


Figure 3.14. Isolated products from the S_{Ni} reaction.

A possible explanation can be the instability of the protective group TMS. In general the stability of a silylated functional group is largely determined by the combined steric bulk of the alkyl groups attached to silicon: as the steric bulk of the alkyl groups increases, the stability of silylated functional groups also increases. For some of the more common silyl ethers (Fig. 3.15), the stability towards acid increases in the order **TMS** (1) < **TES** (64) < **TBDMS** (20,000) < **TIPS** (700,000) < **TBDPS** (5,000,000), and the stability towards base increases in the order **TMS** (1) < **TES** (10-100) < **TBDMS** ~ **TBDPS** (20,000) < **TIPS** (100,000).

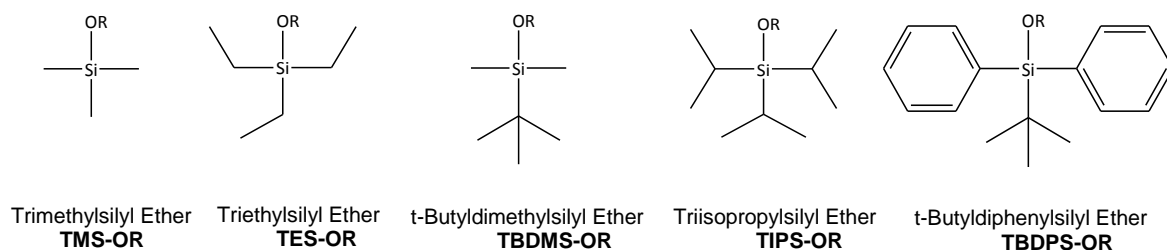


Figure 3.15. Structure of the most common silylating agents.

We therefore decided to try the protection with another silylated functional group, more stable than the TMS group, that can in addition be removed under mild conditions. The greater steric bulk of the TIPS protective group increases its susceptibility toward basic hydrolysis more than other silyl ether groups to acidic and basic hydrolysis⁹².

TIPS was introduced⁹³ by stirring **H1-a** (1 equivalent) with triisopropylsilyl chloride (TIPS-Cl) (1.3 equivalent) and imidazole (1.5 equivalent) in DMF at ambient temperature under argon atmosphere for 16 hours (see Fig 3.16). The mixture was poured into 10% aqueous NaHCO_3 solution and extracted with n-hexane three times. The combined organic layers were washed with 0.5 M HCl and then with water, dried (sodium sulfate) and concentrated *in vacuo*. The resulting residue was purified by flash chromatography.

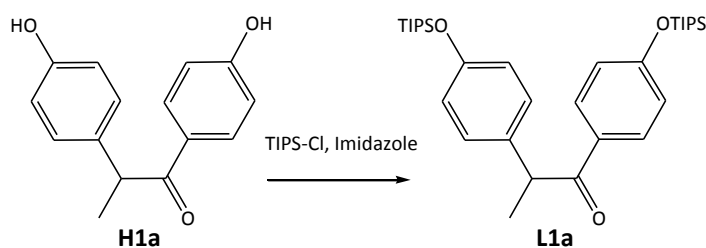


Figure 3.16. Standard protection procedure with triisopropylsilyl chloride (TIPS-Cl).

Finally, **L1a** reacted with lithium(trimethylsilyl)acetylide 0.5 M in the well known reaction described above (Section 3.2.4), but the substitution (S_{Ni}) at the carbonyl group did not take place. The failure of the reaction may be attributed to steric hindrance of the TIPS group, while the lack of reactivity of the carbonyl with lithium(trimethylsilyl)acetylide can be explained by the delocalization of the negative charge through the π -system.

All conditions explored (e.g., BBr_3 , EtSH, TMS, TIPS) for the cleavage of the methoxy groups were unsuccessful. They resulted in either polymerization or decomposition products and therefore were not investigated further.

3.2.8 Synthesis and Chemistry of Hexacarbonyl Dicobalt Complexes

Investigations conducted by Greenfield and co-workers have shown that dicobalt octacarbonyl, contains two types of carbonyl groups, *i.e.*, bridge and terminal carbonyl groups⁹⁴ (see Fig. 3.19).

The two bridge carbonyl groups can be replaced by alkynes in the reaction depicted in Fig. 3.17:

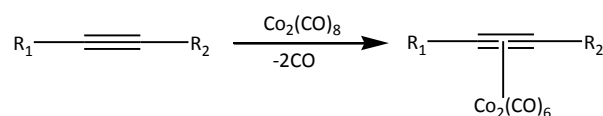
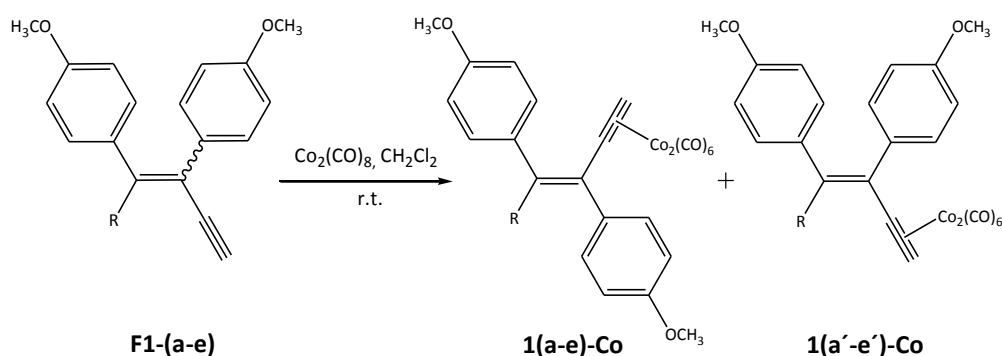


Figure 3.17. Displacement of the two bridge carbonyl groups of the dicobalt octacarbonyl and formation of the alkyne hexacarbonyl dicobalt complex (right).

The coordination of the ligands **F1a-e** to obtain the corresponding cobalt-alkyne complexes **M1a-e** and **M1a'-e'** was easily performed by reaction with an excess of dicobalt octacarbonyl in dry dichloromethane⁹⁵ (see Fig. 3.18).



Compound Form Z	1a-Co	1b-Co	1c-Co	1d-Co	1e-Co
Yield (%)	75	64	54	75	75
R	CH ₃	CH ₂ CH ₃	CH ₂ CH ₂ CH ₃	CH(CH ₃) ₂	CH ₂ CH ₂ CH ₂ CH ₃
Compound Form E	1a'-Co	1b'-Co	1c'-Co	1d'-Co	1e'-Co
Yield (%)	13	15	17	12	11

Figure 3.18. Synthesis of alkyne hexacarbonyl dicobalt complexes.

The reaction was stirred for *approximately* 1 hour: During this time dicobalt octacarbonyl lost its two bridging carbon monoxides, which could be seen by effervescence and an intense colouration (from red to brown) by formation of the complexes. The triple bond of the diphenylalkyne moiety with two perpendicularly oriented p-orbitals made the coordination to $\text{Co}_2(\text{CO})_8$ possible accompanied by elimination of two CO ligands from their coordination places.

The complexes consist of two covalently linked cobalt (0) atoms, each containing three carbon monoxides. The alkyne bond is perpendicular to the Co-Co axis and the CO groups are usually eclipsed across the Co - CO bond as depicted in the Newman projection (see Fig. 3.19). X-ray structural analysis showed the loss of the linearity of the alkyne upon the coordination, therefore its substituents are positioned at an angle of approximately 140 degrees in the complexes and the C-C distance was increased⁶⁵.

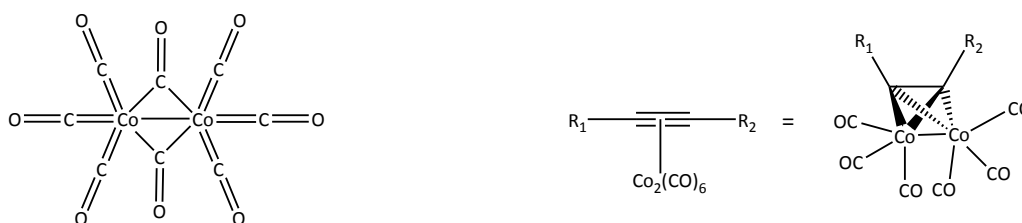


Figure 3.19. Dicobalt octacarbonyl structure(left). Convenient mode of representation and structural model for alkyne- $\text{Co}_2(\text{CO})_6$ complexes (right).

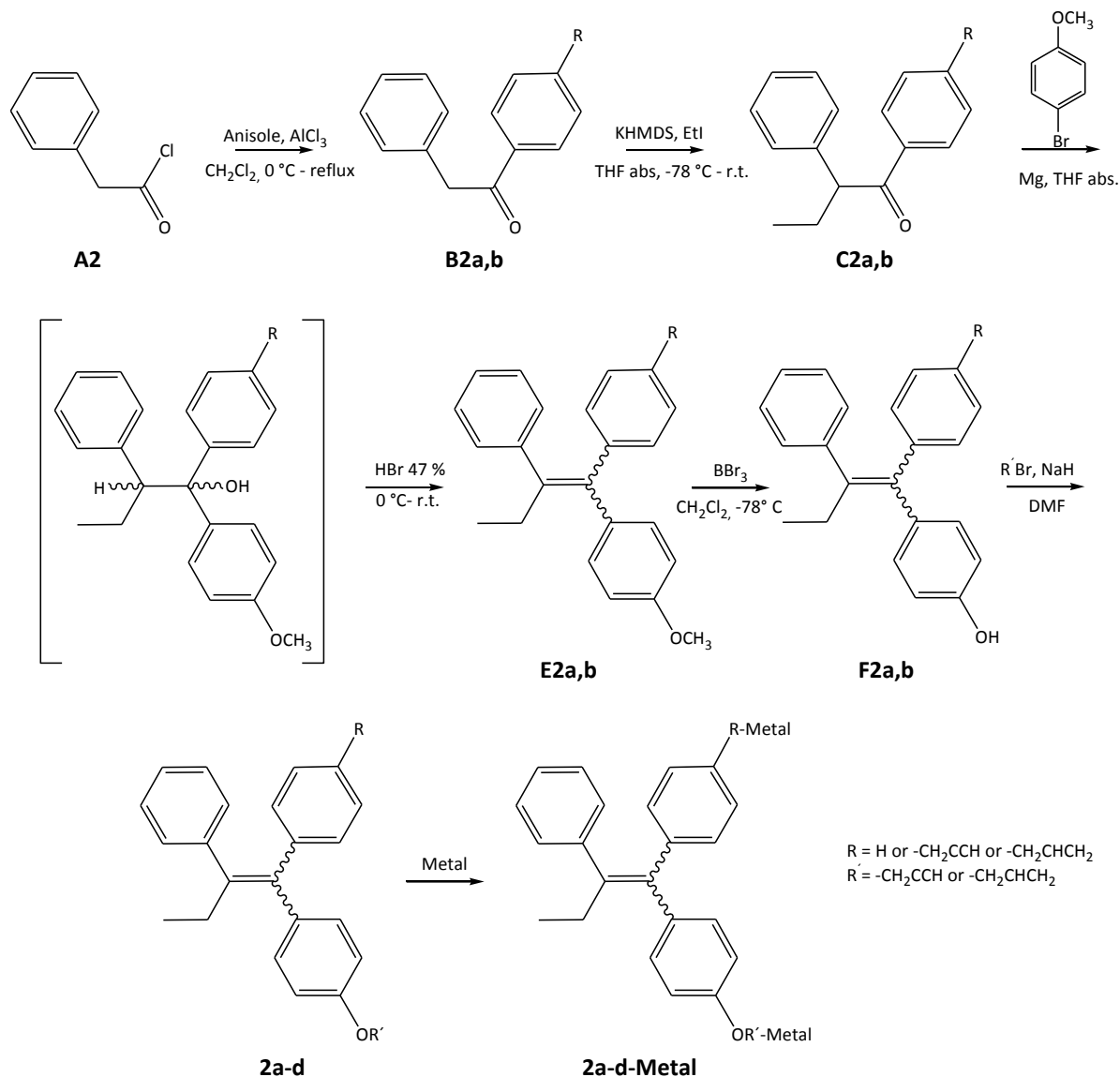
The reaction was monitored by TLC. After 1 hour, the reaction had come to full conversion. The reaction mixture was then evaporated to dryness. As a result of the increased lipophilicity of the compounds upon coordination, it was

now possible to separate the two isomers by column chromatography. The freshly prepared complexes were readily soluble in organic solvents such as diethyl ether and dichloromethane.

1(a-e)-Co and **1(a'-e')-Co** were stable in the solid form when kept under argon atmosphere, but decomposed slowly in solution to form a yellow solution. By $^1\text{H-NMR}$ this solution showed broad peaks suggesting that CO has been oxidized resulting in the loss of CO^{96} .

3.3 Overview on the Preparation of the Triarylalkene Compounds

The synthesis of the 2-ethyl-triarylalkenes compounds is presented in Scheme 2.



Scheme 2.

To synthesize the 2-ethyl-1,1,2-triarylethene a successful method was used, which was developed by Dodds and co-workers^{97,2} and modified to advantage. The successive O-alkylation and preparation of the desired complexes is sequentially described in detail in the following sections.

3.3.1 Preparation of 1-(4-methoxyphenyl)-2-phenylethanone

Similar to the procedure described in Section 1.2.2 the desired 1-(4-methoxyphenyl)-2-phenylethanone **B2b** was obtained by Friedel-Crafts acylation from 2-phenylacetyl chloride **A2** with anisole in presence of aluminium chloride.

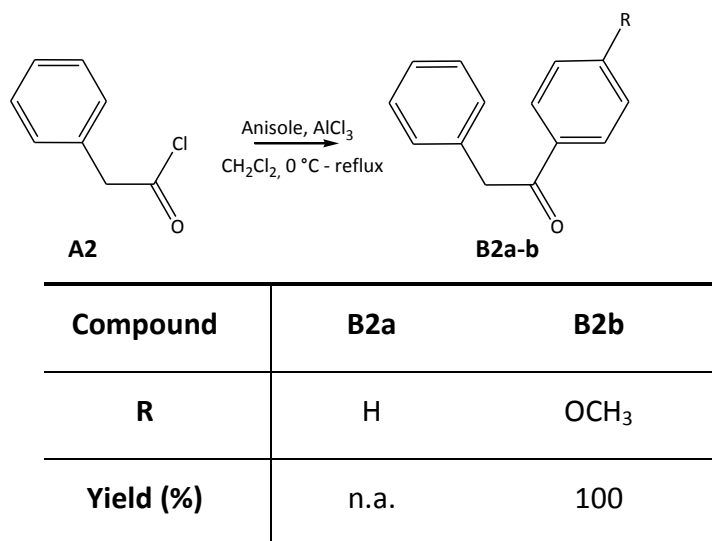


Figure 3.20. Synthesis of the 1-(4-methoxyphenyl)-2-phenylethanone compound.

The crude product was recrystallized from diethyl ether/ethanol as described above.

3.3.2 Alkylation of the ethanone

The commercially available 1,2-diphenylethanone **B2a** and the synthesized 1-(4-methoxyphenyl)-2-phenylethanone **B2b** were both successfully alkylated with ethyl iodide under basic conditions (see Fig. 3.21) according to the procedure described in Section 1.2.3.

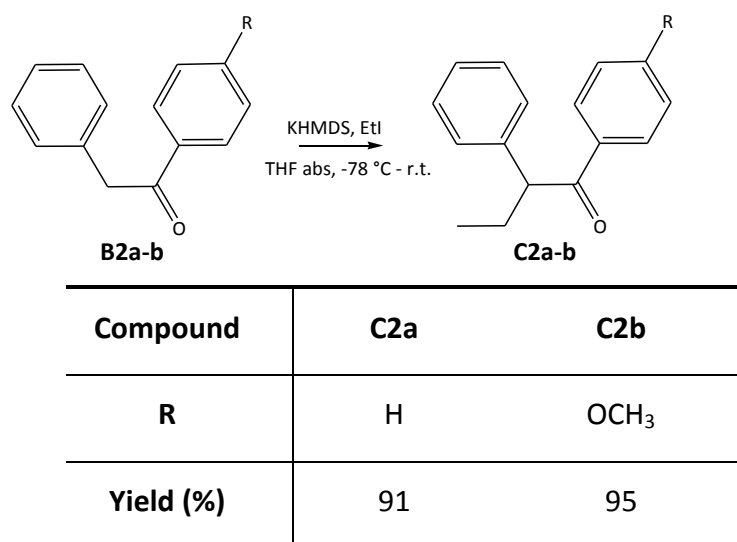
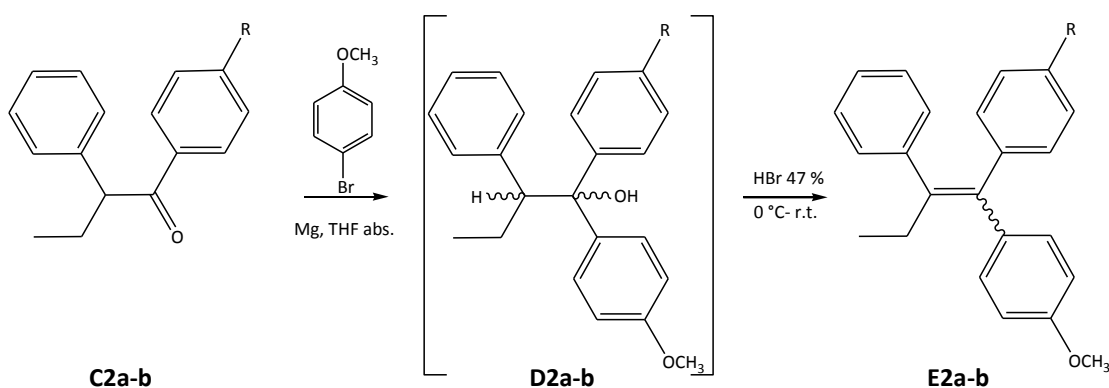


Figure 3.21. Alkylation of 1,2-diphenylbutanone **B2a** and 1-(4-methoxyphenyl)-2-phenylbutanone **B2b** with ethyl iodide.

An excess of KHMDS was added at -78°C to a solution of the ketone. After stirring for 1 hour at this temperature, the ethyl iodide dissolved in THF was added dropwise and the reaction was stirred at room temperature overnight. After work-up of the reaction mixture, the residues obtained were the pure products **C2a** and **C2b**, which could be used directly in the next step without further purification.

3.3.3 Grignard reaction

The synthesis of 1-(4-methoxyphenyl)-1,2-diphenylbutene **E2a** and 1,1-bis(4-methoxyphenyl)-2-phenylbutene **E2b** as depicted in Fig. 3.22 was performed by Grignard reaction in satisfactory yields:



Compound	E2a	E2b
R	H	OCH ₃
Yield (%)	86	77

Figure 3.22. Synthesis of the (*E*)- and (*Z*)-1-(4-methoxyphenyl)-1,2-diphenylbuten **E2a** and 1,1-bis(4-methoxyphenyl)-2-phenylbuten **E2b**.

The first step was to generate the Grignard reagent from 4-bromoanisole and magnesium in THF. To promote the reaction, iodine was used as a catalyst. The Grignard reagent was refluxed for approximately 1 hour. Once magnesium traces had completely disappeared, a solution of the corresponding ketone dissolved in THF was added, and it was converted into the corresponding carbinoy magnesium bromide. After refluxing for 12 hours, the mixture was directly hydrolyzed by HCl 6 N, in order to dissolve precipitated Mg(OH)₂. Due to its high reactivity the carbinol was not isolated, but simultaneously dehydrated *in situ* to the desired 2-alkyl-1,1,2-triarylethylene product by using 47% hydrobromide acid or H₃PO₄. After dehydration, the compounds were extracted with dichloromethane, and the crude products were concentrated, isolated by suction filtration and purified by crystallisation from ligroin/diethyl ether.

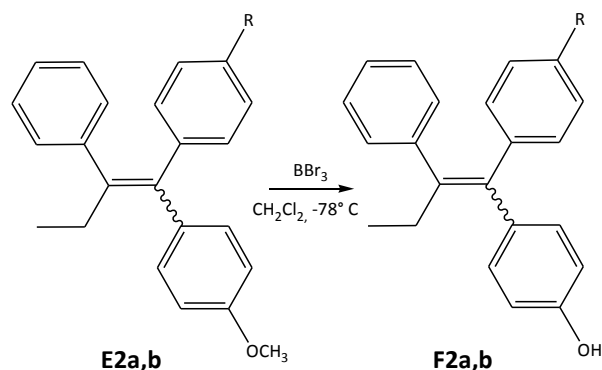
The compound 1-(4-methoxyphenyl)-1,2-diphenylbutene **E2a** was obtained as a mixture of (*E*)- and (*Z*)-isomers, whose separation was possible as a result of the poor solubility of the (*Z*)-isomer in diethyl ether. (*Z*)-**E2a** was precipitated from the solution of diethyl ether/ligroin (4-1) as pure colorless crystals, successively isolated by suction filtration and washed with diethyl ether. The filtrates containing the rest of (*E*)- and (*Z*)-form were accumulated and purified by column chromatography. The structures were confirmed by ¹H-NMR and mass spectrometry analyses.

In contrast to the method described in Section 1.2.4, in this procedure the (*Z*)-configuration as result of the position of substituents at the double bond was favoured. Usually (*E*)-isomers correspond with the *trans* form and (*Z*)-isomers correspond with *cis* form. But in this case (*Z*)- corresponds to the *trans* form^f.

^f Because of steric effects the *trans* forms are more stable. When two large groups are further away from each other (*trans* form), they can line up and fit together in a more stable way than the *cis* form.

3.3.4 Ether cleavage

In order to obtain hydroxylated triphenylalkenes derivatives, it was attempted to demethylate compounds **E2a,b** with boron tribromide:



Compound	F2a	F2b
R	H	OH
Yield (%)	79	89

Figure 3.23. Ether cleavage of (Z)-**E2a** and **E2b**.

Boron tribromide, diluted in dry CH_2Cl_2 , was added *via* syringe to a solution of the appropriate methyl ether in dry dichloromethane at -60°C and stirred approximately 1 hour at this temperature. The ether cleavage occurred by increasing the temperature from -60°C to room temperature, in which one molecule of BBr_3 reacted with three molecules of ether (see Fig. 3.23), this resulted in a boron complex. Hence, the red solution was stirred at room temperature for an additional 24 hours. The demethylation reaction was monitored by thin layer chromatography. The excess of boron tribromide and the formed complex (Fig. 3.24) were destroyed by the addition of MeOH to the cooled reaction mixture and the solvent was removed under reduced pressure⁹⁸.

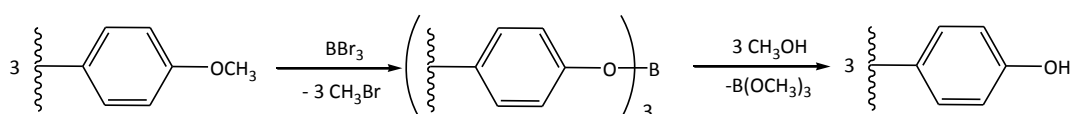
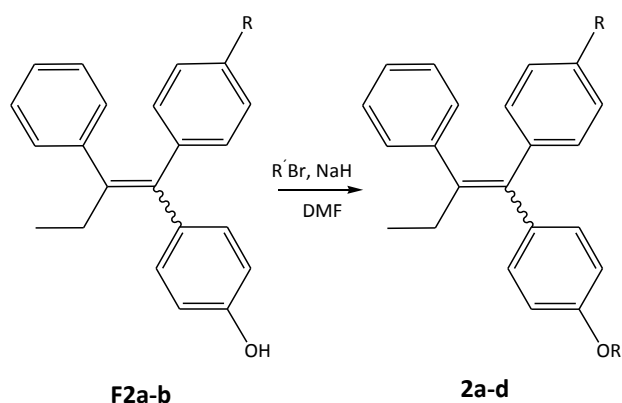


Figure 3.24. Demethylation reaction mechanism.

The products were purified by column chromatography on silica gel ($\text{CH}_2\text{Cl}_2/\text{MeOH}$), but **F2b** was obtained again as a mixture of (*E*)- and (*Z*)- isomers, as a result of the cleavage which gave OH groups conjugated with the electron withdrawing double bond. Further attempts of separation⁹⁹ were unsuccessful. We also found that the use of different demethylating agents (e.g. Pyr-HCl or ethanethiole as described above) produced the same isomers mixture¹⁰⁰. It is important to keep in mind that also time reaction influences the isomers ratio, as will be discussed in the section below. The structures of **F2a** and **F2b** were confirmed by $^1\text{H-NMR}$ and mass spectrometry.

3.3.5 O-Alkylation

The compounds **2a-d** were obtained by treating the hydroxyl function with allyl- and propargyl-bromide, respectively (see Fig. 3.25).



Compound	2a	2b	2c	2d
R	H	$-\text{OCH}_2-\text{C}\equiv\text{CH}$	H	$-\text{OCH}_2-\text{CH}=\text{CH}_2$
R'	$-\text{CH}_2-\text{C}\equiv\text{CH}$	$-\text{CH}_2-\text{C}\equiv\text{CH}$	$-\text{OCH}_2-\text{CH}=\text{CH}_2$	$-\text{CH}_2-\text{CH}=\text{CH}_2$
Yield (%)	79	75	80	57

Figure 3.25. Generation of 1-(4-alkyloxyphenyl)-1,2-diphenylbut-2-ene **2a-2c** and a bis-p-alkyloxyphenyl-2-phenylbut-2-ene **2b-2d** by O-alkylation.

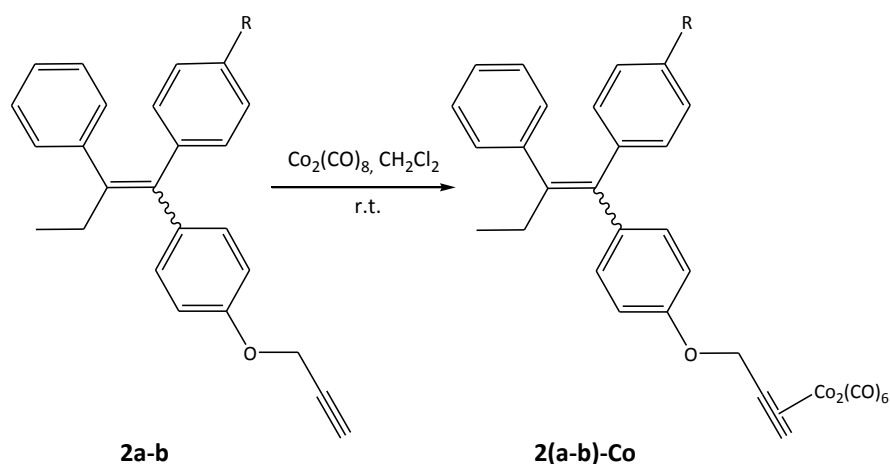
The alkylation, such as the transfer of an alkyl group to the aromatic substrates, proceeded by deprotonation first from the alcohol by a Brønsted base to

furnish a phenoxide. The resulting phenolate anion was stabilized by the aromaticity of the molecule that could delocalize the negative charge by resonance. In aprotic solvents such as DMSO, DMF and ethers only O-alkylation occurred because C-alkylation disrupted the aromatic conjugation.

For this purpose a solution of the corresponding p-hydroxyphenyl molecule **F2a,b** in DMF was added at room temperature to a stirred suspension of sodium hydride (1 g of a 50% dispersion in mineral oil from which the oil was removed by washing with n-hexane) in DMF under argon. After stirring for 30 min the alkylbromide was added and the mixture was stirred for an additional 30 min. Finally, the reaction was poured into saturated aqueous ammonium solution and extracted three times with diethyl ether. The combined extracts were washed five times with water, dried and evaporated to dryness. The residue was crystallized from ethanol.

3.3.6 Preparation of the alkyne hexacarbonyl dicobalt complexes

Cobalt-alkyne complexes were prepared according to the literature procedure¹⁴ previously reported (see chapter 3.2.8).



Compound	2a-Co (Z)	2b-Co
R	H	-OCH ₂ -C≡CH-Co
Yield (%)	79	87

Figure 3.27. Formation of alkyne hexacarbonyl dicobalt complexes .

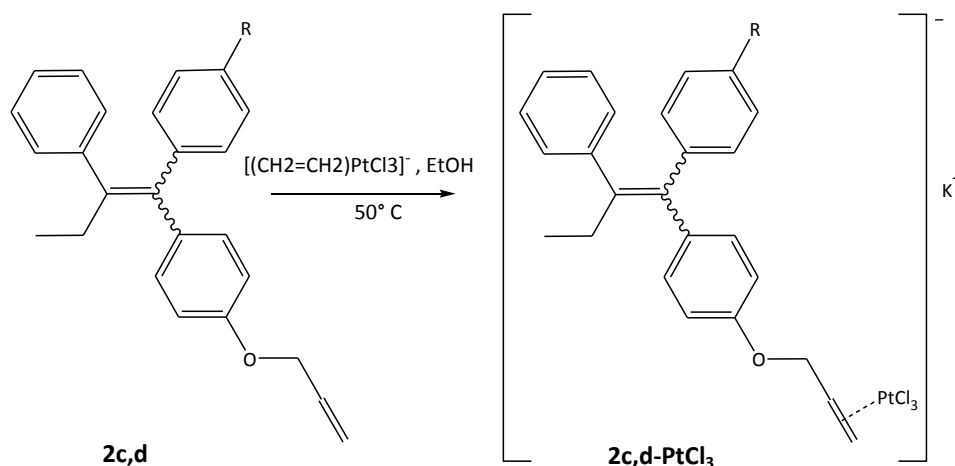
The alkyne was dissolved in dry dichloromethane under an atmosphere of argon and dicobalt octacarbonyl was added in excess. The reaction occurred with all types of alkynes. When the alkyne was in stoichiometric amounts, especially **2b** which contained two triple bonds, each reacted with dicobalt octacarbonyl¹⁰¹.

The reaction mixture was stirred for approximately 1 hour at room temperature until no effervescence was observed. The solution was directly evaporated to dryness. The deeply coloured complexes, which for their weak intermolecular forces of attraction possess high volatility and solubility, could be easily purified by flash column chromatography on silica.

The complexes **2a-Co** and **2b-Co** were conserved under argon in order to prevent the decomposition.

3.3.7 Synthesis of Zeise complexes

The preparation of the platinum complexes (*Z*)-**2c-PtCl₃** and **2d-PtCl₃** was performed by using the reactivity of the olefin **2c** and **2d** in presence of Zeise's salt, previously prepared¹⁰² (see Fig 3.28).



Compound	(Z)-2c-PtCl ₃	2d-PtCl ₃
R	H	-OCH ₂ -CH=CH ₂ -PtCl ₃
Yield (%)	76	82

Figure 3.28. Synthesis of Zeise complexes **2c-PtCl₃** and **2d-PtCl₃** with olefin ligands.

Zeise's salt can be described as ethylene platinum chloride (see Fig. 3.30), in which the carbon atoms of the ethylene ligand, whose C-C axis is perpendicular to the PtCl₃ plane, are equidistant from the Pt atom⁷².

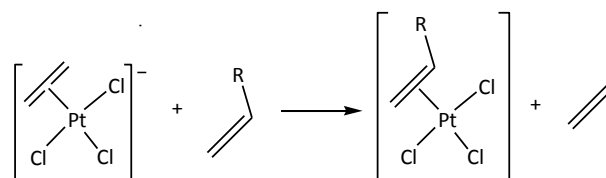


Figure 3.30. Olefin displacement from complexes of platinum (II) is a rapid reaction. Reaction occurs readily, the volatility of ethylene tending to drive it to completion.

The reaction was performed under argon atmosphere using standard Schlenk techniques. The ethanol was dried over Mg and benzophenone, and distilled prior to use. A mixture of [(CH₂=CH₂)PtCl₃]⁻K⁺ (0.1 mmol) and the ligand **2c-d** (1.1 mmol) was stirred at 50° C for a minimum of 3 hours. At this temperature the displacement reaction is accelerated. Then the clear solution was concentrated in *vacuo* to 1 ml and the precipitate filtered off. To the clear yellow filtrate diethyl ether (10 ml) was added dropwise, the precipitate was filtered, washed two times with diethyl ether (2 ml) and dried briefly in *vacuo*¹⁰³. On longer exposure to air and light, the complexes became covered with a black crust, so that they were stored in dark in an dessicator.

4 Proton NMR and Mass Spectrometry Analyses

4 Proton NMR and Mass Spectrometry Analyses

In this work the purity of the ligands as well as the metal complexes was monitored by thin layer chromatography and their corresponding structures were characterized using $^1\text{H-NMR}$ spectroscopy, mass spectra and elemental analyses. Data of $^1\text{H-NMR}$ spectra are presented in ppm. Chemical shifts are reported in the delta [δ] system of units relative to tetramethylsilane (TMS) as an internal standard. High resolution mass spectrometry was used to identify the composition and the purity of both ligands and complexes.

4.1 3,4-Diarylalkenyne Ligands

Double bonds do not exhibit free rotation at room temperature, giving rise to stereoisomerism⁹ (see Fig. 4.1).



Figure 4.1. (*Z*)- indicates priority groups on the same side (right), while (*E*)- indicates priority groups on opposite sides (left).

In the case of the 3,4-diarylalkenyne ligands the $^1\text{H-NMR}$ spectra showed superimposed signals. For example, the spectrum of compound **F1b** in CDCl_3 solution (see Fig. 4.2) showed a triplet at 1.02 ppm (CH_3 protons on the side chain), a quartet at 2.88 ppm (CH_2 protons on the side chain) and showed the alkyne proton at 3.18 ppm as a singlet. The methoxy protons at 3.69 and 3.71 ppm gave rise to a singlet and the aromatic protons can be seen at 6.64-7.06 ppm as doublets ($J=8.8$ Hz and $J=8.7$ Hz).

⁹ The stereodescriptors *cis* and *trans* can only be used to indicate the relative arrangement of similar groups. When an alkene possesses nonsimilar groups, usage of *cis-trans* terminology would be ambiguous and the stereodescriptors (*E*)- and (*Z*)- must be used.

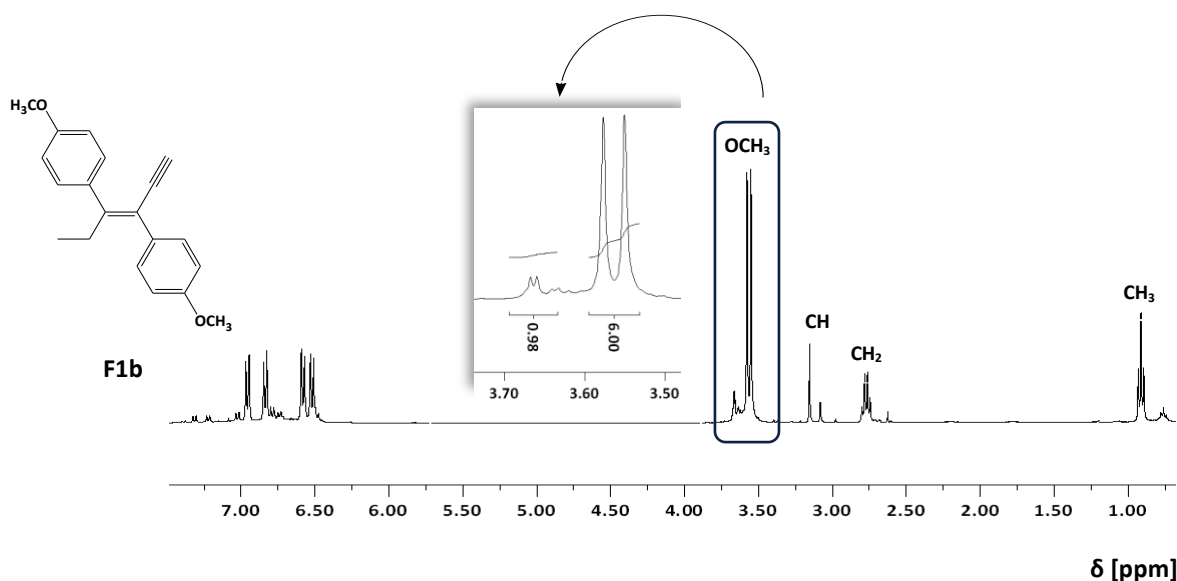


Figure 4.2. $^1\text{H-NMR}$ spectrum of **F1b**. Remarkd is the peak corresponding to the $-\text{OCH}_3$ signal in both isomer. The isomers ratio was 6 to 1 as shown in the detail.

It would be difficult to establish which of the isomers of **F1e** gives rise to the spectrum presented in Fig. 4.3 by inspection. The configuration of the olefins **F1a,e** was established performing using NOE (Nuclear Overhauser Effect) NMR experiments and determining which groups are closer together in space¹⁰⁴. In the spectrum, key signals were irradiated one by one and the remaining resonances were observed to assess whether there was an observable enhancement.

In the (*E*)-isomer, irradiation of the triplet CH_2 protons (belonging to the propyl group) would be expected to provide a NOE *enhancement* of both aromatic doublets $\text{H}_2\text{-H}_6$ and $\text{H}_2\text{-H}_6'$ and the vicinal proton (multiplet). In the (*Z*)-isomer, the same irradiation would be expected to provide an enhancement of only one aromatic doublet, the alkyne singlet and the multiplet of the vicinal proton. It was found that the major form present in the spectrum was the (*Z*)-configuration as shown in the Fig. 4.3 below.

4 Proton NMR and mass spectrometry analyses

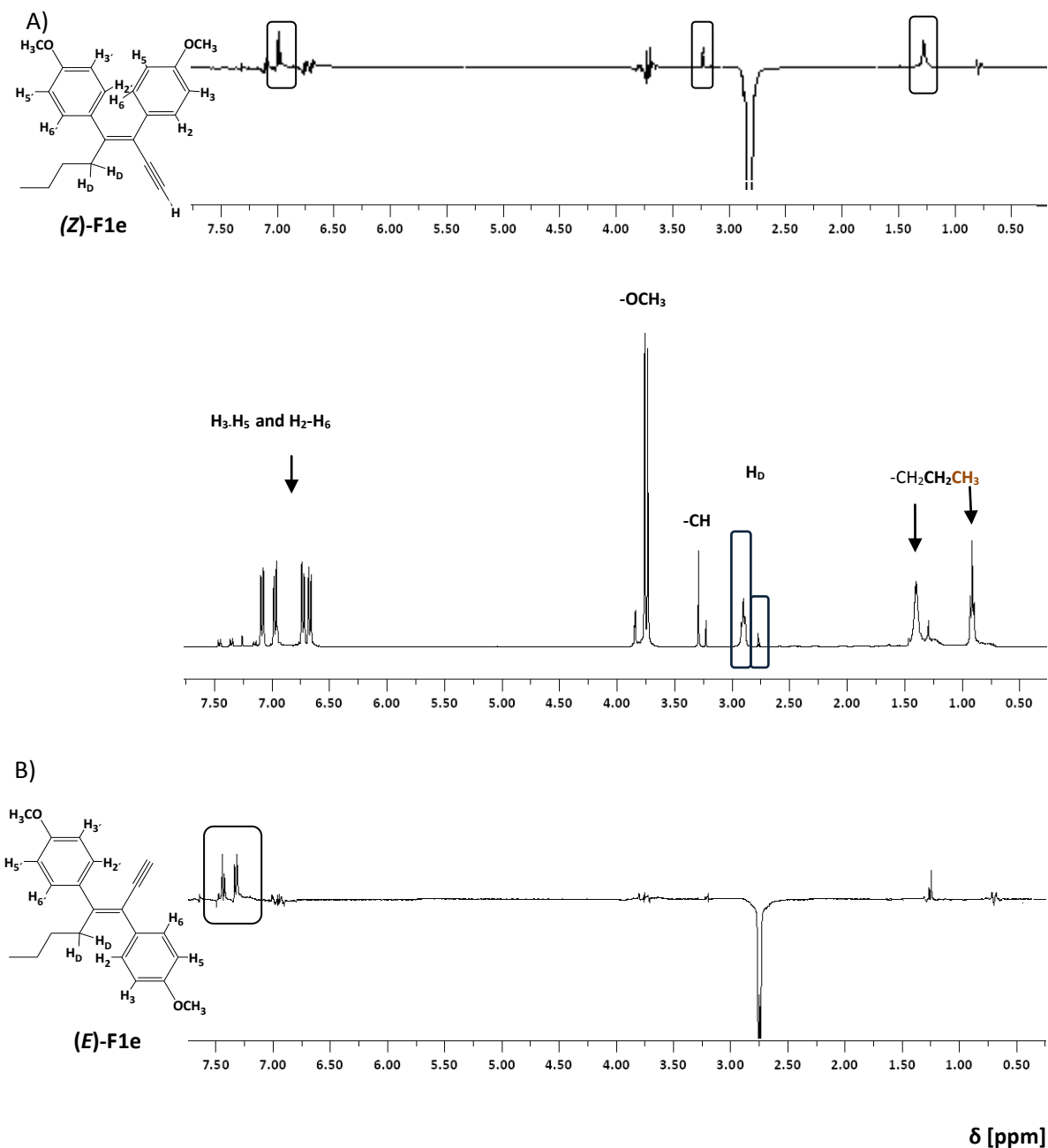


Figure 4.3. $^1\text{H-NMR}$ and NOE $^1\text{H-NMR}$ spectra of **F1e**. The assignment of the signals of the two different isomers was supported by NOE experiments taken in CDCl_3 . A) By irradiating the H_D at 2.87 ppm was measured a strong enhancement with the aromatic doublet at 6.94 ppm, with the CH proton of the alkyne group at 3.27 ppm and the vicinal proton (multiplet at 1.36 ppm). These confirm the (*Z*)-configuration. B) By irradiating the H_D at 2.76 ppm was measured a strong enhancement with both aromatic doublets (at 7.27 and 7.48 ppm), and the vicinal proton (multiplet at 1.26 ppm). These confirm the (*E*)-configuration.

Other confirmations of the structures of the ligands were obtained by mass spectra as well as elemental analyses CHN.

4.1.1 3,4-Diarylalkenyne Complexes with Dicobaltoctacarbonyl

As already described by Ott and co-workers⁶⁴, upon the coordination to cobalt the complete geometry of the alkyne was changed into a (*Z*)-alkene and this modification was documented by ¹H-NMR spectroscopy (see Fig. 4.4).

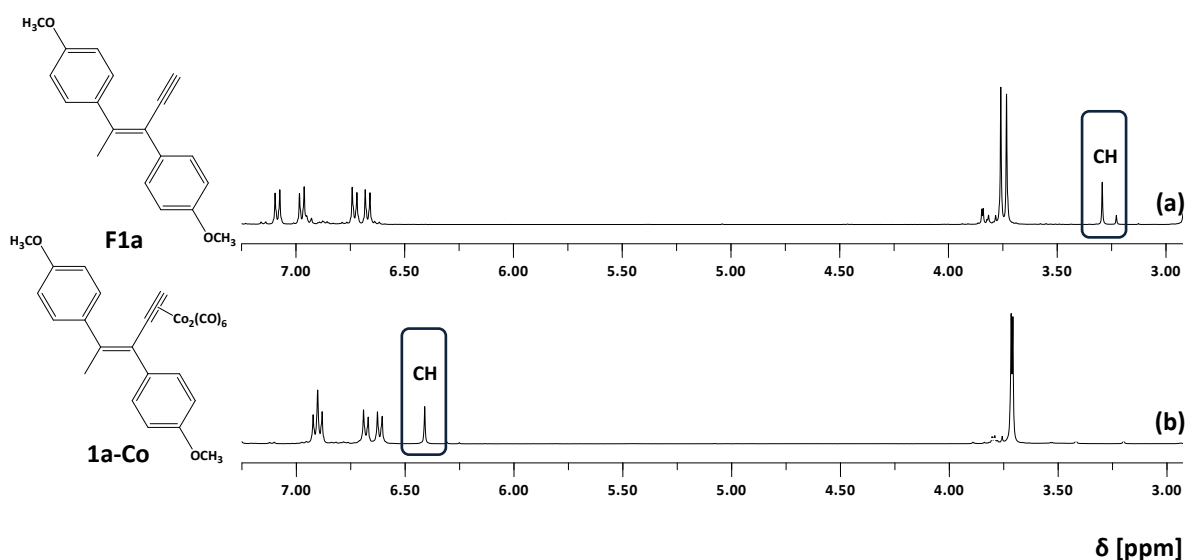


Figure 4.4. ¹H-NMR spectra of the ligands **F1a** (above) and **1a-Co** (below) in CDCl₃. Remarked are the peaks corresponding to the terminal hydrogen of the triple bond in both cases. This proton in **F1a** showed a chemical shift δ [ppm] of 3.29 against 6.41 in **1a-Co**.

It is noteworthy that a considerable downfield shift for the terminal hydrogen of the triple bond in the cobalt complexes could be observed. Furthermore, the metal cluster increased the lipophilicity of the molecules. Also the two aromatic doublets got closer-converged and appeared in the spectrum as a false triplet at 6.90 ppm. By thin layer chromatography (diethyl ether/ligroin 2:1) the separation of two spots corresponding to each isomer was visible. Other confirmations of the structures of the compounds were carried by EI (Electron Impact) mass experiments in which a very characteristic fragmentation consistent in a consecutive loss of CO ($m/z = 28$, see Fig 4.5.) was observed.

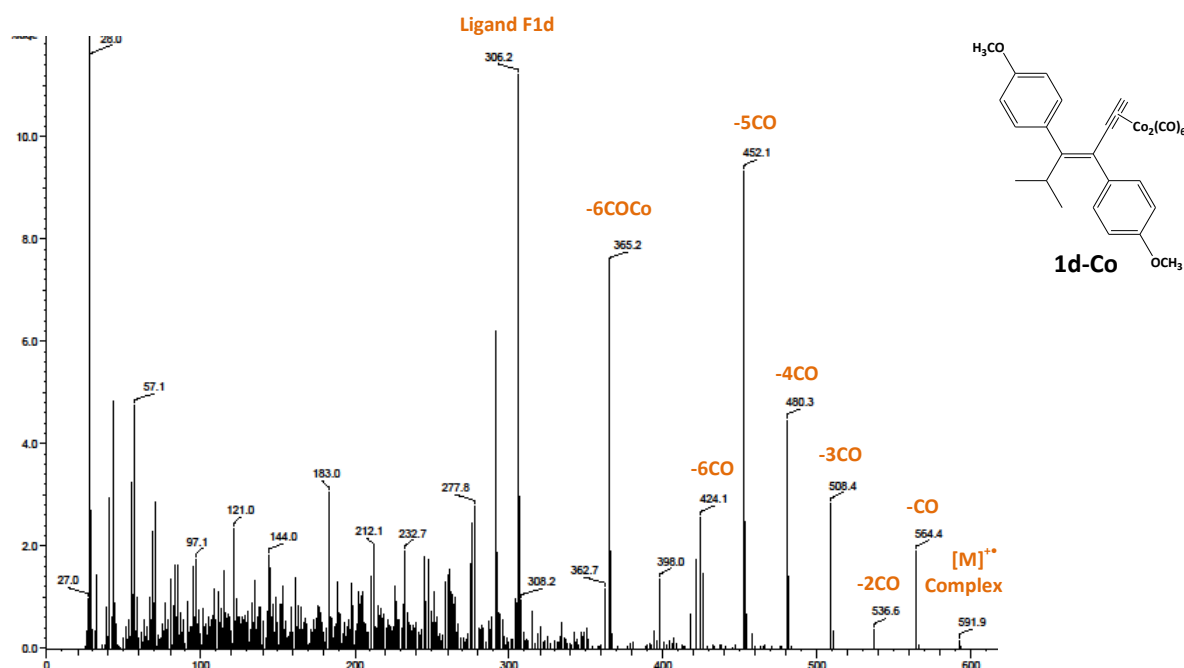


Figure 4.5. The mass spectrum of **1d-Co** shows the base peak at m/e 591.9 and the peaks relative to the consecutive loss of CO.

Elemental analyses of all presented (*E*)- and (*Z*)-isomers were within 0.4% of the calculated values and documented the high purity.

4.2 1,1,2-Triarylalkene Ligands

The geometrical identity of the triarylalkene ligands could be ascertained readily from $^1\text{H-NMR}$ spectra.

E2a, which was initially obtained as a mixture of (*E*)- and (*Z*)-isomer (Fig. 4.6 (a)) was further purified to give the desired (*Z*)-**E2a** compound (Fig. 4.6 (b)). Thus, its spectrum in CDCl_3 solution showed the CH_3 protons on the side chain as a triplet at 0.92 ppm and the CH_2 protons as a clean quartet at 2.44 ppm. As reported in the literature¹⁰⁵ the methoxy group at 3.67 ppm as well as the **AA'BB'** pattern for the disubstituted aromatic ring of the (*Z*)-isomer (that was more lipophilic, $R_f = 2.3$ cm against $R_f = 2.7$ cm, by thin layer chromatography with diethyl ether/ligroin 4:1) is substantially upfield (0.3 ppm) relative to the corresponding resonance in the (*E*)-isomer (see Fig. 6).

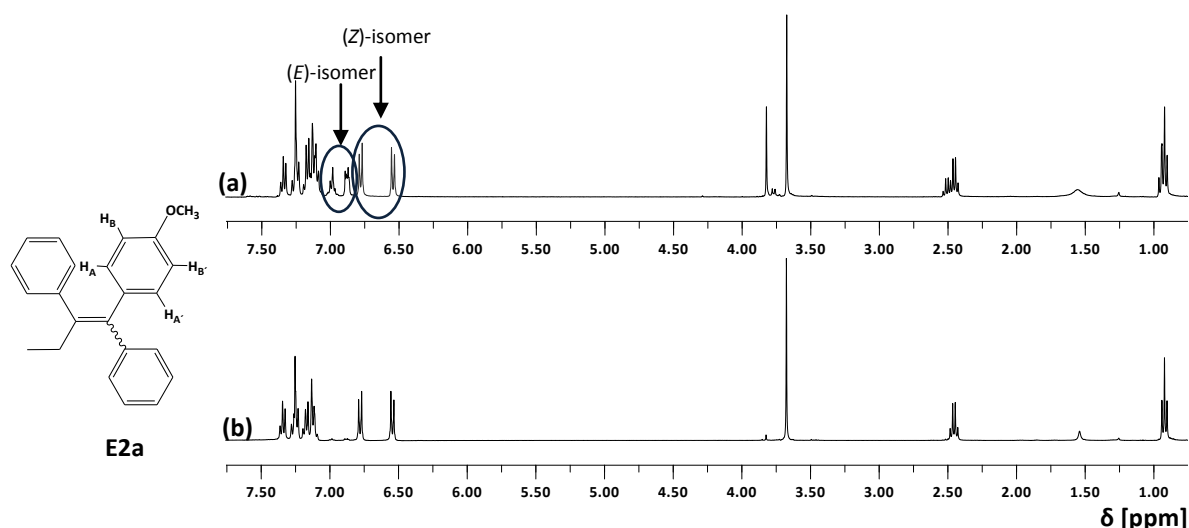


Figure 4.6. (a) The $^1\text{H-NMR}$ spectrum of the crude compound **E2a** exhibits aromatic protons as $\text{AA}'\text{BB}'$ systems in the range of 6.54-6.78 ppm, in contrast with the (*E*)-configuration that shows the same signals at 6.87- 7.02 ppm. (b) $^1\text{H-NMR}$ spectrum of the pure (*Z*)-**E2a** isomer.

The major isomer (*Z*)-**E2a** was isolated after crystallization, while the oil still contained the mixture of both isomers. In the mass spectra of **E2a** and **E2b** the peaks of molecular ions were observed at m/z 314 (100%) and 344 (100%) respectively.

4.2.1 Hydroxy-Substituted 1,1,2-Triaryalkene Ligands

The ether cleavage was complete and could be confirmed by the $^1\text{H-NMR}$ -spectra of **F2a** and **F2b** taken in DMSO. For example, compound **F2a** displayed a broad singlet at 4.15 ppm (-OH proton) with no absorption in the region at 3.67 ppm corresponding to the methoxy protons of the starting material **E2a**. The aromatic protons and ethyl protons remain visible at normal fields.

It is important to emphasize that the cleavage of the methoxy group by the pure (*Z*)-**E2a**, still led to a mixture of (*E*)- and (*Z*)-isomers, which could not be separated from each other. The downfield chemical shift for the protons on the di-substituted aromatic ring at 6.76 and 6.78 ppm was consistent with (*Z*)- stereochemistry which placed the protons of the $\text{AA}'\text{BB}'$ pattern relatively far from the region of positive shielding of the -OH group at 4.15 ppm.

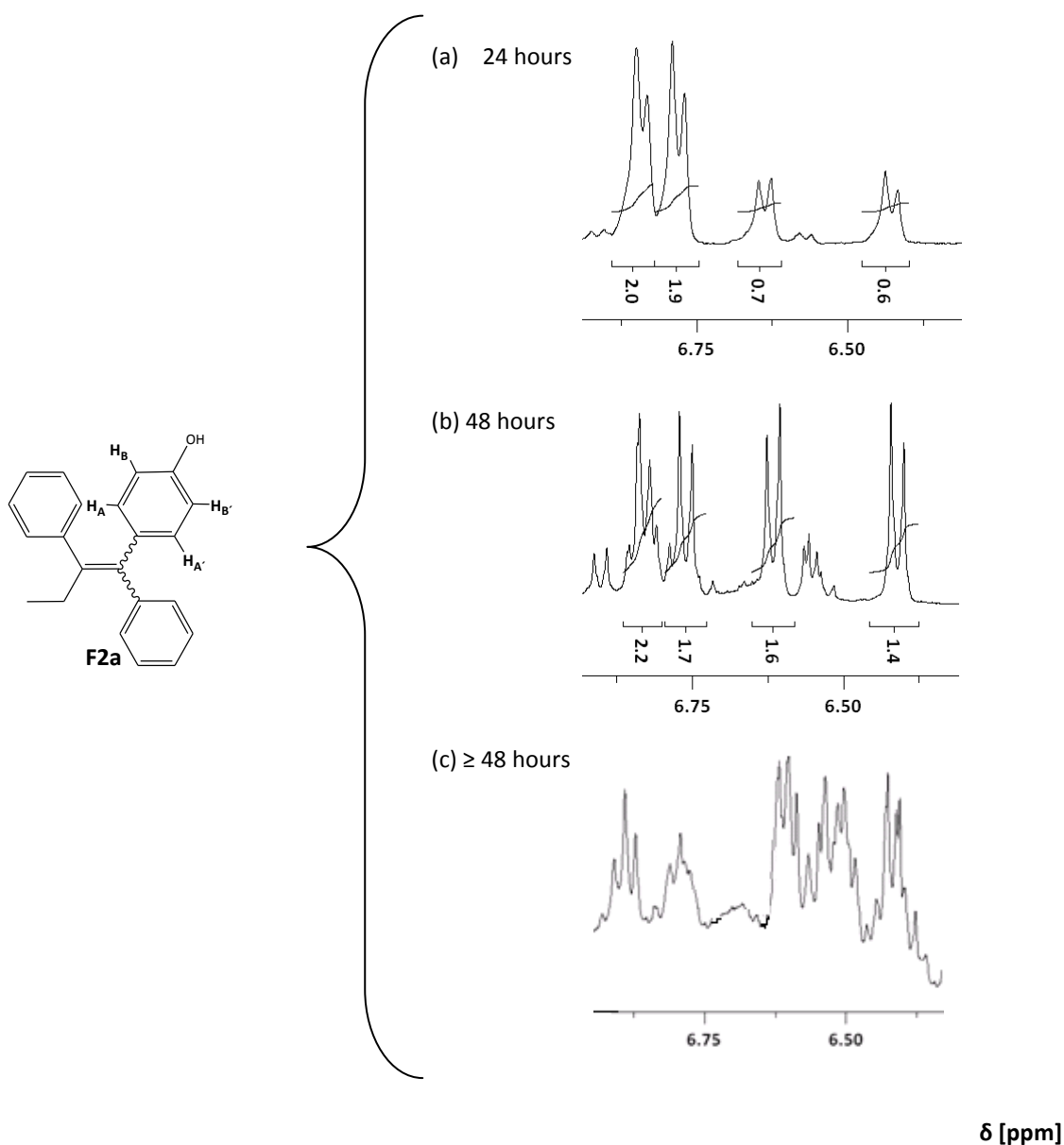


Figure 4.7. (a) Portion of the $^1\text{H-NMR}$ spectrum of the system $\text{AA}'\text{BB}'$ of **F2a**, which shows after 24 hours a 3:1 (*E*)-/(*Z*)- ratio; (b) portion of the $^1\text{H-NMR}$ spectrum of the system $\text{AA}'\text{BB}'$ of **F2a** between 24 and 48 hours; (c) portion of the $^1\text{H-NMR}$ spectrum of the system $\text{AA}'\text{BB}'$ of **F2a** after 48 hours.

By adjusting the conditions under which an isomers mixture is formed it was possible to establish kinetic control. The (*E*)-/(*Z*)-ratio depended on the reactions times: after stirring 24 hours the crude compound **F2a** had a 6:1 (*E*)-/(*Z*)-ratio; by stirring 48 hours the ratio became 1:1. Stirring for a longer period of time caused decomposition of the original molecule, probably by polymerization (not investigated further, see Fig. 4.7). In the mass spectrum of **F2a** and **F2b**, the base-parent peak was shown at m/z 300 and 316 respectively, while ele-

mental analyses were within 0.4% of the calculated values and documented the high purity of the compounds.

4.2.2 1,1,2-Triaryalkene Complexes with Zeise's Salt

The exchange of ethylene on the Zeise's salt by the olefin on the ring of **2c** could be documented by $^1\text{H-NMR}$ experiments (see Fig. 4.8). After the O-alkylation there still was a mixture of the two isomers of **2c**, which could not be separated. In its spectra the signals were strongly superimposed. Absorption of H_3 was a multiplet centered at 5.99 ppm, while H_1 and H_2 showed double doublets at 5.26-5.39 ppm. The coupling constant calculated for H_1 ($J= 10$ Hz) indicated that it was split *cis* by H_3 . On the other hand the constant of H_2 ($J= 17$ Hz) characterized a *trans* arrangement, according to the literature¹⁰⁶. In the spectrum of the complex **2c-PtCl₃** the signals broadened and did not split but shifted. In particular a chemical shift at upfield of H_3 (5.20 ppm) was observed, which can be explained as a result of weakening the character of the double bond under metal coordination. H_1 and H_2 signal shifted at 4.43 ppm, whereas H_4 and H_5 were showed at 4.13 and 4.64 ppm.

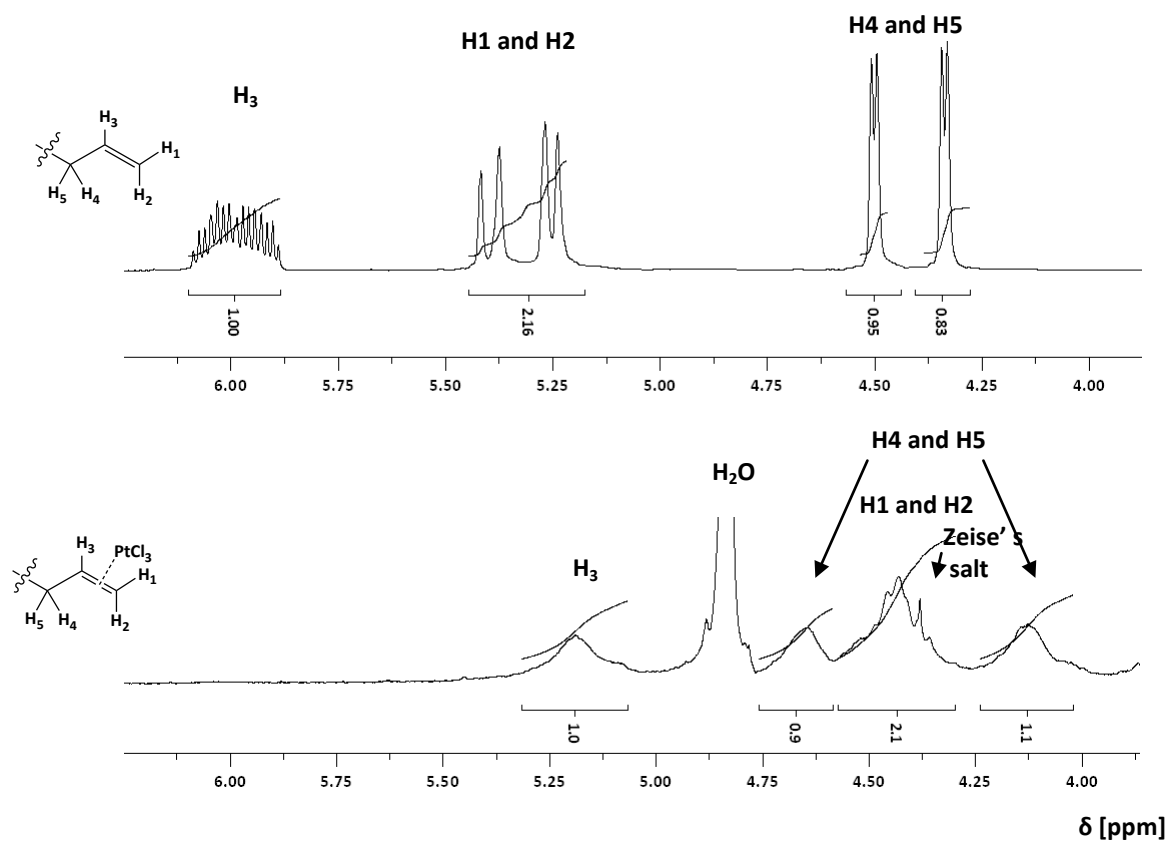


Figure 4.8. (a) ¹H-NMR spectrum taken in CDCl₃ of the aliphatic chain on the disubstituted aromatic ring of **2c**; (b) ¹H-NMR spectrum taken in CD₃OD of the aliphatic chain on the disubstituted aromatic ring of **2c-PtCl₃** upon coordination of the olefin to Zeise's salt.

To confirm the structure of the Zeise complexes, electrospray-ionization (ESI) in positive voltage mode was used. ESI is a mild ionization process and typically yields -quasi molecule ions- with little or no fragmentation. Characteristic for the complex **2c-PtCl₃** were $[M+K]^+ = 718$ in positive mode and $[M-H]^+ = 641$ in negative mode.

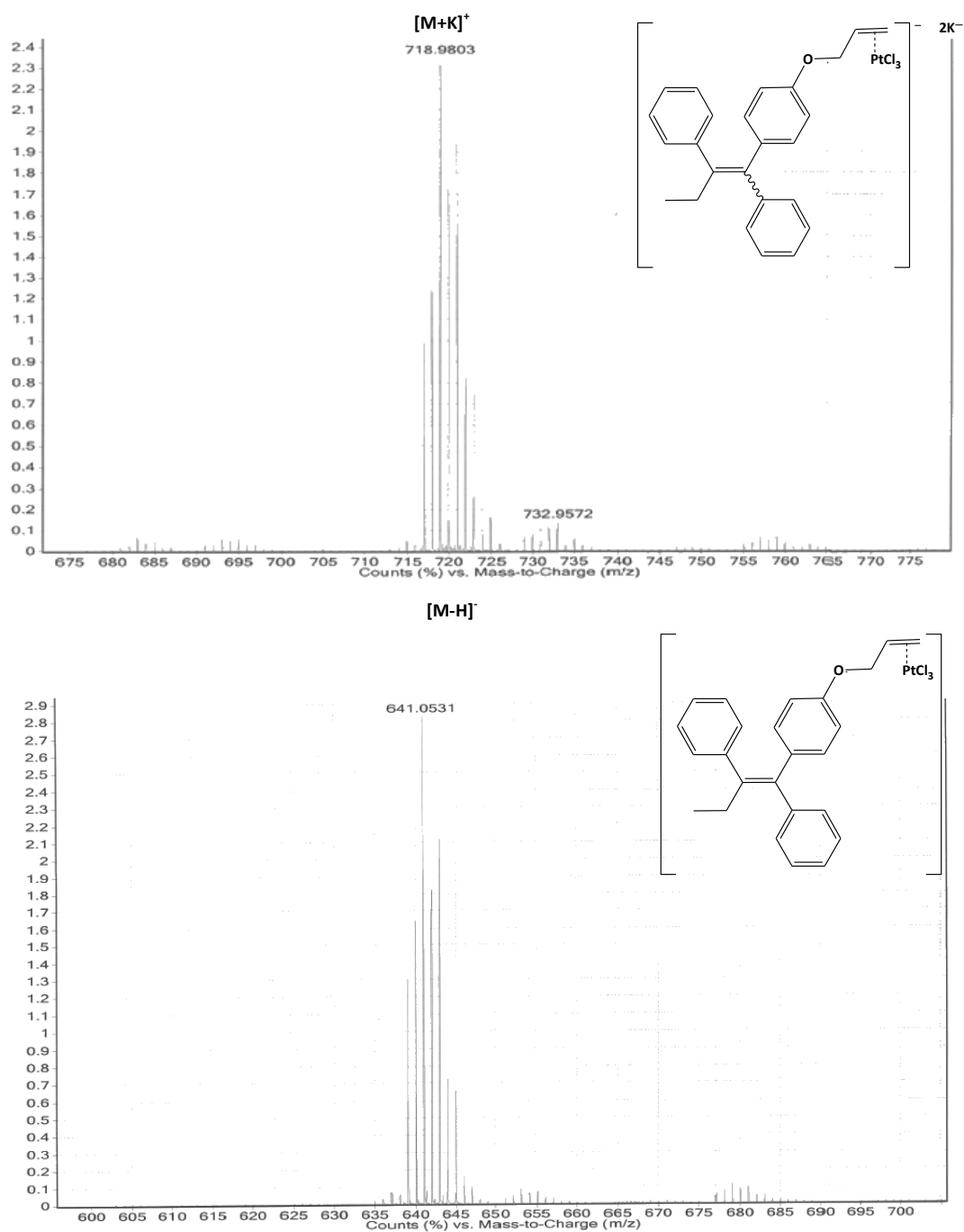


Figure 4.9. ESI-MS spectrum of the complex **2c-PtCl₃**. The molecular structure of the complex is shown in the insert.

5 Pharmacological Evaluation

5 Pharmacological Evaluation

The majority of breast cancer research is conducted using established breast cancer cell lines as *in-vitro* models, since they are easy to handle and represent an unlimited self-replicating source that can be grown in almost infinite quantities. In addition, they exhibit a relatively high degree of homogeneity and are easily replaced from frozen stocks if lost through contamination¹⁰⁷. However, the problem with in the *in-vitro* testing is the marked genetic instability of tumor cells entailing an extreme clonal variation, which increases with a growing number of passages^{108,109}. Sets of instructions have to be followed to reduce errors occurring during analytical procedures and ensure accurate evaluations.

5.1 Cell Lines Used

5.1.1 MCF-7 (hormone dependent cancer cell line)

The human breast cancer cell line MCF-7 was derived at the Michigan Cancer Foundation (MCF) in the early 1970s from a pleural effusion of a 69-year-old woman with metastatic (infiltrating ductal carcinoma of the breast) breast cancer¹¹⁰. This cell line has retained several characteristics that are particular to mammary epithelium, including the ability to grow as a monolayer, forming domes and responding to hormones. MCF-7 cells are shown to be ER-positive (70 - 90 fmol/mg protein)¹¹¹, in particular ER α represents the largely predominant form, while ER β is not present at high concentration^{112,113}. They further have a basal level of COX-1 and a barely detectable and transient COX-2 inducible expression¹¹⁴.

5.1.2 MDA-MB-231 (hormone independent cancer cell line)

MDA-MB-231 is a breast cancer cell line, derived from a metastatic carcinoma, obtained from a 51-year-old patient in 1973. Among other characteristics, this cell line is ER-negative and shows a low expression of COX-1, but a constitutive level of COX-2.

5.1.3 MCF-7-2a and U2-OS/ α , β

The MCF-7-2a cell line was obtained from ER-positive MCF-7 cells stably transfected with the ERE_{wtc}luc plasmid¹¹⁵. ERE_{wtc}luc, is a DNA sequence which contains the ERE (estrogen response element) of the DNA as enhancer sequence and the reporter gene *luc*, which encodes for luciferase enzyme.

Cell line U2-OS, formerly known as 2T cell line, was derived from a 15-year-old girl with a moderately differentiated osteogenic sarcoma of the tibia (shinbone). The cultures were started in 1964 from a non-necrotic intraosseous part of the tumor (2T) obtained at the time of amputation of the left leg. The patient died 8 months after the operation of widespread metastases¹¹⁶.

U2-OS/ α , β cells were transiently transfected with the plasmid pSG5-ER α (U2-OS/ α) or pSG5-ER β FL (U2-OS/ β) together with the reporter plasmid p(ERE)₂-luc⁺.

5.2 *In-Vitro* Chemosensitivity Assay

In accordance with established procedures^{117,118}, the synthesized compounds and the antitumor drug cisplatin were evaluated for growth inhibition and antiproliferative effects on cultured breast cancer cell lines MCF-7 and MDA-MB-231.

The *in-vitro* testing was carried out on exponentially dividing cells of the above mentioned lines. The technique enables the overall growth curves of cells by large scale spectrophotometric measurement and can be briefly described as follows:

- The human cell lines were grown in monolayer culture (culture conditions: culture medium, 37 °C, 5 % CO₂, humidified atmosphere).
- A cell suspension (at defined density) at 7700 cells/ml culture medium (MCF-7) and at 3200 cells/ml (MDA-MB-231), respectively was transferred to 96-well microtiter plates (100 μ l per well) and cultivated for 3 days.
- Addition of a solution containing the test compounds in various concentrations (solvent: DMF). Sixteen wells were used for each test concentration and for the control, which contained the corresponding amount of DMF.

- After the proper incubation time of 4 (plate representing t_0 used for the determination of the initial cell biomass) to 7 days, the medium was removed and 100 μ l of glutardialdehyde solution (0.5 ml of glutardialdehyde +12.5 mL of phosphate-buffered saline (PBS), pH 7.4) was added for fixation. The plates are stored at 4 °C under phosphate buffered saline (PBS) (180 μ l).
- Cells were stained with a 0.02 M solution of crystal violet (100 μ l) for 30 minutes. To remove the excess stain, cells were washed several times with water.
- Plates were incubated on a softly rocking rotary shaker with 180 μ l of ethanol (70%) for 3 hours. A microplate autoreader (FLASHscan S12) at 590 nm was used to measure the optical density of each well.
- The mean absorption of the initial cell biomass plate was subtracted from the mean absorption of each experiment and control. The corrected control was set to 100%.

The method is very simple and reproducible and provides in short time large sets of data about the activity of potential anticancer drugs. The effectiveness of the compounds is expressed as corrected T/C_{corr} (%) or τ (%) values according to the following equations:

$$\text{Cytostatic effect: } \frac{T}{C_{\text{corr}}} (\%) = \frac{T - C_0}{C - C_0} \times 100 \quad \text{Eq. 1}$$

$$\text{Cytocidal effect: } \tau (\%) = [(T - C_0)/C_0] \times 100 \quad \text{Eq. 2}$$

where T (test) and C (control) are the optical densities values at 590 nm of the crystal violet extract of the cells in the wells (i.e. the chromatin bound crystal violet extracted with ethanol 70%), measured at the time of test end, and C_0 is the density of the cell extract immediately before treatment (at the time of compound

addition)¹¹⁹. The solvent, employed in equal concentration to prepare all compound solutions, is used as a control or blank.

In case of a cytotoxic effect, the density of cell extract in the test system is lower than in the control system and the effect has to be calculated directly from the density of cell extract at $t = 0$ (C_0) (Eq. 2).

The calculated T/C_{corr} and τ values can be interpreted as follows:

$T/C_{corr} > 80\%$	no antiproliferative effect
$80\% > T/C_{corr} \geq 20\%$	antiproliferative effect
$20\% > T/C_{corr} > 0\%$	cytostatic effect
T/C_{corr} or $\tau < 0\%$	cytotoxic effect

In this work, every negative influence produced by a compound on the rate of growth of the cells is called “cytotoxic effect”. The T/C_{corr} values usually represent the maximum inhibitory effects of the test compounds.

5.2.1 Growth Inhibitory Effects on MCF-7 and MDA-MB-231

The IC_{50} value is commonly used as a measure of the drug potency, which is the drug concentration (or dose) inducing a 50% decrease in the maximum effect (response, in this case inhibition of cell growth).

The *in-vitro* chemosensitivity assay uses a concentration-effect model based on a Boltzmann fit (OriginPro 8), which simulates a sigmoidal curve. The IC_{50} value was determined by interpolation from the curve (in logarithmic scale) of the compounds, and it was represented by the inflection point on the curve. The mean and standard deviation for the replicate IC_{50} values were calculated for each determination (two or three independent experiments). The IC_{50} values for all ligands and complexes up to a concentration of 20 μ M, after a period of drug exposure of 96 hours, were measured for a preliminary large-scale screening in a “two-concentrations” assay. Higher values of IC_{50} were expressed as $IC_{50} > 20$ μ M, assuming that the compound is not cytotoxic in the tested range of concentrations. Consequently, only for the substances that were cytotoxic in this test ($IC_{50} \leq 20$ μ M) a time- and concentration- dependent cytotoxicity assay was performed to provide unambiguous information concerning differential sensitivity. For

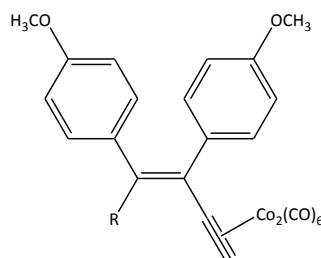
each complex five times of incubation (48, 72, 96 120, and 144 hours) and five different concentrations (ranging from 10 to 1.25 μM) were tested.

5.2.2 Determination of the Antiproliferative Activity

IC_{50} values of all the synthesized compounds and cisplatin were determined after 72 hours of incubation. Cisplatin, which was used as reference, characteristically reduced the cell growth of MCF-7 ($\text{IC}_{50} = 2.6 \pm 1.1 \mu\text{M}$) and MDA-MB-231 ($\text{IC}_{50} = 5.4 \pm 0.9 \mu\text{M}$) cells.

5.2.2.1 3,4-Diarylalkenyne Derivatives

The IC_{50} values of the 3,4-diarylalkenyne hexacarbonyl dicobalt complexes **1(a-e)-Co** and **1(a'-e')**-Co are shown in Table 5.1 and Table 5.2, respectively.

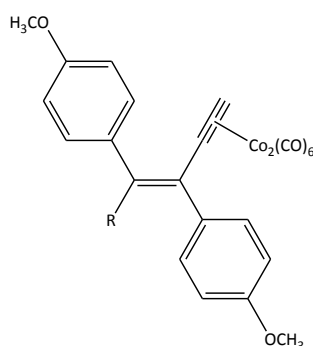


Nr	R	$\text{IC}_{50} [\mu\text{M}]^{[h]}$	
		MCF-7	MDA-MB-231
1a-Co	CH_3	6.9 ± 2.6	2.8 ± 0.7
1b-Co	C_2H_5	7.2 ± 1.1	4.1 ± 1.4
1c-Co	C_3H_7	7.9 ± 0.8	4.6 ± 0.2
1d-Co	$\text{CH}(\text{CH}_3)_2$	12.6 ± 2.4	6.2 ± 1.2
1e-Co	C_4H_9	24.6 ± 3.1	5.4 ± 1.6

Table 5.1. (Z)-3,4-diarylalkenyne hexacarbonyl dicobalt complexes, IC_{50} in $\mu\text{M}/\text{l}$.

^[h] Values represent the mean \pm SD of two or three independent determinations.

The growth inhibitory effects depended on the presence of the metal cluster (all the ligands were inactive with an $IC_{50} > 50 \mu M$). The five complexes revealed an antiproliferative effect on both cell lines, which increased in the following order **1e-Co** < **1d-Co** < **1c-Co** < **1b-Co** < **1a-Co**. The difference in antitumor potency depended on the length of the alkyl chain. In the MDA-MB-231 cell line, the complexes **1(a-c)-Co** were more active than cisplatin ($IC_{50} < 5 \mu M$), in particular **1a-Co** possessed a strong inhibitory potency ($IC_{50} = 2.8 \mu M$). **1d-Co** and **1e-Co** were somewhat less active ($IC_{50} = 6.2$ and $5.4 \mu M$), but their activity still remained similar to that of cisplatin. In MCF-7 cells **1(a-c)-Co** caused only a weak inhibitory effect ($IC_{50} = 6.9 \mu M$, $7.2 \mu M$, respectively), while **1d-Co** and **1e-Co** were only marginally active, indicating a selectivity for MDA-MB-231 cells. Their selectivity is linked to the presence of a long alkyl chain: compound **1e-Co**, which is substituted with a butyl chain, increased the selectivity of about five fold.



Nr	R	$IC_{50} [\mu M]^{[i]}$	
		MCF-7	MDA-MB-231
1a'-Co	CH ₃	10.7 ± 1.9	13.1 ± 2.6
1b'-Co	C ₂ H ₅	13.5 ± 1.3	4.5 ± 0.5
1c'-Co	C ₃ H ₇	14.9 ± 1.6	5.9 ± 1.2
1d'-Co	CH(CH ₃) ₂	17.6 ± 1.0	7.2 ± 1.1
1e'-Co	C ₄ H ₉	27.2 ± 2.8	8.4 ± 2.3

Table 5.2. (*E*)-3,4-diarylalkenyne hexacarbonyl dicobalt complexes, IC_{50} in $\mu M/l$.

^[i] Values represent the mean ± SD of two or three independent determinations.

The change of configuration of the complexes from (*Z*) to (*E*) decreased the growth inhibitory effects. At MCF-7 the IC_{50} values of **1a'-Co** to **1d'-Co** is 2 fold higher than that determinate with the (*Z*)-configuration congeners. The cytotoxicity of **1b'-Co** to **1d'-Co** at MDA-MB-231 is comparable to **1b-Co** to **1d-Co**, while **1a'-Co** is distinctly less active (IC_{50} = 13.1 μ M, IC_{50} (1a-Co) = 2.8 μ M). Nevertheless, it has to be mentioned that **1b'-Co** and **1c'-Co** reached the activity of cisplatin at MDA-MB-231 cells (IC_{50} = 4.5 μ M, IC_{50} = 5.9 μ M, respectively).

A single-end-point determination like the IC_{50} determination does not give exact information about the differential sensitivity of the compounds. Thus, we performed time-dependent experiments at the two cell lines. As reference the time-dependent curves of cisplatin are shown in Fig. 5.1.

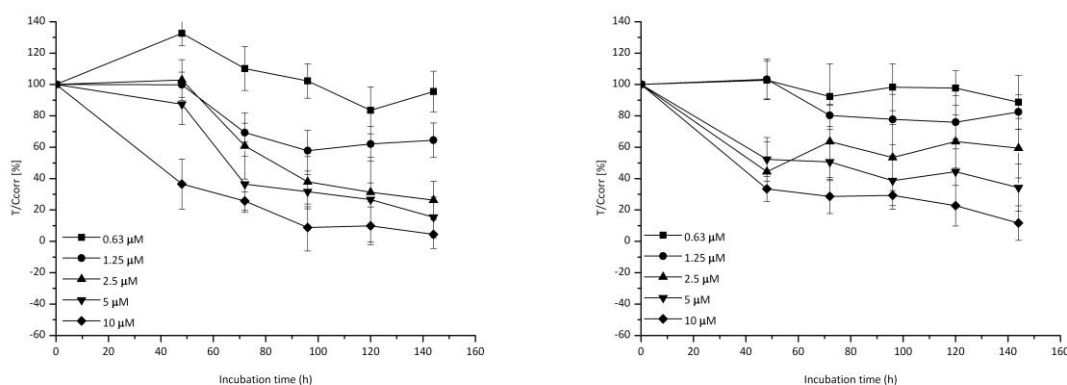


Figure 5.1. Time-activity curves of the antiproliferative effect of cisplatin on human MCF-7 (left) and MDA-MB-231 (right) breast cancer cell lines, at concentrations ranging from 1.25 to 20 μ M.

Comparing the time-activity curves of the complexes **1c-Co**, **1c'-Co** and cisplatin, the onset of antiproliferative effect of **1c-Co** in MDA-MB-231 cells was observed much earlier. After an incubation time of 48 hours, the complex showed cytotoxic effect at 20 μ M, whereas at 10 μ M its antiproliferative effect is comparable to cisplatin (see Fig. 5.2). The time over activity (T/C_{corr}) correlation, indicated a minimal T/C_{corr} (maximum of growth inhibition) which remained constant or increased only slowly during the test period. On the contrary, cisplatin reached its maximum effect toward the end of the test (see Fig. 5.1).

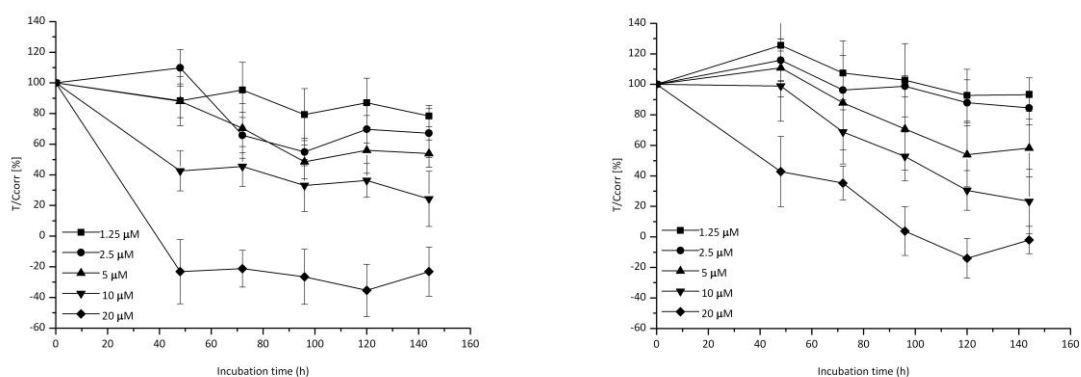


Figure 5.2. Time-activity curves of the antiproliferative effect on human MDA-MB-231 breast cancer cell line of **1c-Co** (left) and **1c'-Co** (right), at concentrations ranging from 1.25 to 20 μM .

Exploring the time-response curves of these complexes at MCF-7 cells, they showed a cisplatin-like curve reaching the maximum effect towards the end of the test (see Fig. 5.3). By comparing the two curves we can also confirm the correlation between inhibitory potency and the configuration of the complex. Namely the (*Z*)-configuration of **1c-Co** increased the activity against MCF-7 compared to its (*E*)-configuration **1c'-Co**. In MDA-MB-231 cells, the configuration of the compounds seemed to play the same role, yielding nearly identical results (data were shown in Fig. 5.2).

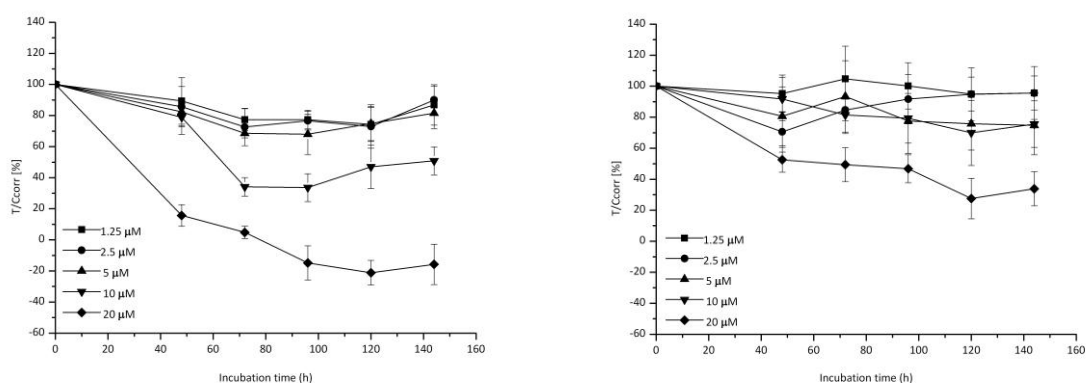


Figure 5.3. Time-activity curves of the antiproliferative effect on human MCF-7 breast cancer cell line of **1c-Co** (left) and **1c'-Co** (right), at concentrations ranging from 1.25 to 20 μM .

Another example of the time-response curve at MDA-MB-231 is shown in Fig. 5.4. **1a-Co** showed a maximum of activity after 48 hours, which is held during the whole time of incubation. Notwithstanding, its isomer **1a'-Co** showed an atyp-

ical time-activity curve, in which a fast onset of proliferation after a rapid reduction of the cell growth was observed. We assume that the cell population recovers after the initial damage.

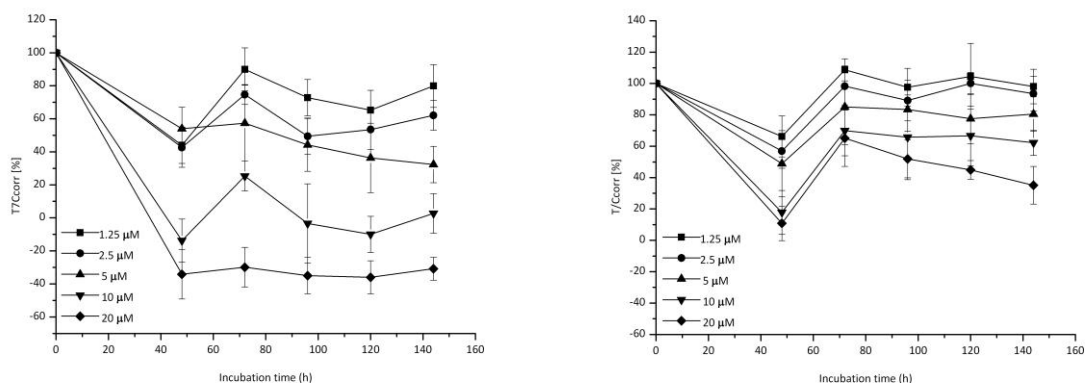


Figure 5.4. Time-activity curves of the antiproliferative effect on human MDA-MB-231 breast cancer cell line of **1a-Co** (left) and **1a'-Co** (right), at concentrations ranging from 1.25 to 20 μM .

The explication of the rising growth curve can be the development of drug resistance, in fact exponential cell growth is guaranteed for at least 250 hours of incubation.

The time-response curves for all other complexes are presented in the Appendix.

5.2.2.2 1,1,2-Triarylalkene Derivatives

In the group of the 1,1,2-triarylalkene derivatives (in Table 5.3), the ligands possessed only a weak growth inhibitory activity as shown in Fig. 5.5.

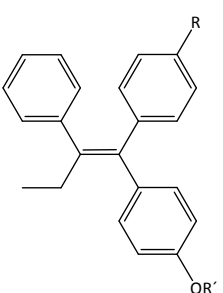
Structure	Ligand	R	R'
	2a	H	-CH ₂ -C≡CH
	2b	-OCH ₂ -C≡CH	-CH ₂ -C≡CH
	2c	H	-CH ₂ -CH=CH ₂
	2d	-OCH ₂ -CH=CH ₂	-CH ₂ -CH=CH ₂

Table 5.3. Main structure of the 1,1,2-triarylalkene compounds and substitution pattern of **2a**, **2b**, **2c** and **2d**.

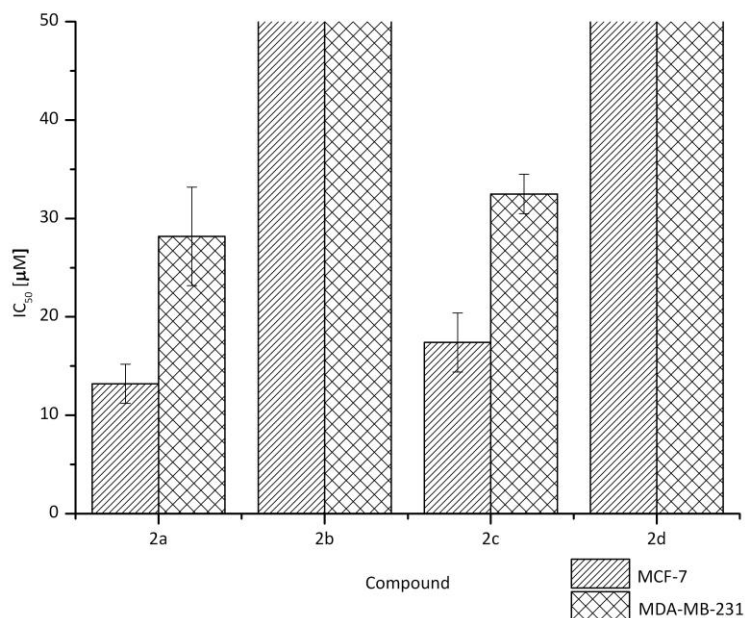


Figure 5.5. IC₅₀ values of triphenylalkene ligands **2a**, **2b**, **2c** and **2d** at MCF-7 (left) and MDA-MB-231, respectively.

Only **2a** and **2c** showed a somewhat higher activity (IC₅₀ = 13.2 μM, IC₅₀ = 17.4 μM, respectively) in MCF-7 cells, but weak activity in MDA-MB-231 (IC₅₀ =

28.2 μM , $\text{IC}_{50} = 32.5 \mu\text{M}$, respectively) indicating two-fold selectivity for MCF-7 cells (Fig. 5.5). Thus, **2a** reached its maximum inhibitory effect after 96 hours, while for **2c** achieved its maximum within 48 hours. After a prolonged time of exposure the growth inhibition did not show a recuperation of the tumor cells and remained constant (see Fig. 5.6).

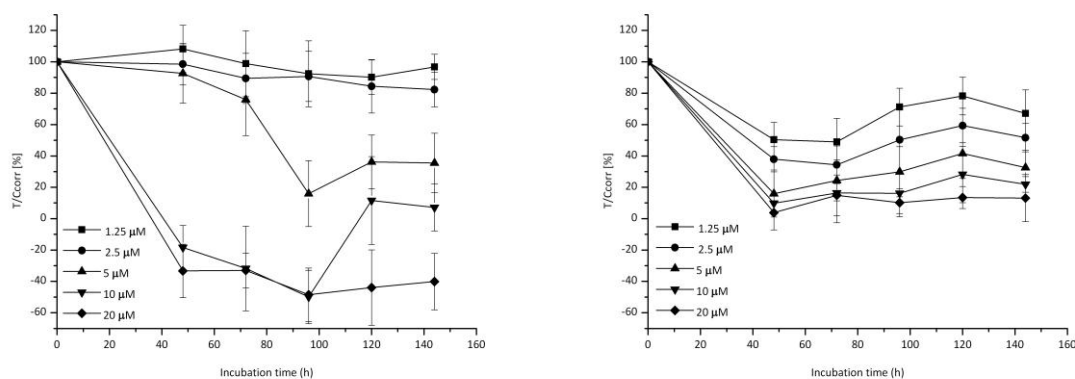


Figure 5.6. Time-activity curves of the antiproliferative effect of **2a** (left) and **2c** (right) on human MCF-7 breast cancer cell line, at concentrations ranging from 1.25 to 20 μM .

Further modifications, like additional alkyl groups at the phenyl moiety, led to compounds with any influence in the tumor cell growth. Hence, in **2b** and **2d** the inhibitory effect in both cell lines decreased drastically ($\text{IC}_{50} > 20 \mu\text{M}$). The complexes **2a-Co**, **2b-Co**, **2c-PtCl₃** and **2d-PtCl₃** did not present inhibitory effects on the growth of MCF-7 and MDA-MB-231 cells. IC_{50} values for these compounds were not presented.

5.3 Luciferase Assay

The *in-vitro* luciferase assay system in MCF-7-2a and U2-OS/ α,β cells can give a prediction over the possible estrogenic and antiestrogenic properties of the synthesized compounds. In molecular biological studies, luciferase is one of the most commonly used gene reporter, applied to study cellular gene expression and gene regulation. In particular, the luciferase gene, cloned from the firefly *Photinus pyralis*, is found to be a good bioluminescent reporter. This gene encodes for firefly luciferase, a monomeric enzyme (61 kD), that is commonly used because of its enzyme activity closely coupled to protein synthesis; when the expression of luciferase gene (*luc*) is promoted, the protein obtained (Luciferase) can be detected *in vitro* (cellular extracts) by its produced light.

The photon emission is achieved through oxidation of beetle luciferin in a multi-step reaction that requires ATP, Mg^{2+} and O_2 (Fig. 5.7). In the first step, the activation of the protein produces a reactive mixed anhydride intermediate. In the subsequent step, the luciferyl-AMP intermediate reacts with oxygen to create a transient dioxetane, which breaks down to the oxidized product oxyluciferin. As a result, a flash of light is generated¹²⁰ that rapidly decays over about 15 seconds after the addition of substrate to the enzyme.

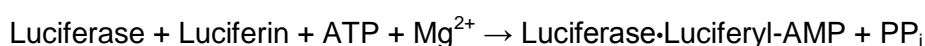


Figure 5.7. Two-step chemiluminescent reaction catalyzed by luciferase¹²⁰

Under conventional reaction conditions the enzyme turns over very slowly. A Promega kit that contains coenzyme A (CoA) is used to increase the turnover and yield maximal luminescence intensity that can be maintained for at least 60 seconds¹²¹.

The maximum of the luciferase expression with the stably transfected cells MCF-7-2a and U2-OS is reached after 48 hours of culture. Consequently after 50 hours the cells are destroyed by a lysis buffer. The produced light is measured in relative light units (RLU) with a luminometer (390 - 520 nm) and it is performed for 10 seconds (sensitive range of the luminometer). The wavelength of the emit-

ted light ranges from 490 to 630 nm¹²². Luciferase was assayed using the Promega luciferase assay reagent.

An active substance exerts its effects by binding to the ligand binding domain (LBD) of the ER. As a consequence it induces a conformational change in the ER, which dimerizes as homodimers (ER α /ER α). The hormone-receptor complexes bind to the EREs present in the plasmid and lead to the expression of luciferase, which correlates well with the estrogenic potency of the active substance^{123,124}.

5.3.1 Estrogenic Activity

The agonistic potency is estimated by determining whether and how much the stimulation of luciferase expression is induced by the test substances depending on their concentration. Therefore, the MCF-7/2a and U2-OS/ α,β cell lines are incubated with seven concentrations of each compound (range from 10^{-11} to 10^{-5} M), as well as the pure solvent as background and estradiol (10^{-8} M) as positive control. The assay terminates by determining the luciferase activity (RLU). Finally, the RLU-values are correlated with the quantity of protein (quantified according to Bradford¹²⁵) of each sample with the mass of luciferase. Estrogenic activity is expressed as percentage activation and was calculated in relation to luciferase expression of a 10^{-8} M estradiol control (100%) and based on pure solvent background (0%). In order to compare the potential agonistic effect of different compounds, usually two values are used, including the relative activation value at the concentration of 10^{-6} M and the EC₅₀ value, the compound concentration causing 50% relative activation.

5.3.2 Antiestrogenic Activity

To evaluate the antagonistic activity, MCF-7/2a and U2-OS/ α,β cells were incubated with a constant concentration of estradiol (10^{-9} M) in combination with increased concentrations of the test compounds (10^{-11} to 10^{-6} M). The concentration of the compound which is necessary to reduce the effect of estradiol of 50% is the IC₅₀ value, which is taken from the concentration activation curve¹²⁶.

5.3.2.1 3,4-Diarylalkenyne Derivatives

All the 3,4-diarylalkenyne derivatives and their corresponding dicobalt complexes were tested for agonistic and antagonistic effects at concentrations ranging from 10^{-11} to 10^{-6} M. All the compounds failed to evoke transcriptional activation of the luciferase gene. Based on the analyses of the crystal structure of the DES-ER α LBD complexes (see chapter 1.6, Fig. 1.6), it was found that a phenolic hydroxy group is a critical binding anchor of a ligand in the ER LBD. In contrast, methoxy groups drastically decreased the hormonal potency¹²⁷. This is probably the reason why 3,4-diarylalkenyne derivatives did not show transcriptional activity.

These compounds exert a strong cytotoxic effect in MCF-7 cells. Hence, we concluded that their antiproliferative effects did not result from an interaction with the ER.

5.3.2.2 1,1,2-Triarylalkene Derivatives

The 1,1,2-triarylalkene compounds are analogues of tamoxifen (TAM), an ER ligand displaying antagonistic properties in breast tissue and agonistic properties in the skeleton, uterus, and cardiovascular system¹²⁸. As prerequisite for this selective modulation of the ER a basic side chain located in the 4-position of the C1-phenyl ring is necessary.

Manipulation of the tamoxifen scaffold has been explored^{129,130}, but very few researchers have attempted to change the key side-chain $-O(CH_2)_2N(CH_3)_2$. The importance of the nitrogen atom¹³¹ was discovered by experiments in which the substituents on the alkyl amine were modified. That led to a decrease of antiestrogenicity. In order to diminish the basicity of the amine substitutions were attempted, e.g. replacing the alkylamino side-chain with N-oxides, quaternary salts, or by adding fluorinated to tethers. All of these modifications weakened antiestrogenic potency. The cause is to search on the reduction of ability of the nitrogen atom to form hydrogen bonds. Only the substitution of the amino side-chain by a carboxylic acid entity, which may interact with Asp 351 of the ER α LBD, led to an increase of antiestrogenic activity¹³².

In subsequent studies it was found that replacement of the aminoalkoxy group in TAM by a non-basic group, led to compounds more active than tamoxifen¹³³. On the basis of these facts, we introduced an alkyl group (propargyl group

= **2a**; allyl group = **2c**) in this position and in the 4-position of the C2-phenyl ring (propargyl group = **2b**; allyl group = **2d**) and evaluated the ER subtype (ER α or ER β) selectivity on the molecular level in stably transfected MCF-7/2a and transiently transfected U2-OS/ α,β cells. Furthermore, we investigated the ability of cobalt to influence estrogenic potency.

All the triarylalkene ligands did not show agonistic or antagonistic properties. Because of the high activity of the **2a** and **2c** in the hormone-dependent MCF-7 cell lines and their lack of ability to antagonize the effects of estradiol (E2), an antiestrogenic mode of action seems rather improbable.

In contrast, the complexes **2a-Co** and **2b-Co** were able to induce luciferase expression (see Fig. 5.8). The Co₂(CO)₆ unit appeared to be essential for the estrogenic activity. Others have also reported the importance of the hexacarbonyl dicobalt moiety for estrogenic action⁶⁵ (see chapter 1.7.2).

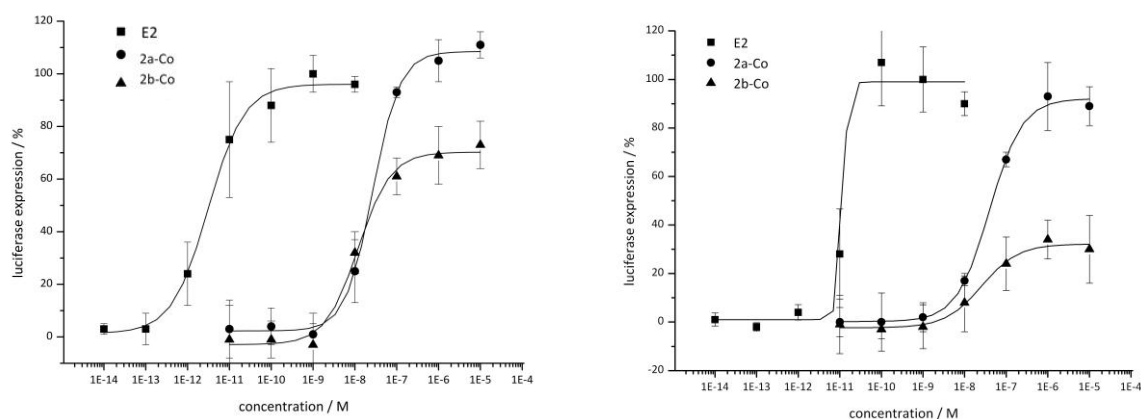


Figure 5.8. Activation-concentration curves of 1,1,2-triarylalkene hexacarbonyl dicobalt complexes **2a-Co**, **2b-Co** and estradiol **E2** at U2-OS/ α (left) and U2-OS/ β cells (right). The curves are representative examples of a single determination performed in quadruplicate.

2a-Co and **2b-Co** showed the highest potency in U2-OS/ α (EC_{50} = 27 nM and EC_{50} = 1.2 nM, respectively) and in U2-OS/ β (EC_{50} = 40 nM and EC_{50} = 2.5 nM, respectively). Interestingly, in MCF-7/2a cells they were only marginally active (data not shown).

This data can be explained as a result of a greater sensitivity of the U2-OS cells to hormones compared to MCF-7 cells. In fact the transfection of the U2-OS with the ER expression plasmid leads to higher ER levels. On the contrary the stably transfected MCF-7 cells with the ERE_{wtc}luc reporter plasmid do not re-

respond to ER stimulation despite ER binding and are therefore less sensitive to hormones. The observation that U2-OS cells are more sensitive than MCF-7 cells has been made before in our group¹³⁴.

Compound	U2-OS/ α		U2-OS/ β	
	IA ^[i] [%]	EC ₅₀ [nM]	IA ^[3] [%]	EC ₅₀ [nM]
E2	100 ± 7	0.004	100 ± 13	0.01
2a-Co	105 ± 8	27	93 ± 14	40
2b-Co	69 ± 11	1.2	34 ± 8	2.5

Table 5.4. Values were calculated as the mean of three independent experiments and SD < 20%.

As shown in Table 5.4 **2a-Co**, with only one alkyl substituent at the phenyl ring, presented transactivation at both ER α and ER β (full agonism). On the other hand, the introduction of a further substituent group at phenyl ring in **2b-Co**, decreased the estrogenic activity in ER α and led to marginal activity at ER β . Its low intrinsic activity (it did not reach the maximum effect) and its high potency (EC₅₀ = 1.2), suggested that **2b-Co** is a partial agonist. Probably the higher lipophilicity is responsible for diminishing the intrinsic activity, however the mechanism has remained elusive. The compounds did not display any anti-estrogenic activity.

Agonistic / antagonistic estrogenic effect is only one of the possible pharmacological evaluations. Further tests are necessary, in order to evaluate the pharmacological potential of these compounds.

^[i] IA = intrinsic activity.

5.4 Binding to COX-1 and COX-2

5.4.1 Cyclooxygenase Isoenzymes

As demonstrated in earlier studies^{135,136} a further possible target in cancer chemotherapy are the cyclooxygenase enzymes (COX-1 /2), also known as prostaglandin H synthase (PGH synthase). Prostaglandin E2 (PGE2) is a primary product of arachidonic metabolism and is synthesized via the cyclooxygenase and prostaglandin synthase pathways. PGE2 production is a commonly used method for the detection of COX-1 and COX-2 modulation and prostaglandin synthases. It was found that the COX-1 and COX-2 pathway, which convert arachidonic acid (hydrolytically liberated from membrane phospholipids) to PGH₂ (the precursor of prostaglandins PGs, tromboxanes and prostacyclins) (see Fig. 5.9), is involved in the development and growth of several different neoplastic lesions and is frequently overexpressed in invasive and *in situ* breast cancers cells¹³⁷.

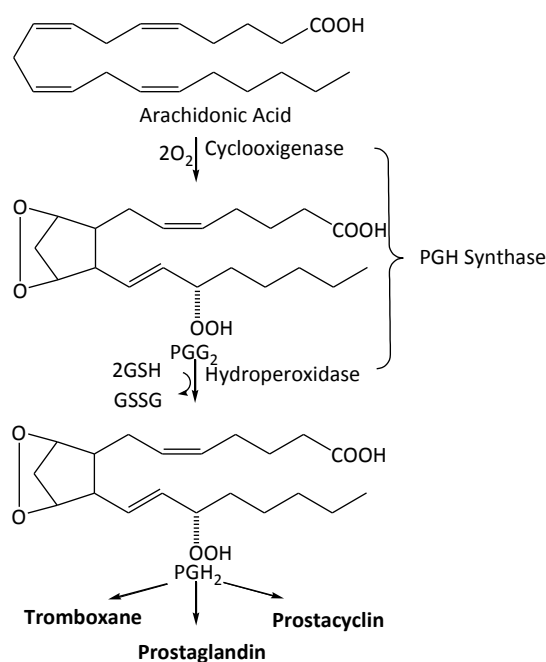


Figure 5.9. Conversion of arachidonic acid to prostaglandin¹³⁸. COX catalyzes the first step of their biosynthesis.

The existence of an inducible isoform of COX was described by the group of Needleman¹³⁹. The two isoforms, which are encoded by different genes, vary

in their tissue distributions and regulation of expression, although they present an amino acid sequence homology of approximately 60% in structural analyses.

COX-1 is constitutively expressed in many cell types, including thrombocytes and those present in kidney, stomach and vascular endothelium. It is synthesized and regulated as a so-called 'housekeeping enzyme' involved in physiological adaptation.

In contrast COX-2 is inducible; the induction can occur during tissue damage or inflammation in response to cytokines (tumour necrosis factor- α , interleukin-1), mitogens and growth factors¹⁴⁰.

COX-3, identical in sequence to COX-1, is the third and most recently discovered by Simmons and co-workers but is not functional in humans.

It is difficult to generalize the physiological roles of individual prostaglandins, in fact the same compound can sometimes exert even opposite effects on different types of target cell. At last prostaglandin effects are complex and depend on the type of target cells, among other factors. They are important in the regulation of thrombocyte aggregation, inflammatory processes, pain and fever induction, the regulation of vessel perfusion, and many other processes¹⁴⁰.

5.4.2 COX Inhibitory Assay System

We studied the influence of the Zeise' s compounds on isolated ovine COX-1 and human recombinant COX-2 activity. Therefore, the level of the major COX metabolite prostaglandin E₂ (PGE₂) in arachidonic acid-stimulated MDA-MB-231 breast tumor cells is quantified by enzyme-linked immuno sorbent assay (ELISA) (COX Inhibitor Screening Assay; Cayman Chemical Company, Ann Arbor, MI)¹⁴¹. The experiments were performed according to the manufacturer's instructions¹⁴². Briefly described, there is a competition between PGs and a PG-acetylcholinesterase (AChE) conjugate (PG tracer) for a limited amount of PG antiserum. 96-wells plates are used for the assay. Each plate contains the mouse monoclonal anti-rabbit IgG, which has been previously attached to the well. Each well contains the rabbit antiserum-PG (either free or tracer), the PG tracer and the sample PG, respectively. The concentration of the PG tracer is held constant, while the concentration of PG varies. The amount of the PG tracer, which is able to bind to the PG antiserum will be inversely proportioned to the concentration of

PG in the well during the incubation. To remove any unbound reagents, the plate is washed. Afterwards to the well is added Ellman's Reagent (which contains the substrate to AChE), that catalyzes the reaction described in Fig. 5.10. The product of this reaction (5-thio-2-nitrobenzoic acid) has a distinct yellow color and absorbs strongly at 415 nm ((FLASHscan S12Victor 2, Perkin Elmer). Results were calculated as the means of duplicate determinations¹⁴³.

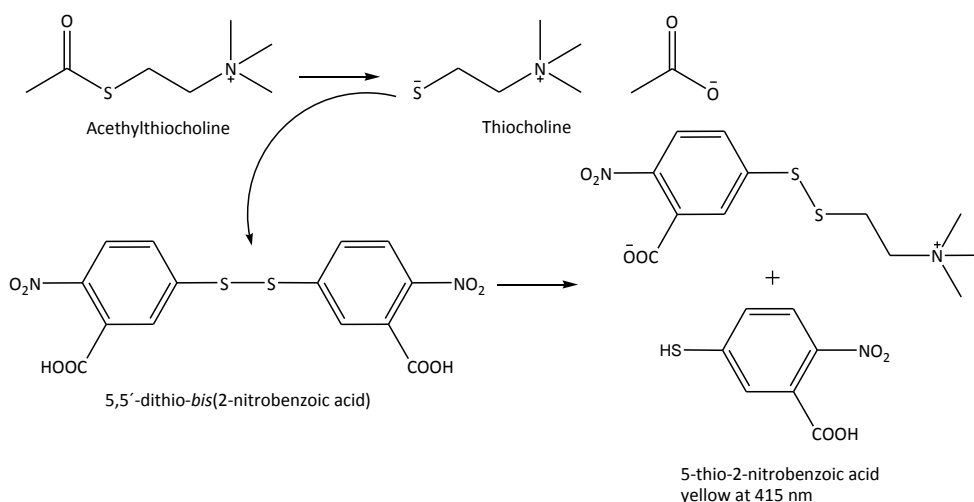


Figure 5.10. Reaction catalyzed by acetylcholinesterase in COX inhibitor screening assay kit.

5.4.2.1 1,1,2-Triarylalkenes Zeise's Complexes

Both subtypes of the cyclooxygenase enzymes (COX-1 and COX-2) are the targets for the design of anti-inflammatory drugs as well as in cancer therapy¹⁴⁴. Since Zeise's complexes gained interest as labeling agents of bioactive molecules, because they possess the ability to inhibit cyclooxygenase, on the contrary to other platinum complexes, e. g. cisplatin or potassium tetrachloroplatinate, which did not show inhibitory property, indicating a specific mode of action of Zeise's salt.

Thus, we investigated the inhibitory potency of the 1,1,2-triarylalkenes Zeise's complexes **2c-PtCl₃** and **2d-PtCl₃** in an ELISA using the isolated isoenzymes (Fig. 5.11).

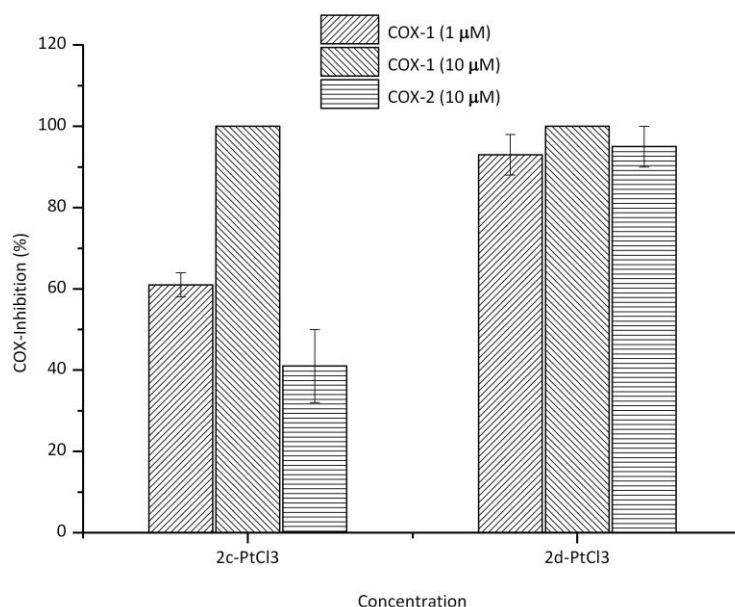


Figure 5.11. Inhibition of COX-1 and COX-2 enzymatic activity by the Zeise' s complexes **2c-PtCl₃** and **2d-PtCl₃** at concentration of 1 and 10 μM.

A drug concentration of 1 μM and 10 μM was used for the experiments. At the concentration used **2c-PtCl₃** showed a high inhibitory activity at COX-1 (61% at 1 μM and 100 % at 10 μM) and lower inhibition at COX-2 (41% at 10 μM). On the contrary **2d-PtCl₃**, which contains a further Zeise' s unit, was much more active at both isoenzymes (COX-1: 93% at 1 μM and 100 % at 10 μM; COX-2: 95 % at 10 μM). The COX inhibitory effects showed a clear structural dependence. The Zeise' s unit was necessary for high inhibitory activity. Its specific mode of action was explained by studies of Meieranz¹⁰¹, by LC-MS experiments, in which COX-1 was incubated with Zeise's salt and enzymatically digested. It emerged that Tyr385, which is located in the active site of COX and represents the essential amino acid for the oxidation of arachidonic acid, was platinated.

No correlation existed between growth inhibition of breast cancer cells and COX activity.

6 Conclusions

6 Conclusions

In this work, two series of new non-steroidal organometallic compounds for the treatment of breast cancer were presented.

In section 1 hormone therapy and development of novel bioactive molecules were described focusing on the treatments and diagnosis techniques that were already available for breast cancer. The ability of agonistic compounds to promote cell proliferation was briefly presented as well as the mode of action of the antiestrogenic drug tamoxifen, which represents the most common agent concerning the treatment of ER-positive breast tumors. Unfortunately, in the course of this treatment tumors become resistant to tamoxifen. This drug resistance has promoted more efforts in the synthesis of compounds with new therapeutic spectra. In particular, the use of metal-based compounds as potential therapeutic agents has become an interesting field in medical research. One major advantage of organometallic compounds is the fact that they offer a high kinetic stability, having bonds with a more covalent character. The evaluation of the biological properties of organometallic compounds, especially cobalt as well as Zeise's salt derivatives, represent the principal topic of this work.

In the first part, we have designed and synthesized a series of 3,4-diarylalkenyne hexacarbonyl dicobalt complexes (**1(a-e)-Co** and **1(a'-e')-Co**). These compounds bear a cobalt alkyne chain instead of one of the two ethyl chains of diethylstilbestrol. Instead of the other ethyl chain these compounds bear a shorter or longer alkyl chain. The modified diethylstilbestrol derivatives (3,4-diarylalkenyne) were synthesized in three main steps:

- Synthesis of the 3,4-diarylalkenyne moiety
- Deprotection of the methoxy groups
- Incorporation of the cobalt into the alkenyne scaffold

In the first step 3,4-diarylalkenyne moieties with various alkyl chain lengths were obtained by a S_N1 reaction. This reaction led to a mixture of (*Z*)- and (*E*)-isomers, which could not be separated. However, the assignment of the signals of the (*Z*)-

and (*E*)-isomers was achieved by $^1\text{H-NMR}$ NOE experiments, which indicated the presence of the (*E*)- isomers as the major form (6:1 ratio).

Regarding the deprotection step we explored different methods for the cleavage of the methoxy group with the purpose to obtain molecules which combine cytotoxic properties and possible ER activity. This aim could not be reached due to the fact that the compounds bear an alkyne function, which is liable to degradation during the deprotection step. We decided to use a silyl ether function instead of the methoxy group as protecting group which allowed milder conditions for the deprotection step. Unfortunately, our attempts using first TMS and later TIPS failed. We decided not to investigate further, because all conditions explored (e.g., BBr_3 , EtSH) for the cleavage of the methoxy groups were unsuccessful. The results of these reactions were either polymerization or decomposition of the used compounds.

In the last step, the corresponding alkyne ligands (**F1a-e**) reacted with $\text{Co}_2(\text{CO})_8$ in absolute dichloromethane resulting in the cobalt-alkyne complexes (**1(a-e)-Co** and **1(a'-e')-Co**). It is noteworthy that the metal moiety increases the lipophilicity of the molecules allowing the separation of both (*Z*)- and (*E*)-isomers by flash column chromatography.

The antiproliferative activity of the synthesized compounds was investigated using two different breast cancer cell lines (hormone-dependent MCF-7 cells as well as on hormone-independent MDA-MB-231 cells). The results of these biological investigations demonstrated that an attachment to $\text{Co}_2(\text{CO})_6$ increases the inhibition of cell proliferation. Only marginal cytotoxicity was detected for the free ligands. Furthermore, antitumor potency depended on the length of the alkyl chain as well as the configuration. The short alkyl chain and (*Z*)-configuration of the complexes increased antiproliferative activity against in both MCF-7 and MDA-MB-231 cells. For all tested compounds, the observed inhibiting activity was stronger in MDA-MB-231 cells compared to MCF-7 cells. Further experiments such as cellular uptake and accumulation (using atomic absorption spectroscopy), could be useful to elucidate these effects.

Aiming a more detailed exploration of their mode of action, we investigated whether ER is involved in this mechanism. Estrogenic and antiestrogenic activity was analyzed using MCF-7/2a, U2-OS/ α , and U2-OS/ β cancer cells. None of the

tested compounds did show any estrogenic or antiestrogenic activity on these cell lines. Therefore, an ER-mediated cytotoxicity can be excluded. One reason for the lack of estrogenic or antiestrogenic activity might be the fact that the methoxy group in these compounds prevents the binding of the ligand to the ER LBD¹²⁹.

In the second part of this thesis, a series of modified tamoxifen (1,1,2-triarylalkene) derivatives have been developed combining the antiestrogenic properties of the tamoxifen scaffold with the cytotoxic properties derived from the addition of a cobalt cluster.

The synthesis of these compounds was performed in accordance to the synthesis of the 3,4-diarylalkenyne derivatives mentioned before, followed by Grignard reaction. A mixture of (*Z*)- and (*E*)-isomers was obtained, whose separation was possible as a result of the poor solubility of the (*Z*)-isomer in diethyl ether. The subsequent deprotection of the (*Z*)-isomer using BBr₃ afforded again a mixture of both isomers. However the ratio of the two isomers could be adjusted by varying the reaction time. Derivatization of the alkyl side-chains introducing an alkyne or alkene functionality prior to the introduction of a metal moiety was successful. The compounds of the 1,1,2-triarylalkene series were found to isomerize quite rapidly. Hence, (*Z*)- and (*E*)-isomers were not separated and the biological tests were performed using a mixture of both isomers.

The compounds were first tested for their antiproliferative activities. Only the free ligands **2a** and **2c** presented some antiproliferative activities in MCF-7 cells, and even weaker inhibiting effects in MDA-MB-231 cells. The compounds with alkyl groups on the side-chain at the other phenyl moiety (**2c** and **2d**) did not display any influence on tumor cell growth.

The complexes with the Co₂(CO)₆ cluster incorporated into the alkyne function (**2a-Co**, **2b-Co**) did not present inhibiting effects on the growth of MCF-7 and MDA-MB-231 cells.

The free ligands as well as the complexes were further tested in an established luciferase assay in order to understand the mode of action on the molecular level and to evaluate the ER subtype selectivity. The free ligands did not induce any agonistic or antagonistic properties on ER. For that reason an estrogenic-antiestrogenic mode of action seems rather unlikely for those compounds. In contrast, the complexes **2a-Co** and **2b-Co** were able to induce luciferase expres-

sion. These results led us to the conclusion that the $\text{Co}_2(\text{CO})_6$ unit plays an important role for the estrogenic activity.

Differences were also observed on the estrogenic activity on both subtypes. **2a-Co**, with only one alkyl substituent at the phenyl ring, presented trans-activation activity on both $\text{ER}\alpha$ and $\text{ER}\beta$. **2b-Co**, with a second alkyl substituent at the other phenyl ring, presented estrogenic activity in $\text{ER}\alpha$ and only a marginal activity in $\text{ER}\beta$. A possible reason for this moderate intrinsic activity, might be the higher lipophilicity, caused by the second substituent. By all means the mechanism has remained elusive and molecular modeling experiments would be of great interest to explore how the cobalt-alkyne functionality can favor the binding to the LBD of ER. In the literature, a possible interaction with Asp 351 is described for similar compounds.

Interestingly, **2a-Co** and **2b-Co** showed the highest estrogenic activity in U2-OS/ α and in U2-OS/ β cells, whereas in MCF-7/2a cells they were only marginally active. These results accentuated the higher sensitivity of U2-OS cells for hormones compared to MCF-7 cells.

Finally the low cytotoxic effects compared to their remarkable estrogenic activity of the cobalt-alkyne complexes, make an ER-mediated cytotoxicity mode of action unlikely. Therefore, as the mechanism of action could not be elucidated in this work, future studies should be conducted on the subject.

Moreover, in consideration of the fact that Zeise's salt is able to inhibit cyclooxygenase enzymes, we added it to the alkene function on the side-chain, by displacement of the olefin from platinum (II) binding *via* the double bond. The complexes **2c-PtCl₃** and **2d-PtCl₃** did not present antiproliferative activity in MCF-7 and MDA-MB-231 cells. We investigated the COX-1 and COX-2 inhibitory effects at isolated isoenzymes. Due to this we used a PGE_2 assay with MDA-MB-231 cells, which show a constitutive COX-2 expression. **2c-PtCl₃** and **2d-PtCl₃** were found to be potent inhibitors of COX-1 and COX-2. The COX inhibitory effects showed a clear structural dependence. Interestingly, **2c-PtCl₃** showed a preference for COX-1, although **2d-PtCl₃** strongly inhibited both isoenzymes with the same potency. A possible explanation is that the Zeise' unit was necessary for high activity: **2d-PtCl₃**, which has two Zeise' units in its structure, can highly increase the inhibition. As the free ligands did not show any COX-inhibition, we

suggest that the inhibitory properties derived from a specific mode of action of Zeise's salt.

Drawing any conclusion is difficult, because no correlation existed between growth inhibition of breast cancer cells and COX activity. Furthermore, the compounds did not display any anti-estrogenic activity.

This work offered a number of pharmacologically active compounds. It emerged that different metal clusters on the ligand's scaffold can modulate biological properties like estrogenic or COX-inhibiting activity.

Cellular accumulation experiments on 3,4-diarylalkenyne derivatives could be useful to elucidate their cytotoxic effects originated after drug exposure. Since their biological target still remains unknown, it is also possible that these compounds could be used for the treatment of other diseases. For the synthesized 1,1,2-triarylalkene derivatives apoptotic and DNA interaction studies could help to understand their antitumor mode of action.

7 Experimental Section

7 Experimental section

7.1 Synthesis and structural analysis

7.1.1 General considerations

7.1.1.1 Solvents and chemicals

All chemicals, reagents and solvents were purchased – if not stated – from Sigma-Aldrich, VWR, Merck, Acros or Alfa Aesar. The laboratory consumables were purchased from Braun, Nunc, Merck and Sarstedt.

Dichloromethane was dried over molecular sieve 4A for 48 hours and then stirred with phosphor(V) oxide for 8 hours and distilled. THF and diethylether were freshly distilled under N₂ gas and dried over potassium-sodium alloy. Pyridine was stirred with CaCl₂ for 2 hours and distilled.

7.1.1.2 Thin-layer chromatography (TLC) and column chromatography

Reactions were all monitored by thin-layer chromatography (TLC), performed on precoated silica gel plates (Kieselgel 60 F254, Merck). Visualization on TLC was achieved by UV light at 254 and / or 366 nm. Column chromatography was performed with silica gel 60 (0.063-0.200 mm, Merck). The silica gel were first bloated in the used eluent and then filled into the column. The sample was solved in a little of the corresponding eluent unless otherwise noted and loaded onto the column.

7.1.1.3 Melting points

Melting points are measured using a Büchi B-545 melting point apparatus (Flawil, Switzerland) and are uncorrected.

7.1.1.4 Nuclear magnetic resonance

The ¹H-NMR spectra were performed on the Avance/DPX 400 spectrometer (by Bruker Analytische Messtechnik GmbH) at 400 MHz (for 1H) with TMS as internal standard. The used NMR solvents are detailed in each spectrum. Chemical shift

values are quoted in parts per million (ppm, δ) and coupling constants J are quoted in Hertz (Hz). Coupling constants (J) are quoted in Herz (Hz) with the following splitting abbreviations: s = singlet, d = doublet, t = triplet, m = multiplet, and dd = double doublet.

7.1.1.5 Mass spectrometry

FAB-MS-spectra were determined using a CH5DF/FAB(+) instrument. EI-MS-spectra were recorded with a CH-7A-Varian MAT (70eV) instrument (Palo Alto, USA)

7.1.1.6 Elemental analysis

Elemental analyses were run with a Vario EL Elementaranalysator (Hanau, Germany).

7.1.2 Synthetic procedures and analytical data

7.1.2.1 Synthesis of the acid chloride

4-methoxyphenylacetylchloride (A1)

4 methoxyphenylacetic acid (10g, 60 mmol) and thionyl chloride (7g, 60 mmol) were refluxed for 1 hour. After the gas development ended, the reaction was wakuum-distilled in order to destroy the excess of SOCl_2 . The crude product was directly-immediately used for the next reaction (without any purification) yielding a red liquid.

Red liquid $\text{C}_9\text{H}_9\text{O}_2\text{Cl}$ 184.62

Yield: 11g, 60 mmol, 100%

Phenylacetyl chloride (A2)

With the same method from phenylacetic acid (10g, 73 mmol) and thionyl chloride (8.7 g, 73 mmol).

Red liquid $\text{C}_8\text{H}_7\text{OCl}$ 154.59

Yield: 11g, 73 mmol, 100%

7.1.2.2 General method to synthesize the ethanone

The acetylchloride was added dropwise to a suspension of aluminium chloride and anisole in 20 mL dry dichloromethane under cooling at 0°C. The resulting reaction mixture was heated to reflux for half an hour and then was allowed to stir at room temperature for 1 hour. The reaction was then poured slowly into ca 50 mL ice-water and the layers were separated. The aqueous phase was extracted with CH₂Cl₂ (1x50 mL). The combined organic layer was washed with H₂O, NaOH 20%, dried over Na₂SO₄ and filtered. After removal of the solvent under reduced pressure, the crude product was recrystallized from diethylether/ethanol.

1,2-bis(4-methoxyphenyl)ethanone (B1)

4-Methoxyphenylacetylchloride **A1** (10 g, 54 mmol) was added dropwise at 0°C to a suspension of aluminium chloride (8.6 g, 65 mmol) and anisole (5.9 mL, 54 mmol) in 20 mL of dry dichloromethane. The purification of the product was obtain with-through cristallization from ether/ethanol to afford the compound **B1** as a colorless crystals (mp 110°C)

C₁₆H₁₆O₃ 256,3

Yield: 12.4 g, 48 mmol (89.8%)

¹H NMR (400 MHz, CDCl₃): δ = 3.77 (s, 3H, OCH₃); 3,85 (s, 3H, OCH₃); 4.16 (s, 2H, CH₂); 6.85 (AA'BB'⁻³J = 8.6 Hz, 2H, ArH-3, ArH-5); 6.91 (AA'BB'⁻³J = 8.9 Hz, 2H, Ar'H-3, Ar'H-5); 7.17 (AA'BB'⁻³J = 8.6 Hz, 2H, ArH-2, ArH-6); 7.98 (AA'BB'⁻³J = 8.9 Hz, 2H, Ar'H-2, Ar'H-6)

MS (EI, 50°C): m/z (%) = 256 [M]⁺⁺ (6.04), 135 [C₈H₇O₂]⁺ (100), 121 [C₇H₇OCH₂]⁺ (9.68).

1-(4-methoxyphenyl)-2-phenylethanone (B2b)

Aluminium chloride (10.3 g, 70 mmol) and anisole (7 mL, 60 mmol) were suspended in 20 mL dry CH₂Cl₂ and phenylacetylchloride **A2** (10 g, 0.06 mol) was added under cooling. The crude product was recrystallized from diethyl ether/ethanol to yielding the compound **B2b** as a colorless crystals (mp 68-69° C).

C₁₅H₁₄O₂ 226.28

Yield: 12.1 g, 53 mmol, (89%)

¹H NMR (400 MHz, CDCl₃): δ = 3.86 (s, 3H, OCH₃); 4.24 (s, 2H, CH₂); 6.93 (AA'BB'³J = 8.6 Hz, 2H, ArH-3, ArH-5); 7.29 (m, 5H, Ar'H); 8.00 (AA'BB'³J = 8.5 Hz, 2H, ArH-2, ArH-6)

MS (EI, 50°C): m/z (%) = 226 [M]⁺ (1,6), 135 [C₈H₇O₂]⁺ (100).

7.1.2.3 Alkylation of the ethanone - general method -

1,2 Åq of KHMDS (Potassium bis(trimethylsilyl)amide solution 0.5 M in toluene) were carefully added to a solution of **1** in dry THF, which had been previously cooled to -78° C under a argon atmosphere. After 1 hour, the alkyl iodide dissolved in dry THF was added dropwise. The reaction was allowed to warm to room temperature overnight. After the reaction ended, water was added and the layers were separated. The aqueous phase was washed with ethylacetate and the organic fractions combined, extracted with distilled water and brine. The organic extracts were dried over Na₂SO₄, filtered through a fritted funnel and the filtrate was evaporated to dryness to obtain a colorless oil. The crude product was purified by column chromatography on silica gel with diethyl ether/ligroin only if necessary.

1,2-bis(4-methoxyphenyl)propan-1-one (**C1a**)

KHMDS (37.3 mL, 18.7 mmol) was added via a syringe to a solution of **B1** (4 g, 15.6 mmol) in 100 mL dry THF at -78° C. After 1hour methyl iodide (0.97 mL, 15.6 mmol) dissolved in 40 mL dry THF was added and the reaction was warmed slowly to room temperature. Any purification was required.

Yellow oil

C₁₇H₁₈O₃ 270,32

Yield: 4.2g, 15.6 mmol, 100%

¹H NMR (400 MHz, CDCl₃): δ = 1.48 (d, 3H, CH₃); 3.75 (s, 3H, OCH₃); 3.81 (s, 3H, OCH₃); 4.59 (q, 1H, CH); 6.82 (AA'BB'³J = 8.6 Hz, 2H, ArH-3, ArH-5); 6.85 (AA'BB'³J = 8.9 Hz, 2H, Ar'H-3, Ar'H-5); 7.19 (AA'BB'³J = 8.6 Hz, 2H, ArH-2, ArH-6); 7.93 (AA'BB'³J = 8.9 Hz, 2H, Ar'H-2, Ar'H-6)

MS (EI, 50°C): m/z (%) =270 [M]⁺ (6.2), 135 [C₉H₁₁O]⁺ und [C₈H₇O₂]⁺ (100).

1,2-bis(4-methoxyphenyl)butan-1-one (C1b)

To a solution of **B1** (4 g, 15.6 mmol) in dry THF (100 mL) was added KHMDS (37.4 mL, 18.7 mmol) at -78° C and after 1 hour ethyl iodide (1.25 mL, 15.6 mmol) in 40 mL THF was added. The work-up afford a colorless oil.

$C_{18}H_{20}O_3$ 284.35

Yield: 4.3 g, 15.1 mmol, (98%)

1H NMR (400 MHz, $CDCl_3$): δ = 0.88 (t, 3H, CH_3); 1.81 (m, 1H, CH_2 -ROC-CHRCH $_2$); 2.14 (m, 1H, CH_2); 3.74 (s, 3H, OCH_3); 3.81 (s, 3H, OCH_3); 4.34 (t, 1H, CH); 6.81 (AA'BB' 3J = 8.7 Hz, 2H, ArH-3, ArH-5); 6.85 (AA'BB' 3J = 8.9 Hz, 2H, Ar'H-3, Ar'H-5); 7.21 (AA'BB' 3J = 8.7 Hz, 2H, ArH-2, ArH-6); 7.95 (AA'BB' 3J = 8.9 Hz, 2H, Ar'H-2, Ar'H-6)

MS (EI, 50°C): m/z (%) = 284 [M] $^{+}$ (5.7), 149 [$C_{10}H_{13}O$] $^{+}$ (26.6), 135 [$C_8H_7O_2$] $^{+}$ (100).

1,2-bis(4-methoxyphenyl)pentan-1-one (C1c)

A solution of **B1** (4 g, 15.6 mmol) in dry THF (100 mL) was cooled to -78° C and KHMDS (37.4 mL, 18.7 mmol) was added. After 1 hour was added a solution of propyl iodide (1.52 mL, 15.6 mmol) in 40 mL dry THF and the reaction was stirred to warm overnight. The crude product was purified by a column chromatography on silica gel with ligroin/diethyl ether 4+1 to give a colorless oil.

$C_{19}H_{22}O_3$ 298.16

Yield: 3.9 g, 13 mmol, 84.7%

1H NMR (400 MHz, $CDCl_3$): δ = 0.91 (t, 3H, CH_3); 1.28 (m, 2H, CH_2); 1.77 (m, 1H, CH_2 -ROC-CHRCH $_2$); 2.10 (m, 1H, CH_2); 3.74 (s, 3H, OCH_3); 3.80 (s, 3H, OCH_3); 4.46 (t, 1H, CH); 6.81 (AA'BB' 3J = 8.6 Hz, 2H, ArH-3, ArH-5); 6.85 (AA'BB' 3J = 8.9 Hz, 2H, Ar'H-3, Ar'H-5); 7.21 (AA'BB' 3J = 8.6 Hz, 2H, ArH-2, ArH-6); 7.95 (AA'BB' 3J = 8.9 Hz, 2H, Ar'H-2, Ar'H-6)

MS (EI, 35°C): m/z (%) = 298.2 [M] $^{+}$ (5.9), 163.2 [$C_{11}H_{15}O$] $^{+}$ (21.8), 135 [$C_8H_7O_2$] $^{+}$ (100), 121.2 [C_8H_9O] $^{+}$ (46.3)

1,2-bis(4-methoxyphenyl)-3-methylbutan-1-one (C1d)

2-iodopropanone-isopropyl iodide (1.2 ml, 12 mmol) dissolved in 30 mL dry THF was added to a solution of **B1** (3 g, 12 mmol) in 80 mL THF freshly distilled and KHMDS (28 mL, 14 mmol) at -78° C. After the work-up, the product was obtained

with a column chromatography on silica gel (ligroin/diethyl ether 4+1) as colorless oil.

$C_{19}H_{22}O_3$ 298.16

Yield: 2 g, 6.7 mmol, 57 %

1H NMR (400 MHz, $CDCl_3$): δ = 0.75 (d, 3H, CH_3); 1.98 (d, 3H, CH_3); 2.54 (m, 1H, CH); 3.75 (s, 3H, OCH_3); 3.82 (s, 3H, OCH_3); 4.10 (d, 1H, CH); 6.80 (AA'BB' 3J = 8.6 Hz, 2H, ArH-3, ArH-5); 6.87 (AA'BB' 3J = 8.8 Hz, 2H, Ar'H-3, Ar'H-5); 7.24 (AA'BB' 3J = 8.7 Hz, 2H, ArH-2, ArH-6); 7.97 (AA'BB' 3J = 8.8 Hz, 2H, Ar'H-2, Ar'H-6)

MS (EI, 35°C): m/z (%) = 298.3 $[M]^{+}$ (6.7), 163.2 $[C_{11}H_{15}O]^+$ (36.9), 135 $[C_8H_7O_2]^+$ (100), 121.2 $[C_8H_9O]^+$ (18.5).

1,2-bis(4-methoxyphenyl)hexan-1-one (C1e)

B1 (3g, 12 mmol) in dry THF (80 mL), KHMDS (28 mL, 14 mmol) and 1-iodobutane (1,3 mL, 12 mmol) in THF (30 mL) were stirred from -78° C to room temperature. A column chromatography (mobile phase: ligroin/diethyl ether 2+1) of the crude product produce a colorless oil.

$C_{20}H_{24}O_3$ 312,17

Yield: 2.4 g, 8 mmol, 66,6%

1H NMR (400 MHz, $CDCl_3$): δ = 0.85 (t, 3H, CH_3); 1.28 (m, 4H, CH_2CH_2); 1.80 (m, 1H, CH_2); 2.14 (m, 1H, CH_2); 3.69 (s, 3H, OCH_3); 3.74 (s, 3H, OCH_3); 4.45 (t, 1H, CH); 6.80 (AA'BB' 3J = 8.6 Hz, 2H, ArH-3, ArH-5); 6.83 (AA'BB' 3J = 8.9 Hz, 2H, Ar'H-3, Ar'H-5); 7.22 (AA'BB' 3J = 8.6 Hz, 2H, ArH-2, ArH-6); 7.96 (AA'BB' 3J = 8.9 Hz, 2H, Ar'H-2, Ar'H-6)

MS (EI, 35°C): m/z (%) = 312.3 $[M]^{+}$ (4.3), 177.3 $[C_{12}H_{17}O]^+$ (18.5), 135 $[C_8H_7O_2]^+$ (100), 121.2 $[C_8H_9O]^+$ (47.7).

7.1.2.4 Introduction of the alkyne unit

To a dry round-bottom flask containing Lithium (trimethylsilyl) acetylide, at -78° C was added dropwise the compound **C1a-e** in freshly distilled THF. The reaction mixture was stirred for 12 hours under argon to room temperature. Then saturated ammonium chloride was slowly added to the reaction followed by distilled water and the resulting solution extracted with diethyl ether (4 x 100 mL). The organic layers were combined, dried (Na_2SO_4) and filtered. After removal of the sol-

vent, the resulting brown oil was dissolved under argon in dry pyridine and diethyl ether and cooled to 0°C. Thionyl chloride was carefully added dropwise and the reaction was allowed warm to room temperature overnight. The reaction mixture was hydrolyzed by adding chopped ice and HCl 1 M. The layers were separated whereupon the aqueous layer was extracted with ether (3 times) and the combined organic fractions washed with HCl 1 M (3 times) and brine. After drying over Na₂SO₄ the solvent was evaporated and the remaining product was purified by column chromatography on silica gel with diethyl ether/ligroin.

(E)-(Z)-(3,4-bis(4-methoxyphenyl)pent-3-en-1-ynyl)trimethylsilane E1a

To a pre-cooled (-78° C) solution of lithium (trimethylsilyl) acetylide (37.4 mL, 18.7 mmol) in THF was added **1Ca** (4.22 g, 15.6 mmol) in dry THF (20 mL). The reaction was stirred to warm. After the work-up the crude product, was dissolved in diethyl ether abs. (10 mL) and pyridine abs. (8 mL), and cooled at 0° C. SOCl₂ (2.27 mL) was added very carefully and the reaction was allowed to stir overnight, stopped with ice and HCl 1M and extracted with diethyl ether (3 times). The brown oil was purified by a column chromatography on silica gel with ligroin/diethyl ether (2+1).

C₂₂H₂₆O₂Si (350.5 g/mol)

Yield: 3g, 8.5 mmol, 55.6 % yellow oil

¹H NMR (400 MHz, CDCl₃): δ = 0.22 (s, 9H, CH₃-Si); 1.01 (t, 3H, CH₃); 2.85 (q, 2H, CH₂); 3.71 (s, 3H, OCH₃); 3.73 (s, 3H, OCH₃); 6.63 (AA'BB'³J = 8.8 Hz, 2H, ArH-3, ArH-5); 6.69 (AA'BB'³J = 8.7 Hz, 2H, Ar'H-3, Ar'H-5); 6.92 (AA'BB'³J = 8.7 Hz, 2H, ArH-2, ArH-6); 7.03 (AA'BB'³J = 8.8 Hz, 2H, Ar'H-2, Ar'H-6)

MS (EI, 50° C): m/z (%) = 350 [M]⁺ (100), 335 [M⁺-CH₃] (16.3), 320 [M⁺-2CH₃] (17.0), 305 [M⁺-3CH₃] (13.7), 277 [C₁₉H₁₇O₂]⁺ (10.4).

(E)-(Z)-(3,4-bis(4-methoxyphenyl)pent-3-en-1-ynyl)trimethylsilane E1b

From lithium (trimethylsilyl) acetylide (27.9 mL, 13.9 mmol) and **C1b** (3.3 g, 11.6 mmol) in dry THF (20 mL). The mixture was left to react further with SOCl₂ (1.6 mL) Column chromatography (ligroin/diethyl ether 2+1) afforded compound **E1b** as a yellow oil.

C₂₃H₂₈O₂Si 364,5

Yield: 2,4 g, 6.6 mmol, (57%)

¹H NMR (400 MHz, CDCl₃): δ = 0.18 (s, 9H, CH₃-Si); 2.39 (s, 3H, CH₃); 3.69 (s, 3H, OCH₃); 3.70 (s, 3H, OCH₃); 6.61 (AA'BB'³J = 8.8 Hz, 2H, ArH-3, ArH-5); 6.65 (AA'BB'³J = 8.7 Hz, 2H, Ar'H-3, Ar'H-5); 6.91 (AA'BB'³J = 8.7 Hz, 2H, ArH-2, ArH-6); 7.01 (AA'BB'³J = 8.8 Hz, 2H, Ar'H-2, Ar'H-6)

MS (EI, 50°C): m/z (%) = 364 [M]⁺ (100), 349 [M⁺-CH₃] (21.6), 334 [M⁺-2CH₃] (8.4), 319 [M⁺-3CH₃] (5.2), 291 [C₂₀H₁₉O₂]⁺ (11.2).

(E)-(Z)-(3,4-bis(4-methoxyphenyl)hept-3-en-1-ynyl)trimethylsilane E1c

Starting from lithium (trimethylsilyl) acetylide (30.3 mL, 15.1 mmol) and **C1c** (3.77 g, 12.6 mmol) in dry THF (20 mL). After the work-up the crude product dissolved in pyr abs. (8 mL) and diethyl ether abs. (10 mL), reacted with SOCl₂ (1.8 mL, 12.6 mmol). The product was purified by a column chromatography (ligroin / diethyl ether 2+1) to give a yellow oil.

C₂₄H₃₀O₂Si 378.6

Yield: 1.9 g, 5 mmol, (33.4%)

¹H NMR (400 MHz, CDCl₃): δ = 0.22 (s, 9H, CH₃-Si); 0.93 (t, 3H, CH₃); 1.43 (m, 2H, CH₂); 2.84 (t, 2H, CH₂); 3.64 (s, 3H, OCH₃); 3.66 (s, 3H, OCH₃); 6.60 (AA'BB'³J = 8.8 Hz, 2H, ArH-3, ArH-5); 6.66 (AA'BB'³J = 8.7 Hz, 2H, Ar'H-3, Ar'H-5); 6.92 (AA'BB'³J = 8.7 Hz, 2H, ArH-2, ArH-6); 7.04 (AA'BB'³J = 8.7 Hz, 2H, Ar'H-2, Ar'H-6)

MS (EI, 50°C): m/z (%) = 378 [M]⁺ (81.2), 363 [M⁺-CH₃] (34.9), 349 [M⁺-2CH₃] (30.4), 334 [M⁺-3CH₃] (6.2), 305 [C₂₁H₂₁O₂]⁺ (4.7).

(E)-(Z)-(3,4-bis(4-methoxyphenyl)-5-methylhex-3-en-1-ynyl)trimethylsilane

E1d

From lithium (trimethylsilyl) acetylide (11.3 mL, 5.6 mmol) and **C1d** (1.4 g, 4.7 mmol) in dry THF (15 mL). The mixture was left to react further with SOCl₂ (0.7 mL, 4.7 mmol) Column chromatography (ligroin / diethyl ether 2+1) afforded compound **E1d** as a yellow oil. cambia testo

C₂₄H₃₀O₂Si 378.6

Yield: 1.2 g, 3.2 mmol, (66%)

¹H NMR (400 MHz, CDCl₃): δ = 0.23 (s, 9H, CH₃-Si); 1.07 (d, 6H, CH₃CH₃); 3.66 (m, 1H, CH); 3.70 (s, 3H, OCH₃); 3.75 (s, 3H, OCH₃); 6.59 (AA'BB'³J = 8.8 Hz,

2H, ArH-3, ArH-5); 6.72 (AA'BB'³J = 8.6 Hz, 2H, Ar'H-3, Ar'H-5); 6.85 (AA'BB'³J = 8.6 Hz, 2H, ArH-2, ArH-6); 7.01 (AA'BB'³J = 8.8 Hz, 2H, Ar'H-2, Ar'H-6)

MS (EI, 90°C): m/z (%) = 378 [M]⁺ (61.6), 363 [M⁺-CH₃] (2.4), 348 [M⁺-2CH₃] (13.7), 333 [M⁺-3CH₃] (6.3), 305 [C₂₁H₂₁O₂]⁺ (21.9).

(E)-(Z)-(3,4-bis(4-methoxyphenyl)oct-3-en-1-ynyl)trimethylsilane E1e

From lithium (trimethylsilyl) acetylide (5.9 mL, 2.9 mmol) and **C1e** (0.78 g, 2.5 mmol) in dry THF (15 mL). SOCl₂ (0.36 mL, 2.5 mmol) Column chromatography (ligroin / diethyl ether 2+1) gave compound **E1e** as a yellow oil.

C₂₅H₃₂O₂Si 392,6

Yield: 0.82 g, 2,1 mmol, (83.7%)

¹H NMR (400 MHz, CDCl₃): δ = 0.23 (s, 9H, CH₃-Si); 0,90 (t, 3H, CH₃); 1.37 (m, 4H, CH₂CH₂); 2.85 (t, 2H, CH₂); 3.73 (s, 3H, OCH₃); 3.75 (s, 3H, OCH₃); 6.64 (AA'BB'³J = 8.7 Hz, 2H, ArH-3, ArH-5); 6.70 (AA'BB'³J = 8.6 Hz, 2H, Ar'H-3, Ar'H-5); 6.93 (AA'BB'³J = 8.6 Hz, 2H, ArH-2, ArH-6); 7.04 (AA'BB'³J = 8.7 Hz, 2H, Ar'H-2, Ar'H-6)

MS (EI, 50°C): m/z (%) = 392 [M]⁺ (61.6), 377 [M⁺-CH₃] (2.4), , 362 [M⁺-2CH₃] (13.7), 347 [M⁺-3CH₃] (6.3), 319 [C₂₂H₂₃O₂]⁺ (21.9).

7.1.2.5 Cleavage of the trimethylsilyl group

After dissolution of silylated compounds in abs. methanol, was added potassium hydroxide at room temperature and the reaction mixture was stirred under argon overnight. Subsequently, the mixture was poured into distilled water and extracted with diethyl ether (3 times). The organic layers were pooled, dried over Na₂SO₄ and the solvent was removed by rotary evaporation leaving a yellow-brown oil.

(E)-(Z)-4,4'-(pent-2-en-4-yne-2,3-diyl)bis(methoxybenzene) F1a

Starting from **E1a** (1 g, 2 mmol) in MeOH (15 mL) and KOH (0,13 g, 2.4 mmol) it was obtained a yellow oil.

C₁₉H₁₈O₂ 278.3

Yield: 0.5 g, 1.8 mmol, (91%)

¹H NMR (400 MHz, CDCl₃): δ = 2.44 (s, 3H, CH₃); 3.33 (s, 1H, C≡CH); 3.74 (s, 3H, OCH₃); 3.75 (s, 3H, OCH₃); 6.67 (AA'BB'³J = 8.8 Hz, 2H, ArH-3, ArH-5); 6,70

(AA'BB'³J = 8.8 Hz, 2H, Ar'H-3, Ar'H-5); 6.97 (AA'BB'³J = 8.8 Hz, 2H, ArH-2, ArH-6); 7.06 (AA'BB'³J = 8.8 Hz, 2H, Ar'H-2, Ar'H-6)

MS (EI, 50° C): m/z (%) = 278 [M]⁺ (100), 263 [C₁₈H₁₅O₂]⁺ (28.8)

(E)-(Z)-4,4'-(hex-3-en-1-yne-3,4-diyl)bis(methoxybenzene) F1b

To a solution of **E1b** (0.5 g, 1.4 mmol) in dry MeOH (10 mL) was added KOH (95 mg, 1.7 mmol). After the work-up was obtained a yellow oil.

C₂₀H₂₀O₂ 292.4

Yield: 0.4 g, 1.4 mmol, (100%)

¹H NMR (400 MHz, CDCl₃): δ = 1.02 (t, 3H, CH₃); 2.88 (q, 2H, CH₂); 3.18 (s, 1H, C≡CH); 3.69 (s, 3H, OCH₃); 3.71 (s, 3H, OCH₃); 6.64 (AA'BB'³J = 8.8 Hz, 2H, ArH-3, ArH-5); 6.70 (AA'BB'³J = 8.7 Hz, 2H, Ar'H-3, Ar'H-5); 6.94 (AA'BB'³J = 8.7 Hz, 2H, ArH-2, ArH-6); 7.06 (AA'BB'³J = 8.8 Hz, 2H, Ar'H-2, Ar'H-6)

MS (EI, 50°C): m/z (%) = 292 [M]⁺ (100), 277 [C₁₉H₁₇O₂]⁺ (32.1), 262 [C₁₈H₁₄O₂]⁺ (11.4), 246 [C₁₈H₁₄O]⁺ (13.8).

(E)-(Z)-4,4'-(hept-3-en-1-yne-3,4-diyl)bis(methoxybenzene) F1c

A solution of **E1c** (1 g, 2.6 mmol) and KOH (0.17 g, 3.1 mmol) in dry MeOH (15 mL) was stirred at room temperature for 24 hours. The reaction mixture was stopped and extracted with ether to give a yellow oil.

C₂₁H₂₂O₂ 306.4

Yield: 0.8 g, 2.6 mmol, (100%)

¹H NMR (400 MHz, CDCl₃): δ = 0.85 (t, 3H, CH₃); 1.34 (m, 2H, CH₂); 2.77 (t, 2H, CH₂); 3.18 (s, 1H, C≡CH); 3.63 (s, 3H, OCH₃); 3.65 (s, 3H, OCH₃); 6.56 (AA'BB'³J = 8.8 Hz, 2H, ArH-3, ArH-5); 6.61 (AA'BB'³J = 8.7 Hz, 2H, Ar'H-3, Ar'H-5); 6.86 (AA'BB'³J = 8.7 Hz, 2H, ArH-2, ArH-6); 6.97 (AA'BB'³J = 8.8 Hz, 2H, Ar'H-2, Ar'H-6)

MS (EI, 50°C): m/z (%) = 306 [M]⁺ (100), 291 [C₂₀H₁₉O₂]⁺ (3.7), 277 [C₁₉H₁₆O₂]⁺ (55.1).

(E)-(Z)-4,4'-(5-methylhex-3-en-1-yne-3,4-diyl)bis(methoxybenzene) F1d

KOH (0.095 g, 1.7 mmol) was added to a solution of **E1d** (0.23 g, 0.62 mmol) in dry MeOH (10mL). The reaction was stirred at room temperature for one day. The product was obtained after the work-up as a yellow-green oil.

C₂₁H₂₂O₂ 320.4

Yield: 0.2 g, 0.62 mmol, (100%)

¹H NMR (400 MHz, CDCl₃): δ = 1.05 (d, 6H, R'CR(CH₃)₂); 3.30 (s, 1H, C≡CH); 3.74 (m, 1H, CH(CR)₂); 3.70 (s, 3H, OCH₃); 3.75 (s, 3H, OCH₃); 6.60 (AA'BB'³J = 8.8 Hz, 2H, ArH-3, ArH-5); 6.72 (AA'BB'³J = 8.7 Hz, 2H, Ar'H-3, Ar'H-5); 6.86 (AA'BB'³J = 8.7 Hz, 2H, ArH-2, ArH-6); 7.02 (AA'BB'³J = 8.8 Hz, 2H, Ar'H-2, Ar'H-6)

MS (EI, 50°C): m/z (%) = 320 [M]⁺ (61.6), 307 [C₂₀H₁₉O₂]⁺ (72.3), 392 [C₁₉H₁₆O₂]⁺⁺ (27.9).

(E)-(Z)-4,4'-(oct-3-en-1-yne-3,4-diyl)bis(methoxybenzene) F1e

To a solution of **E1e** (1.45 g, 3.7 mmol) in dry MeOH (25 mL), was added KOH (0.25g, 4.5 mmol). After stirring for one day, the reaction was stopped with distilled water and extracted with diethyl ether. It was afford a yellow-green oil.

C₂₂H₂₄O₂ 334.43

Yield: 1.2 g, 3.7 mmol, (100%)

¹H NMR (400 MHz, CDCl₃): δ = 0.88 (t, 3H, CH₃); 1.37 (m, 4H, CH₂CH₂); 2.86 (t, 2H, CH₂); 3.26 (s, 1H, C≡CH); 3.70 (s, 3H, OCH₃); 3.72 (s, 3H, OCH₃); 6.63 (AA'BB'³J = 8.7 Hz, 2H, ArH-3, ArH-5); 6.69 (AA'BB'³J = 8.7 Hz, 2H, Ar'H-3, Ar'H-5); 6.94 (AA'BB'³J = 8.7 Hz, 2H, ArH-2, ArH-6); 7.05 (AA'BB'³J = 8.7 Hz, 2H, Ar'H-2, Ar'H-6)

MS EI, 50°C): m/z (%) = 334 [M]⁺ (100), 319 [C₂₀H₁₉O₂]⁺ (81.2), 304 [C₁₉H₁₆O₂]⁺⁺ (35.6).

7.1.2.6 General Method for the Preparation of Cobalt-Alkyne Complexes

The alkyne was dissolved in dry dichloromethane under argon at room temperature and dicobalt octacarbonyl was added in excess. The dark reaction was stirred for ca 1 h, until the bubbling has finished and the product has completely formed- the product formation was observed by thin layer chromatography. The solution was subsequently-directly evaporated to dryness and the crude product was purified by flash column chromatography on silica gel (mobile phase: diethyl ether-ligroin).

The complexes were conserved under argon in freezer in order to prevent the decomposition.

1a-Co

From **E1a** (0.2 g, 0.72 mmol) dissolved in CH_2Cl_2 (20 mL) and $\text{Co}_2(\text{CO})_8$ (0.27 g, 0.79 mmol). The crude product was purified by flash column chromatography with ligroin/diethyl ether (9+1) in order to obtain the separation of the two isomers as a red-brown oil.

$\text{C}_{25}\text{H}_{18}\text{Co}_2\text{O}_8$ 564.27

(Z)-1a-Co

Yield: 0.3 g, 5.3 mmol, (75%)

MS (EI, 125°C): m/z (%) =564 $[\text{M}]^{+}$ (0.8), 536 $[\text{M}^{+}\text{-CO}]$ (1.93), , 508 $[\text{M}^{+}\text{-2CO}]$ (0.7), 480 $[\text{M}^{+}\text{-3CO}]$ (8.93), 452 $[\text{M}^{+}\text{-4CO}]$ (9.3), 424 $[\text{M}^{+}\text{-5CO}]$ (29.1), 396 $[\text{M}^{+}\text{-6CO}]$ (11.2), 337 $[\text{M}^{+}\text{-6COCO}]$ (27.4), 278 $[\text{C}_{19}\text{H}_{18}\text{O}_2]$ (27.1).

Calculated: C% 53.21 H% 3.22

Found: C% 53.41 H% 3.49

(E)-1a-Co

Yield: 0.052 g, 0.92 mmol, (13%)

MS (EI, 125°C): m/z (%) =564 $[\text{M}]^{+}$ (1.6), 536 $[\text{M}^{+}\text{-CO}]$ (0.9), , 508 $[\text{M}^{+}\text{-2CO}]$ (0.7), 480 $[\text{M}^{+}\text{-3CO}]$ (0.9), 452 $[\text{M}^{+}\text{-4CO}]$ (3.93), 424 $[\text{M}^{+}\text{-5CO}]$ (8.5), 396 $[\text{M}^{+}\text{-6CO}]$ (13.4), 337 $[\text{M}^{+}\text{-6COCO}]$ (10.7), 278 $[\text{C}_{19}\text{H}_{18}\text{O}_2]$ (7.4).

Calculated: C% 53.21 H% 3.22

Found: C% 53.43 H% 3.50

1b-Co

From **E1b** (0,2 g, 0.68 mmol) dissolved in CH_2Cl_2 (20 mL) and $\text{Co}_2(\text{CO})_8$ (0.26 g, 0,75 mmol). The crude product was purified by flash column chromatography with ligroin/diethyl ether (9:1) in order to obtain the separation of the two isomers.

$\text{C}_{26}\text{H}_{20}\text{Co}_2\text{O}_8$ 578,30

(Z)-1b-Co

Yield: 0.25 g, 0.43 mmol, (64.1%)

MS (EI, 125°C): m/z (%) =578 [M]⁺⁺ (0.8), 549 [M⁺-CO] (0.8), 522 [M⁺-2CO] (1.33), 494 [M⁺-3CO] (4.2), 466 [M⁺-4CO] (5.0), 438 [M⁺-5CO] (12.3), 410 [M⁺-6CO] (4.2), 351 [M⁺-6COCO] (11.1), 292 [C₁₉H₂₀O₂] (23.9).

Calculated: C% 54.00 H% 3.49

Found: C% 54.03 H% 3.75

(E)-1b-Co

Yield: 0.06 g, 0.10 mmol, (15.2%)

MS (EI, 125°C): m/z (%) =578 [M]⁺⁺ (0.7), 549 [M⁺-CO] (0.6), , 522 [M⁺-2CO] (0.7), 494 [M⁺-3CO] (1.0), 466 [M⁺-4CO] (2.7), 438 [M⁺-5CO] (5.9), 410 [M⁺-6CO] (7.7), 351 [M⁺-6COCO] (7.4), 292 [C₁₉H₂₀O₂] (20.7).

Calculated: C% 54.00 H% 3.49

Found: C% 54.02 H% 3.60

1c-Co

From **E1c** (0.2 g, 0.65 mmol) dissolved in CH₂Cl₂ (20 mL) and Co₂(CO)₈ (0.24 g, 0.72 mmol). The crude product was purified by flash column chromatography with ligroin/diethyl ether (9:1) in order to obtain the separation of the two isomers.

C₂₇H₂₂Co₂O₈ 592,33

(Z)-1c-Co

Yield: 0.21 g, 0.35 mmol, (53.8%)

MS (EI, 125°C): m/z (%) =592 [M]⁺⁺ (0.6), 564 [M⁺-CO] (1.2), , 536 [M⁺-2CO] (1.3), 508 [M⁺-3CO] (4.1), 480 [M⁺-4CO] (6.2), 452 [M⁺-5CO] (15.5), 424 [M⁺-6CO] (2.3).

Calculated: C% 54.75 H% 3.74

Found: C% 54.88 H% 3.96

(E)-1c-Co

Yield: 0.04 g, 0.06 mmol, (17%)

MS (EI, 125°C): m/z (%) =592 [M]⁺⁺ (0.7), 564 [M⁺-CO] (1.9), , 536 [M⁺-2CO] (1.6), 508 [M⁺-3CO] (2.8), 480 [M⁺-4CO] (4.5), 452 [M⁺-5CO] (9.3), 424 [M⁺-6CO] (2.6) 365 [M⁺-6COCO] (7.5), 306 [C₂₁H₂₂O₂] (11.2).

Calculated: C% 54.75 H% 3.74

Found: C% 54.91 H% 3.95

1d-Co

From **E1d** (0.15 g, 0.49 mmol) dissolved in CH₂Cl₂ (20 mL) and Co₂(CO)₈ (0.18 g, 0.54 mmol). The crude product was purified by flash column chromatography with ligroin/diethyl ether (9:1) in order to obtain only the E-isomer as a red-brown oil. The Z-isomer was unfortunately obtained in a very small quantities.

C₂₇H₂₂Co₂O₈ 592.33

(Z)-1d-Co

Yield: 0.22 g, 0.37 mmol, (75%)

MS (EI, 125°C): m/z (%) =592 [M]⁺⁺ (0.6), 564 [M⁺-CO] (1.2), , 536 [M⁺-2CO] (1.3), 508 [M⁺-3CO] (4.1), 480 [M⁺-4CO] (6.2), 452 [M⁺-5CO] (15.5), 424 [M⁺-6CO] (2.3).

Calculated: C% 54.75 H% 3.74

Found: C% 55.41 H% 4.03

(E)-1c-Co

Yield: 0.03 g, 0.06 mmol, (12%)

MS (EI, 125°C): m/z (%) =592 [M]⁺⁺ (0.7), 564 [M⁺-CO] (1.9), , 536 [M⁺-2CO] (1.6), 508 [M⁺-3CO] (2.8), 480 [M⁺-4CO] (4.5), 452 [M⁺-5CO] (9.3), 424 [M⁺-6CO] (2.6) 365 [M⁺-6COCo] (7.5), 306 [C₂₁H₂₂O₂] (11.2).

Calculated: C% 54.75 H% 3.74

Found: C% 54.91 H% 3.95

1e-Co

From **E1e** (0.5 g, 1.56 mmol) dissolved in CH₂Cl₂ (50 mL) and Co₂(CO)₈ (0.59 g, 1.72 mmol). The crude product was purified by flash column chromatography with ligroin/diethyl ether (9:1) in order to obtain only the E-isomer as a red-brown oil.

C₂₈H₂₄Co₂O₈ 606.36

(Z)-1e-Co

Yield: 0.71 g, 1.19 mmol, (75%)

¹H NMR (400 MHz, CDCl₃): δ = 0,91 (t, 3H, CH₃); 1,40 (m, 4H, CH₂CH₂); 2,78 (t, 2H, CH₂); 3,71 (s, 3H, OCH₃); 3,72 (s, 3H, OCH₃); 6.4 (s, 1H, C≡CH); 6,62

(AA'BB'³J = 8,7 Hz, 2H, ArH-3, ArH-5); 6,68 (AA'BB'³J = 8,7 Hz, 2H, Ar'H-3, Ar'H-5); 6,90 (m, 4H, ArH-2, ArH-6, Ar'H-2, Ar'H-6).

MS (EI, 100°C): m/z (%) =606 [M]⁺⁺ (0.8), 578 [M⁺-CO] (1.5),), 550 [M⁺-2CO] (2.3), 522 [M⁺-3CO] (21.4), 494 [M⁺-4CO] (7.7), 466 [M⁺-5CO] (12.2), 438 [M⁺-6CO] (2.6) 379 [M⁺-6COCO] (6.7), 320 [C₂₁H₂₂O₂] (14.8).

Calculated: C% 56.5 H% 5.01 with diethyl ether

Found: C% 56.8 H% 4.59

(E)-1e-Co

Yield: 0.10 g, 0.17 mmol, (11%)

MS (EI, 100°C): m/z (%) =606 [M]⁺⁺ (0.8), 578 [M⁺-CO] (1.5),), 550 [M⁺-2CO] (2.3), 522 [M⁺-3CO] (21.4), 494 [M⁺-4CO] (7.7), 466 [M⁺-5CO] (12.2), 438 [M⁺-6CO] (2.6) 379 [M⁺-6COCO] (6.7), 320 [C₂₁H₂₂O₂] (14.8).

Calculated: C% 56.5 H% 5.01 with diethyl ether

Found: C% 56.8 H% 4.59

2a-Co

From **2a** (0.5 g, 1.47 mmol) dissolved in CH₂Cl₂ (50 mL) and Co₂(CO)₈ (0.61 g, 1.77 mmol). The crude product was purified by flash column chromatography with ligroin/diethyl ether (9:1) in order to obtain only the E-isomer as a red-brown oil.

C₃₁H₂₂Co₂O₇ 624,37

Yield: 0.72 g, 1.15 mmol, (79%)

MS (EI, 100°C): m/z (%) =624 [M]⁺⁺ (0.8), 596 [M⁺-CO] (1.5),), 568 [M⁺-2CO] (2.3), 540 [M⁺-3CO] (21.4), 494 [M⁺-4CO] (7.7), 466 [M⁺-5CO] (12.2), 438 [M⁺-6CO] (2.6) 379 [M⁺-6COCO] (6.7), 353 [C₂₁H₂₂O₂] (14.8).

Calculated: C% 59.63 H% 3.55

Found: C% 56.8 H% 4.59

2b-Co

From **2b** (0.5 g, 1.47 mmol) dissolved in CH₂Cl₂ (50 mL) and Co₂(CO)₈ (0.61 g, 1.77 mmol). The crude product was purified by flash column chromatography with ligroin/diethyl ether (9:1) in order to obtain only the E-isomer as a red-brown oil.

C₄₀H₂₄Co₄O₁₄ 964.34

Yield: 1.23 g, 1.27 mmol, (87%)

MS (EI, 100°C): m/z (%) =964 [M]⁺ (0.8), 936 [M⁺-CO] (1.5), , 908 [M⁺-2CO] (2.3), 880 [M⁺-3CO] (21.4), 494 [M⁺-4CO] (7.7), 466 [M⁺-5CO] (12.2), 438 [M⁺-6CO] (2.6) 379 [M⁺-6COC_o] (6.7), 320 [C₂₁H₂₂O₂] (14.8).

Calculated: C% 49.82 H% 2.51

Found: C% 56.8 H% 4.59

7.1.2.7 Alkylation of the ethanone

A solution of 1,2-diphenylethanone (**B2a**) in dry THF was cooled to -78° C. Under Argon 1.2 Åq of KHMDS were carefully added and the reaction was allowed at -78°C for 1hour, after then ethyl iodide dissolved in dry THF was added dropwise. The mixture was warmed up to room temperature and was stirred for 12 hours. The reaction was decomposed with water and the layers were separated.

The aqueous phase was washed with ethylacetate. The organic fractions were combined, extracted with distilled water, brine, dried over Na₂SO₄, filtered and the filtrate was evaporated to dryness to obtain a colorless oil. The crude product was only if necessary purified by column chromatography on silica gel with diethyl ether/ligroin.

1,2-diphenylbutan-1-one C2a

From 1,2-diphenylethanone (3g, 15,3 mmol) in 80 mL THFabs., KHMDS 0,5M in toluol (36,7 mL, 18,4 mmol) and ethyl iodide (1,22 mL in 30 ML THFabs., 15,3 mmol). Any purification was necessary.

C₁₆H₁₆O 224,3

Yield: 3,1 g, 13,8 mmol, 91,2%

¹H NMR (400 MHz, CDCl₃): δ = 0,90 (s,3H, CH₃);1,87 (m, 1H, CH₂); 2,20 (m, 1H, CH₂);4,44 (t, 1H, CH)

1-(4-methoxyphenyl)-2-phenylbutan-1-one C2b

From **B2a** (3 g, 13,2 mmol) in 80 mL THFabs., KHMDS 0,5M in toluol (31,8 mL, 15,9 mmol) and ethyl iodide (1,1 mL in 30 ML THFabs., 13,2 mmol). Any purification was necessary.

C₁₇H₁₈O₂ 254,32

Yield: 3,2 g, 12,6 mmol, 95%

¹H NMR (400 MHz, CDCl₃): δ = 0,89 (t, 3H, CH₃); 1,84 (m, 1H, CH₂); 2,19 (m, 1H, CH₂); 3,81 (s, 3H, OCH₃); 4,39 (t, 1H, CH); 6,86 (AA'BB'³J = 8,8 Hz, 2H, ArH-3, ArH-5); 7,25 (m, 5H, Ar'H); 7,96 (AA'BB'³J = 8,8 Hz, 2H, ArH-2, ArH-6)

7.1.2.8 Grignard -general method-

From Mg (mmol) and 4-bromoanisole (mmol) in dry THF was generated the Grignard's reagent 4-methoxyphenylmagnesium bromide. To this suspension was added dropwise a solution of the corresponding ketone in THF abs and the mixture was refluxed. After 12 hours the reaction was cooled to room temperature and decomposed with ice and HCl 6N in order to loose(dissolving) the magnesiumhydroxide's precipitate. The two layers were separated and the remaining aqueous solution was extracted with diethyl ether. The organic layer were combined, washed with saturated NaHCO₃ solution and water, dried over Na₂SO₄, filtered and evaporated to dryness to obtain the carbinol.

To complete the dehydration, HBr 47% was added dropwise to a solution of the crude product in THF abs. under cooling. The mixture was stirred for 2 h, poured onto ice, and extracted with dichloromethane. The organic layer was washed with NaHCO₃ solution, water, dried with anhydrous sodium sulphate and concentrated. The residue was recrystallised from light petroleum-diethylether to give the compound.

(Z)-(1-(4-methoxyphenyl)but-1-ene-1,2-diyl)dibenzene E2a

The Grignards reagent was generated from Mg (0.4 g, 0,016 mol) and 4-Bromoanisole (2.1 mL, 0.016 mol) in ca 10-15 mL dry THF. After 1 hour **C2a** (3.1 g, 0.014 mol) was added and the mixture was refluxed for 12 hours. After the work up to the crude product was added H₃PO₄ and a white solid was obtained. The crude product was purified by crystallization from ligroin-diethyl ether

C₂₃H₂₂O 314.42

Yield: 3.8 g, 0.012 mol, 85.7%

¹H NMR (400 MHz, CDCl₃): δ = 0.92 (t, 3H, CH₃); 2,45 (q, 2H, CH₂); 3.67 (s, 3H, OCH₃); 6.54 (AA'BB'³J = 8,7 Hz, 2H, ArH-3, ArH-5); 6.78 (AA'BB'³J = 8.7 Hz, 2H, ArH-2, ArH-6); 7.11-7,36 (m, 10H, Ar'H-Ar'H)

1,1-Bis(4-methoxyphenyl)-2-phenylbut-1-ene E2b

The Grignards reagent was generated from Mg (0,37 g, 15 mmol) and 4-Bromoanisole (1,9 mL, 15 mmol) in ca 10-15 mL dry THF. After 1 hour **C2b** (3,2 g, 12 mmol) was added and the mixture was refluxed for 12 hours. After the work up to the orange oil HBr 47% was added and a white solid was obtained.

C₂₄H₂₄O₂ 344,45

Yield: 3,3 g, 9,6 mmol, 77%

¹H NMR (400 MHz, CDCl₃): δ = 0,93 (t, 3H, CH₃); 2,48 (q, 2H, R₂C=CR-CH₂CH₂); 3,67 (s, 3H, OCH₃); 3,82 (s, 3H, OCH₃); 6,54 (AA'BB'³J = 8,7 Hz, 2H, ArH-3, ArH-5); 6,77 (AA'BB'³J = 8,7 Hz, 2H, ArH-2, ArH-6); 6,88 (AA'BB'³J = 8,6 Hz, 2H, ArH-3, ArH-5); 7,07-7,18 (m, 7H, ArH-ArH)

7.1.2.9 Ether Cleavage with BBr₃

After cooling to -60°C a solution of 1 equiv of the appropriate methylether in dry dichloromethane, Boron tribromide dissolved in CH₂Cl₂ was added via a syringe under Argon atmosphere. The red mixture was warmed to room temperature and stirred for one day. The excess reagent was destroyed by the addition of dry MeOH under cooling (three times) and the solvent was removed under reduced pressure.

(Z)-4-(1,2-diphenylbut-1-enyl)phenol F2a

From **E2a** (0,4 g, 1,3 mmol) and BBr₃ (0,18 mL, 1,9 mmol). The reaction was stirred for 22 hours and a brown oil was obtained.

C₂₂H₂₂O 300,39

Yield: 0,3 g, 1 mmol, 79%

¹H NMR (400 MHz, DMSO): δ = 0,86 (t, 3H, CH₃); 2,43 (q, 2H, CH₂); 4,15 (s, 1H, OH); 6,76 (AA'BB'³J = 8,4 Hz, 2H, ArH-3, ArH-5); 6,78 (AA'BB'³J = 8,4 Hz, 2H, ArH-2, ArH-6); 6,96-7,39 (m, 10H, Ar'H-Ar''H)

4,4'-(2-phenylbut-1-ene-1,1-diyl)diphenol F2b

From **E2b** (1 g, 2,9 mmol) and BBr₃ (0,18 mL, 8,7 mmol). The reaction was stirred for 22 hours and a brown oil was obtained.

C₂₂H₂₀O₂ 316,39

Yield: 0.82 g, 2,7 mmol, 89%

¹H NMR (400 MHz, DMSO): δ = 0,92 (t, 3H, CH₃); 2,47 (q, 2H, CH₂); 6, 39 (AA'BB'³J = 8,5 Hz, 2H, ArH-3, ArH-5); 6,65 (AA'BB'³J = 8,5 Hz, 2H, ArH-2, ArH-6);); 6, 76 (AA'BB'³J = 8,6 Hz, 2H, Ar'H-3, Ar'H-5); 7,01 (AA'BB'³J = 8,6 Hz, 2H, Ar'H-2, Ar'H-6); 7,06-7,17 (m, 5H, (C2)ArH)

7.1.2.10 O-Alkylation

A solution of the corresponding hydroxyl compounds in N,N-dimethylformamide was added at laboratory temperature to a stirred suspension of sodium hydride (g of a 50% dispersion in mineral oil from which the oil had been removed by washing with n-hexane) in DMF under an atmosphere of argon. The mixture was stirred for 30 minutes, after then the alkylbromide was added. The reaction was stirred for a further 30 minutes and then poured into saturated aqueous ammonium chloride solution.

The mixture was extracted three times with diethyl ether and the combined extracts were washed five times with water, dried and evaporated to dryness. The residue was crystallized from ethanol.

(Z)-(E)-(1-(4-(prop-2-ynoxy)phenyl)but-1-ene-1,2-diyl)dibenzene 2a

From **F2a** (0.3 g, 1 mmol) dissolved in 10 mL dry DMF, NaH 60% (0.06 g, 3 mmol) and propargylbromide 80% (0.14 mL, 1.3 mmol).

C₂₅H₂₂O 338.44

Yield: 0.27 g, 0.8 mmol, 79%

¹H NMR (400 MHz, CDCl₃): δ = 0,93 (t, 3H, CH₃); 2,42-2,54 (m, 3H, R₂C=CR-CH₂ und ORC≡CH); 4,54 (d, 1H, OCH₂CR); 4,71 (d, 1H, CH₂CR); 6, 61 (AA'BB'³J = 8,8 Hz, 1H, ArH-3); 6,79 (AA'BB'³J = 8,8 Hz, 2H, ArH-2); 6,68-7,36 (m, 12H, ArH)

Calculated: C% 88.24 H% 6.79 with water

Found: C% 88.02 H% 6.53

Z)-(1-(4-(allyloxy)phenyl)but-1-ene-1,2-diyl)dibenzene 2b

From **F2a** (1 g, 3.3 mmol) dissolved in 15 mL dry DMF, NaH 60% (0.2 g, 0.01 mol) and allylbromide (0,38 mL, 4.3 mmol).

C₂₅H₂₄O 340,46

Yield: 0.86g, 2,5 mmol, 75%

¹H NMR (400 MHz, CDCl₃): δ = 0,92 (t, 3H, CH₃); 2,48 (q, 2H, R₂C=CR-CH₂); 4,33 (d, 1H, OCH₂CR); 4,50 (d, 1H, OCH₂CR); 5,16-5,42 (m, 2H, ORCR=CH₂); 5,89-6,07 (m, 1H, ORCH=CR); 6,54 (AA'BB'³J = 8,6 Hz, 1H, ArH-3); 6,77 (AA'BB'³J = 8,8 Hz, 2H, ArH-2); 6,87-7,33 (m, 12H, ArH)

Calculated: C% 88.20 H% 7.11

Found: C% 87.91 H% 7.09

4,4'-(2-phenylbut-1-ene-1,1-diyl)bis((prop-2-ynoxy)benzene) 2c

From **F2b** (1 g, 3,2 mmol) dissolved in 20 mL dry DMF, NaH 60% (0,46 g, 0,02 mol) and propargylbromide 80% (0,9 mL, 8,2 mmol).

C₂₈H₂₄O₂ 392,18

Yield: 0,84g, 2,1 mmol, 70%

¹H NMR (400 MHz, CDCl₃): δ = 0,92 (t, 3H, CH₃); 2,44-2,55 (m, 4H, R₂C=CR-CH₂ und ORC≡CH); 4,55-4,71 (m, 4H, OCH₂CCR); 6,59-7,35 (m, 13H, ArH)

Calculated: C% 81.92 H% 6.38 with water

Found: C% 88.7 H% 6.04

4,4'-(2-phenylbut-1-ene-1,1-diyl)bis(allyloxybenzene) 2d

From **F2b** (0.5 g, 1,6 mmol) dissolved in 15 mL dry DMF, NaH 60% (0.2 g, 0,01 mol) and allylbromide (0.36 mL, 4.1 mmol).

C₂₈H₂₈O₂ 396.52

Yield: 0.36 g, 0.9 mmol, 57%

¹H NMR (400 MHz, CDCl₃): δ = 0.92 (t, 3H, CH₃); 2.47 (q, 2H, R₂C=CR-CH₂); 4,38-4,56 (m, 4H, OCH₂CR); 5.21 (m, 4H, ORCR=CH₂); 5.94-6.13 (m, 2H, ORCH=CR); 6.54-7.35 (m, 13H, ArH)

Calculated: C% 81.13 H% 7.29 with water

Found: C% 80.74 H% 7.12

8 Pharmacological Part

8 Pharmacological Part

8.1 Cell lines

MCF-7: human, hormone dependent cancer cell line

MDA-MB-231: Human, hormone independent cancer cell line

U2-OS: osteogenic sarcoma cell line

Plasmid: p(ERE)₂-luc⁺

pSG5-ER α

pSG5-ER β

8.2 Cell culture conditions

8.2.1 Growth conditions

Cell line banking and quality control are performed according to the seed stock concept reviewed by Hay¹⁴⁵. MCF-7 and MDA-MB-231 cells are cultivated as a monolayer culture at 37° C in a humidified atmosphere (95% air, 5% CO₂) in 25 cm² culture flasks (T-25) using DMEM (Dulbecco's Modified Eagle Medium) supplemented with FCS 5% (V/V) as growth medium. U2-OS cells were maintained as a monolayer culture at 37 °C under a humidified atmosphere (92.5% air, 7.5% CO₂) in T-25 flasks. All manipulations of cells including seeding are performed in a laminar flow biohood and cell culture was conducted in a traditional cell culture incubator. The medium change is done every few days depending on growth curve of the cells. The MCF-7 and MDA-MB-231 cell lines are passaged weekly and medium is changed after 3-4 days of incubation. Whereas U2-OS are passaged twice per week. When the cells are 70-90% confluent perform a second passage into a new flask. At this moment, the old medium is removed and the cells were washed with PBS. Trypsin solution is distributed over the surface of the flask to detach the cells and is afterwards removed. The flask is incorporated into the incubator for 2 min. At last the cells are resuspended in fresh medium

and an appropriate aliquot volume of cell suspension (approximately 1/10 dilution) is incorporated into new flasks with fresh medium.

8.2.2 Determination of cell concentration

The number of cells is determined with a new building telling chamber, which consist of eight large squares, with a volume of 1 μL each. The cell suspension is up-pipetted with laterally and sucks themselves through capillary strength into the chamber. Before the counting a glass cover panel is pushed with something pressure on the chamber in order to see the Newton's rings. The counting takes place under the optical microscope. During counting it is important that one does not count lying cells doubly on boundary lines. For this it is usually during the counting of a square only the cells on two boundary lines (e.g. to take in account above and left) and on other are appropriate for two lines not. Finally the mean value is multiply by 10^4 in order to obtain the cells number per mL.

8.3 In-vitro chemosensitivity assays

The in-vitro testing of the compounds is carried out on exponentially dividing cancer cells according to a previous published microtiter assay with some modifications(bio). Exponential cell growth is ensured during the complete time of incubation.

8.3.1 Cell seeding

At the beginning of the experiment, an amount of 100 μL of a cell suspension in culture medium at 7.500 cells/mL (MCF-7 and MDA-MB-231) is plated into each well of a 96-well microtiter plate, after determining the cell concentration in the initial cell suspension. The plates are incubated at 37 $^{\circ}\text{C}$ for 3 days in a humidified atmosphere at growing conditions.

8.3.2 Addition of the substances

After dissolving the test compounds in DMF to allow 10 mM stock solutions, they are diluted to the chosen concentrations. The substance solution (10 μL) or DMF are added to the growth medium (5 mL DMEM). Thus, the drug-containing medi-

um (100 µL) are incorporated to the 96-well microtiter plate in order to obtain the final test concentrations. For each test concentration and for the control corresponding to DMF, which are used for the preparation of the stock solutions, are used four wells per plate.

➤ “Two-concentrations” test

The substances are tested in the two higher concentrations (20 and 10 µM). Only for the substances which are cytotoxic in this test (with a T/C_{corr} value < 50% at 20 µM and lower concentration) are performed further cytotoxicity measurements. The substances are pipetted of the 96-wells microtiter plate following the scheme shown in Fig. 1.

DMF	0.1%	DMF	0.1%	substance 4	10
	0.31		0.2%		20
	0.63	substance 1	10	substance 5	10
	1.25		20		20
cisplatin	2.5	substance 2	10	substance 6	10
	5		20		20
	10	substance 3	10	substance 7	10
	20		20		20

Figure 8.1. Pipetting scheme in the “two-concentrations” assay. Concentrations are given in µM.

➤ Time- and concentration-dependent cytotoxicity and IC_{50} determination assays

To determine the IC_{50} values, solutions of each compound are prepared by diluting the stock solutions to give five different concentrations (ranging from 1.25 to 20 µM). The solutions are added to the 96-wells microtiter plate following the scheme in Fig. 2. If the initial tested concentrations produced strong tumour growth inhibition, even at the lowest concentrations, the test is repeated with less concentrated solutions. As negative control were used DMF 0.1 %, which are

pipetted to the wells (16 per plate). Cisplatin at various concentrations (ranging from 0.63 to 10 μM) is used in each test as a positive control. Finally one extra plate (without substance solution) on each test is seeded to determine the initial cell density (t_0 plate).

In the time- and concentration-dependent cytotoxicity assay, is used the same concentrations and pipetting scheme as in the IC_{50} determination test. The main difference is that each substance is added (with the same concentration pattern) in five different plates, in order to fix the cells at five different times. Cisplatin at various concentrations (ranging from 0.63 to 10 μM) is used in each test as a positive control. One extra plate (without substance solution) on each test is seeded to determine the initial cell biomass (t_0 plate).

DMF	Cisplatin					DMF	Substance 1				
	0.63	1.25	2.5	5	10		1.25	2.5	5	10	20
DMF	Substance 2					DMF	Substance 3				
	1.25	2.5	5	10	20		1.25	2.5	5	10	20

Figure 8.2. Pipetting scheme in the “time- and concentration-dependent cytotoxicity” and “ IC_{50} determination” assays. Concentrations are given in μM .

8.3.3 Cell fixation

The initial cell density is determined by addition of glutaric dialdehyde (1% in PBS, 100 μL per well). After the appropriated incubation time had been reached (4–7 days), the medium is removed and the cells are fixed with glutaric dialdehyde (1% in PBS, 100 μL per well). After 15 min of incubation, the solution is decanted and 180 μL of PBS per well was added. The plates are stored at 4° C until staining.

In the case of *the* “two-concentrations” and “IC₅₀ determination” assays the incubation time is 72 (MDA-MB-231) or 96 (MCF-7) hours. In the “time- and concentration-dependent cytotoxicity” assay, the fixation of the cells is carried out after 48, 72, 96, 120 and 144 hours of incubation.

8.3.4 Cell staining and evaluation

The cell biomass is determined by crystal violet staining according to the following procedure: the PBS (pH 7.4) is removed and replaced with 0.02% aqueous crystal violet solution (100 µL/well). All plates are incubated for 30 min at room temperature, washed three times with water, and incubated on a softly rocking rotary shaker with 70% ethanol (180 µL) for further 3–4 hours. For automatic estimation of the optical density of the crystal violet extract, the absorption at 590 nm is measured using a microplate autoreader. The antiproliferative activity is expressed as corrected T/C_{corr} (%) or τ (%) value according to Eq. .1 and .2 respectively (see Section.2). The IC₅₀ values are determined using OriginPro 8, by interpolation from the *curve* which is based on a Boltzmann fit.

8.4 Luciferase assay: estrogenic and antiestrogenic activity

8.4.1 MCF-7-2a and U2-OS cells cultivation and transfection

MCF-7-2a cells are grown in the same conditions like MCF-7 cells as described above in section 9.2.2.1. Four days before starting the experiment, MCF-7-2a cells are cultivated in DMEM supplemented with L-glutamine, antibiotics and dextran/charcoal-treated FCS (ct-FCS, 50 mL/L). Cells from an 80% confluent monolayer are removed by trypsinization and suspended to approximately $\sim 10^5$ cells/mL in the growth medium mentioned above. The cell suspension is then cultivated in six 96-well flat-bottomed plates (0.5 mL cell suspension and 2 mL medium per well) at growing conditions (see above).

U2-OS cells are transferred to DMEM supplemented with ct-FCS, 24 hours before the experiment started. Cells from a nearly confluent monolayer are split and seeded in Petri dishes ($\varnothing = 10$ cm) at a concentration of 1×10^6 cells per dish at least 24 hours prior to transfection. According to the manufacturer’s instruc-

tions, after 6 hours is carried out a transient transfection of the cells with receptor plasmid pSG5-ER α or pSG5-ER β (0.05 μ g) and the reporter plasmid p(ERE)₂-luc⁺ using Fugene 6 (15 μ L). After 18 hours the cells are washed with PBS and harvested by trypsinization and seeded with 96-wells plates at the concentration of 10⁴ cells per well in 100 mL ct-DMEM.

8.4.2 Addition of the substances

8.4.2.1 Dilution from stock solutions

After trasfection, different diluted solutions of the test compounds are added to a 96-well plate. The dilution is obtained following the scheme in Fig. 3. First of all, PBS (90 μ L) is pipetted in each well. In the A line, 10 μ L of a stock solution of E2 (10⁻⁵ M) and of the test compounds (10⁻² M) was added. For each test concentration three wells are used.

	1	2	3	4	5	6	7	8	9	10	11	12
A	E2		10 ⁻⁶	Compound 1		10 ⁻³	Compound 2		10 ⁻³	Compound 3		10 ⁻⁵
B			10 ⁻⁷			10 ⁻⁴			10 ⁻⁴			10 ⁻⁴
C			10 ⁻⁸			10 ⁻⁵			10 ⁻⁵			10 ⁻⁵
D			10 ⁻⁹			10 ⁻⁶			10 ⁻⁶			10 ⁻⁶
E			10 ⁻¹⁰			10 ⁻⁷			10 ⁻⁷			10 ⁻⁷
F			10 ⁻¹¹			10 ⁻⁸			10 ⁻⁸			10 ⁻⁸
G			10 ⁻¹²			10 ⁻⁹			10 ⁻⁹			10 ⁻⁹
H			10 ⁻¹³			10 ⁻¹⁰			10 ⁻¹⁰			10 ⁻¹⁰

Figure 8.3. Dilution scheme of stock solutions in the Luciferase assay.

To afford the chosen concentrations, 10 μ L of each wells in the A line are transferred to each wells in the line B. This carrying method, which is used until the H line, corresponds to a 1:10 dilution.

8.4.2.2 Transfer of the diluted solutions to the microtiter test plates

For the estrogenic and antiestrogenic tests, the medium is removed and replaced with 90 μ L of a new one. The test compounds are carried over from the first plate and diluted directly in the test plate to final concentrations ranging from 10⁻⁵ to 10⁻¹¹ M (estradiol, E2: 10⁻⁸ to 10⁻¹⁴ M) following the scheme in Fig. 4. The plates are incubated for 50 hours.

	1	2	3	4	5	6	7	8	9	10	11	12
A	DMSO		0.01%	DMSO		0.01%	DMSO		0.01%	DMSO		0.01%
B	E2		10^{-8}	Compound 1		10^{-5}	Compound 2		10^{-5}	Compound 3		10^{-5}
C			10^{-9}			10^{-6}			10^{-6}			10^{-6}
D			10^{-10}			10^{-7}			10^{-7}			10^{-7}
E			10^{-11}			10^{-8}			10^{-8}			10^{-8}
F			10^{-12}			10^{-9}			10^{-9}			10^{-9}
G			10^{-13}			10^{-10}			10^{-10}			10^{-10}
H			10^{-14}			10^{-11}			10^{-11}			10^{-11}

Figure 4. Pipetting scheme in the Luciferase assay.

8.4.2.3 Cells lysis and Luciferase activity

After incubation and before harvesting, the cells are washed twice with PBS. The cell culture lysis reagent (50 μ l) is added into each well. After 30 min of lysis at room temperature, the cells are transferred into reaction tubes and centrifuged. Luciferase is assayed using the Promega luciferase assay reagent. Fifty microliters of each supernatant is mixed with 50 μ l of substrate reagent. Luminescence (in relative light units (RLU)) is measured for 10 s using a luminometer. Measurements are corrected by correlating the quantity of protein (quantified according to Bradford¹⁴⁶) of each sample with the mass of luciferase. Estrogenic activity is expressed as percentage activation of a 10^{-8} M estradiol control (100%).

To evaluate the antagonistic activity, the cells are incubated with a constant concentration of E2 (3×10^{-11} M for ER α ; 3×10^{-10} M for ER β) and in combination with increased concentrations (10^{-11} to 10^{-6} M) of inhibitor. The percentage activation is calculated in relation to the luciferase expression of E2 alone. The IC₅₀ value is taken from the concentration activation curve.

8.5 COX inhibitory activity

The inhibition of isolated ovine COX-1 and human recombinant COX-2 of Zeise' s complexes is determined using a "COX inhibitor screening assay kit", which is ready supplied to use from Cayman Chemicals. Experiments are performed according to the manufacturer's instructions.

8.5.1 COX inhibitor screening assay

The COX inhibitor screening assay directly measures $\text{PGF}_{2\alpha}$ by SnCl_2 reduction of COX-derived PGH_2 produced in the COX reaction. The prostanoid product is quantified *via* enzyme immunoassay (EIA) using a broadly specific antiserum that binds to all the major PG compounds. 96-wells plate(s) are used for the assay. Each plate contains the mouse monoclonal anti-rabbit IgG that has been *previously attached* to the well. Each well contains the rabbit antiserum-PG (either free or tracer), the PG tracer and the sample PG, respectively. The concentration of the PG tracer is held constant, while the concentration of PG varies. The amount of the PG tracer which is able to bind to the PG antiserum will be inversely proportioned to the concentration of PG in the well during the incubation. To remove any unbound reagents, the plate is washed. Afterward Ellman's Reagent, which contains the substrate to AChE, is added to the well. The product of this reaction (5-thio-2-nitrobenzoic acid) has a distinct yellow color and absorbs strongly at 415 nm.

8.5.1.1 Procedure of the COX-inhibitor screening assay

10 mmol/ L and 1 mmol/ L of the stock solutions (in DMF) are prepared for the test. The sample (20 μL), the inactive COX-1 or COX-2 (10 μL of each enzyme), and Heme (10 μL) are added to the test tubes (which contains 950 μL of reaction buffer) and pre-incubated for 10 min at $37^\circ\text{C}^{(k)}$. After the substrate arachidonic acid was added, the test tubes were incubated for 2 min at 37°C . To stop the enzyme catalysis HCl 1 M (50 μL) are added to each test tube. Test tubes are removed from the water bath and stannous chloride solution (100 μL) is added to each test tube and vortex in order to reduce PGH_2 to PGF_2 . After incubation for 5 min at room temperature, the reaction mixture became cloudy.

8.5.1.2 Plate set up

The sample is diluted with reaction buffer (950 μL), and pipetted to ELISA 96-wells plate (50 μL per well) following the scheme in Fig. 4. Prostaglandin E_2 screening standard is prepared, obtaining 8 clean test tubes with different con-

^(k) The incubation of the enzymes with the inhibitor can be between 10 and 20 min without affecting enzyme stability, but the incubation must be the same for all the samples in an individual experiments.

centrations. 50 μL from each test tube are pipetted to the plate. PG screening AChE tracer is also added to each well (50 μL) except to the Total Activity (TA) and the Blank (Blk) wells.

Blk	K1	K1	BC1	BC1	S3		S11		S4		S12
Blk	K2	K2	BC2	BC2	S4		S12		S5		
NSB	K3	K3	IA 1	IA 1	S5		S13		S6		S13
NSB	K4	K4	IA 1	IA 1	S6		S14		S7		
B ₀	K5	K5	IA 2	IA 2	S7		S15		S8		S14
B ₀	K6	K6	IA 2	IA 2	S8		S1	COX-1	S9		
B ₀	K7	K7	S1	COX-2	S9		S2		S10		S15
TA	K8	K8	S2		S10		S3		S11		

Figure 8.4. Pipetting scheme of COX-inhibitor screening assay

Blk	Blank, background absorbance caused by Ellman's reagent
TA	Total Activity of the AChE-linked tracer
NSB	Non-Specific Binding of the tracer to the well. Even in absence of specific antibody a very small amount of tracer still binds to the well
B ₀	Maximal Binding of the tracer that the antibody can bind in the absence of free analyte
BC1	Background COX-1
BC2	Background COX-2
IA 1	100 % COX-1 activity
IA2	100 % COX-2 activity
S1-S15	Samples

Each plate is covered with plastic film and incubated for 18 hours at room temperature. Finally the plate cover is removed and the Ellman's reagent (200 μL) is added to each well. Absorption was measured at 415 nm (Victor 2, Perkin Elmer). Results were calculated as the means of duplicate determinations.

8.5.2 PGE₂-assay

The concentration of PGF₂ α was measured using the enzyme immunoassay (EIA) of the same kit. All samples are added as dimethyl sulfoxide (DMSO) solutions to assay solutions, and all determinations were performed in triplicate (N = 3).

A cell suspension of MDA-MB-231 (400 μ L) was diluted with DMEM (40 mL) supplemented with FCS and the resulting 500 μ L of them were distributed in three 24-wells plates. Plates were conserved for one week in *cell* culture incubator. When about 70 % confluency was reached the old medium was replaced with 500 μ L of a new one, which contains 0.1 % of the test compounds stock solution and DMSO. After 23 hours of incubation, arachidonic acid solution was diluted with DMEM to 1/1000 and added to the test plate (50 μ L per well) in order to stimulate COX to convert the acid into PGE₂. The reaction is stopped by transferring 200 μ L of the medium, into the test tubes. The residual medium was removed and cells were washed with PBS. For measuring the Prostaglandin the medium is thinned by the provided EIA-buffer in a relation of 1:25. For quantification 50 μ L of the diluted assay is pipetted on a 96-wells plate. The procedure follow the same way as already described in the COX-assay

8.6 Materials and reactants

8.6.1 Instrumentation

- Accurate weight: BP 211D, Sartorius AG (Göttingen, Germany)
- Steam autoclave sterilizer: 2540 ELV, Systec GmbH (Wettenberg, Germany)
- Incubator Drying Chamber: B 5060 EK-CO₂, Heraeus Instruments (Hanau, Germany)
- Inverted microscope: Axiovert 25C, Carl Zeiss (Jena, Germany)
- Inverted microscope: Axiovert 40CFL, Carl Zeiss (Jena, Germany)
- Microplate reader: Flashscan S12, Analytik Jena AG (Jena, Germany)
- Sterile laminar flow cabinet: Lamin Air HB 2448, Heraeus Instruments (Hanau, Germany)
- Counting chamber: Neubauer 0.100 depth, 0.0025 mm², Carl Zeiss (Jena, Germany)
- Centrifuge: Megafuge 1.0R, Heraeus Instruments (Hanau, Germany); Eppendorf centrifuge 5417R, Eppendorf AG (Hamburg, Germany)

- Water bath: W26, Haake (Karlsruhe, Germany)
- Ultraschall bath Bandelin Sonorex Super RK106 Bandelin
- Eppendorf tube: Multipette® plus
- Multichannel pipette Eppendorf
- 8-channel Absauger : Integra Bioscience
- Magnet agitator : IKAMAG RCT IKA Labortechnik
- Multilabel Counter 1420 microplate : Wallac Victro 2 / Perkin Elmer
- ¹H-NMR spectrometer: Avance/DPX 400, Burker (Karlsruhe, Germany)
- UV-VIS Spectrometer: SPECORD 200, Analytikjena AG (Jena, Germany)
- Mass spectrometer: Agilent 6210 ESI-TOF, Agilent Technologies (Santa Clara, USA)

8.6.2 Used materials

- 96 MicroWell™ Plates: Nunc Brand products
- Single-use cannulas: B.Braun
- Single-use syringes: B.Braun
- Standard-Pasteur pipettes: Roth
- Pipette tips: Sarstedt AG Nümbrecht
- Parafilm: Peching Plastic Packaging, Menasha/USA
- Serological sterile pipettes 2 mL, 5 mL, 10, 25 mL: Sarstedt AG Nümbrecht
- 25 cm² cell culture flasks: Sarstedt AG Nümbrecht

8.6.3 Reactants and solutions

All chemicals, reagents and solvents were purchased – if not stated – from Sigma-Aldrich, VWR, Merck, Acros or Alfa Aesar. The laboratory consumables were purchased from Braun, Nunc, Merck and Sarstedt.

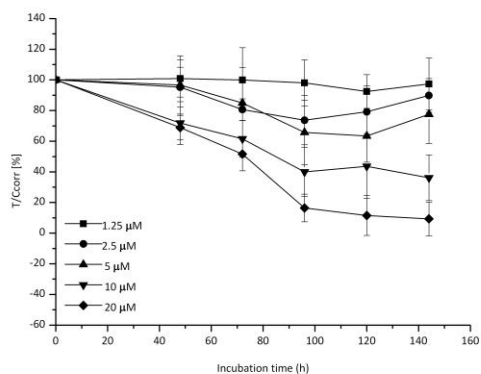
- Dulbecco's Modified Eagle Medium with phenol red and 4.5 g/L glucose (DMEM): PAA Laboratories GmbH (Pasching, Austria)
- Fetal calf serum (FCS): Biochrom AG (Berlin, Germany)

- Human serum albumin (HSA)
- Bradford reagent: 250 mg Serva Blue G, 250 mL ethanol (95%), 500 mL H₃PO₄ (86%) and 250 mL distilled H₂O. To perform the assay 1:5 dilution of the Bradford reagent in distilled H₂O
- Phosphate buffered saline (PBS): 0.2 g KH₂PO₄, 8 g NaCl, 1,44 g Na₂HPO₄·2H₂O, and 0,2 g KCl, dissolved in 1 L distilled H₂O
- Glutardialdehyde solution 1%: Glutardialdehyde 25% diluted in PBS
- Trypsin solution: 0.05% trypsin (ICN, Eschwege, Germany) and 0.02% EDTA in PBS. Sterile filtration of the solution using a 0.22 µm filter
- Hexamethylpararosaniline (crystal violet) solution 0.02%
- dextran/charcoal-treated FCS (Ct-FCS): 5% Norit A, 0.05% Dextran 60 in Tris-Buffer 200 mL (pH 7.5), centrifugation, stirring Pellet with 500 mL FCS for 3 hours at 4° C, filter out
- 17β- Estradiol: Fluka
- Luciferase assay reagents: Promega, Mannheim
- COX Inhibitor Screening Assay Kit: Cayman Chemicals

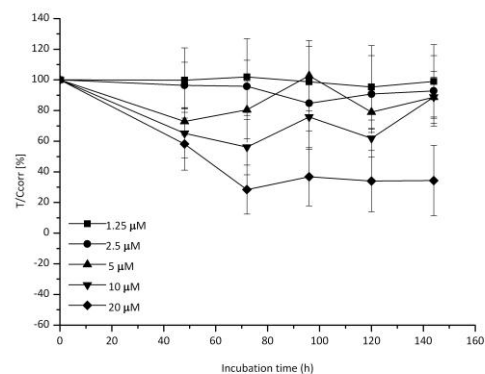
9 Appendix

9 Appendix: Time- and concentration-dependent cytotoxicity diagrams

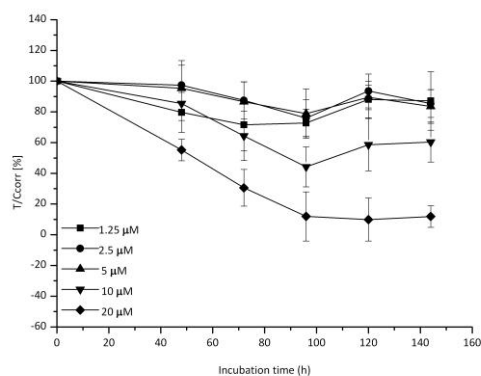
9.1 MCF-7



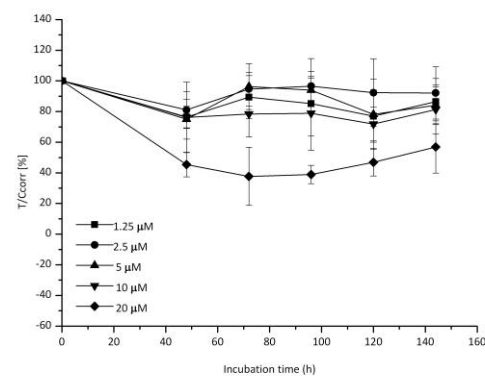
1a-Co



1a'-Co

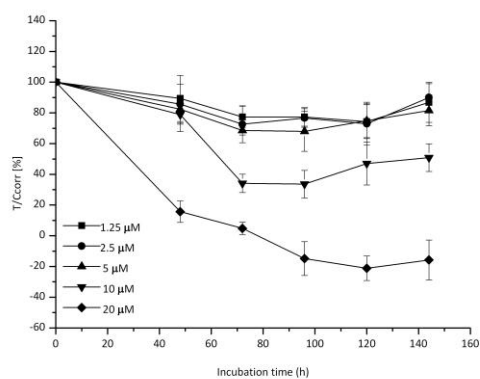


1b-Co

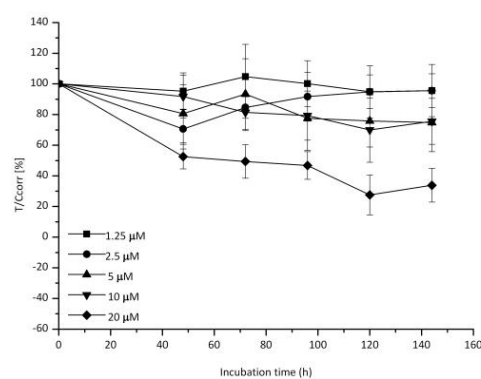


1b'-Co

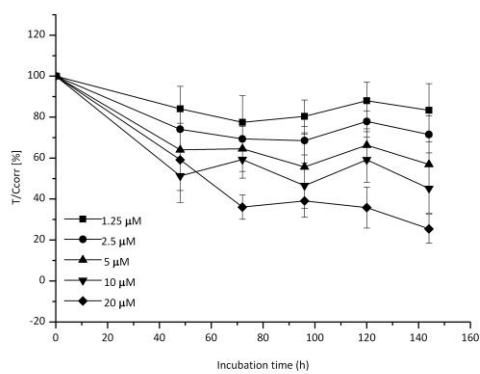
9 Appendix: Time- and concentration-dependent cytotoxicity diagram



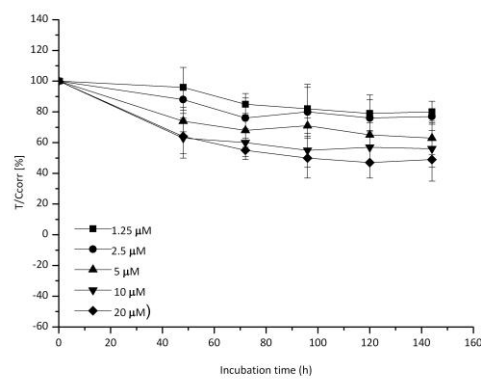
1c-Co



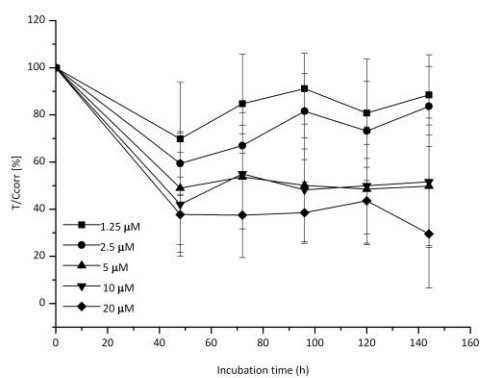
1c'-Co



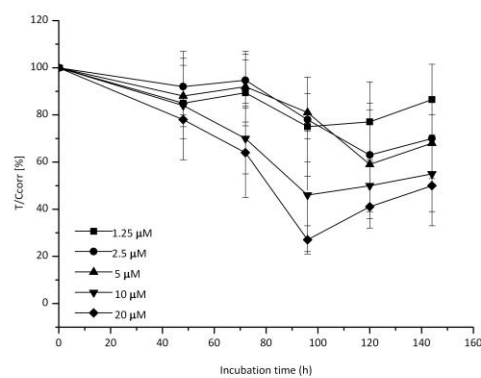
1d-Co



1d'-Co

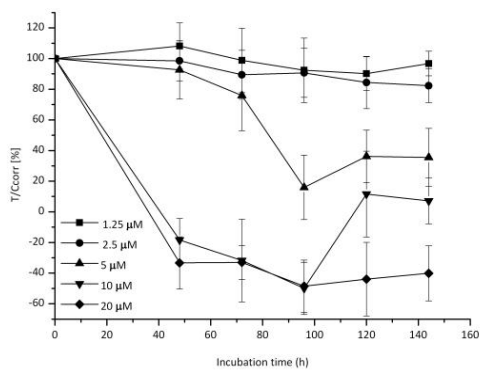


1e-Co

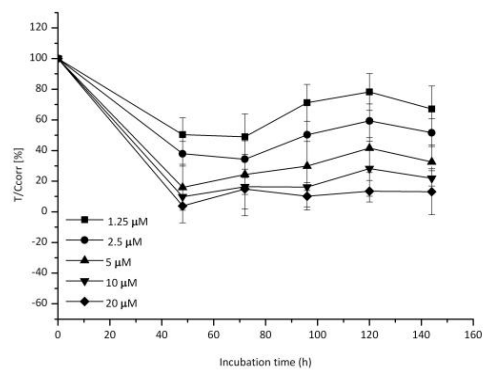


1e'-Co

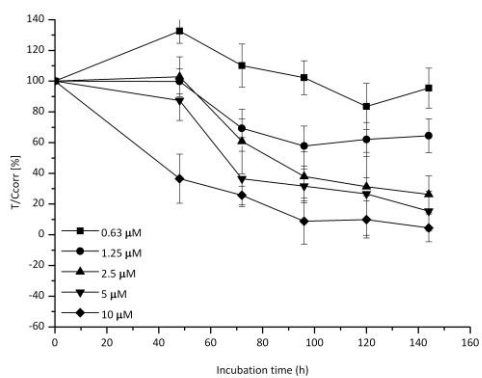
9 Appendix: Time- and concentration-dependent cytotoxicity diagram



2a

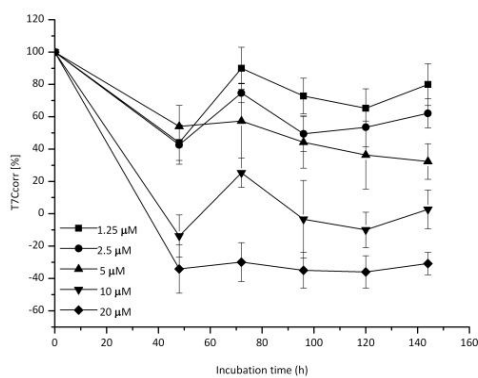
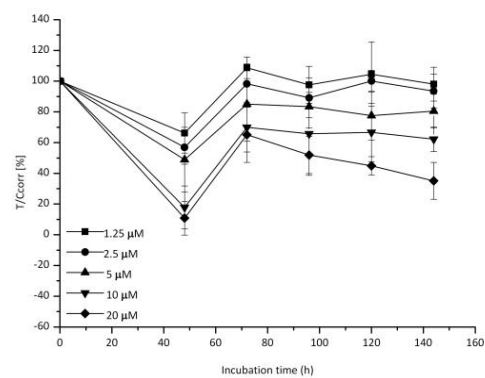
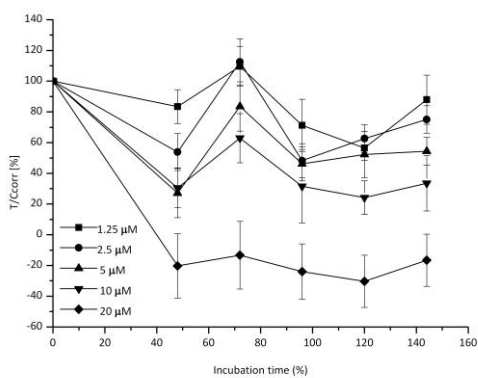
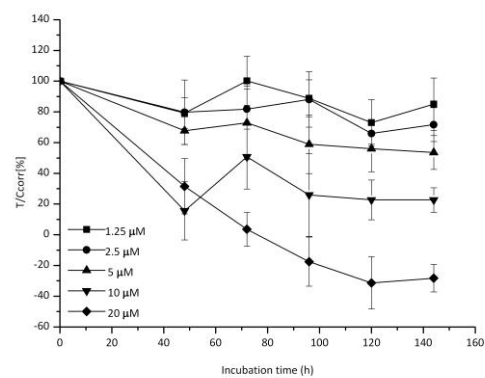
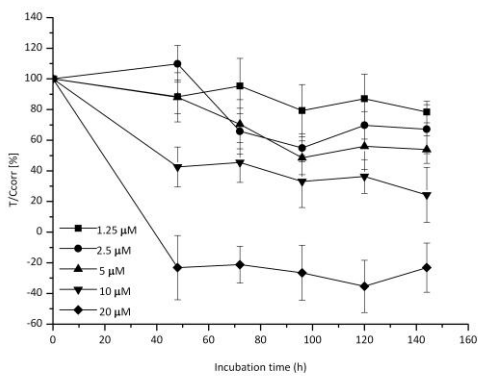
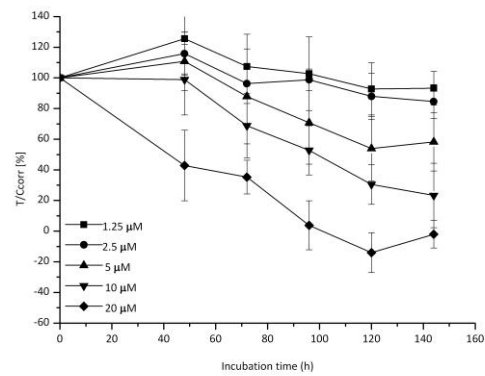


2c

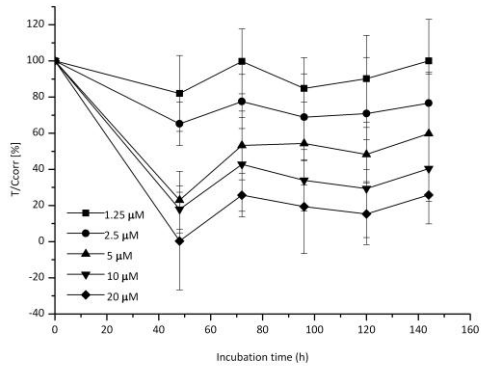


cisplatin

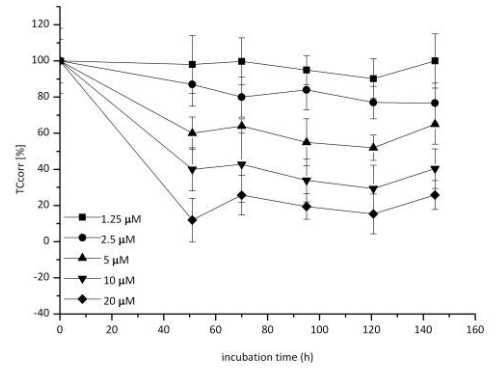
9.2 MDA-MB-231

**1a-Co****1a'-Co****1b-Co****1b'-Co****1c-Co****1c'-Co**

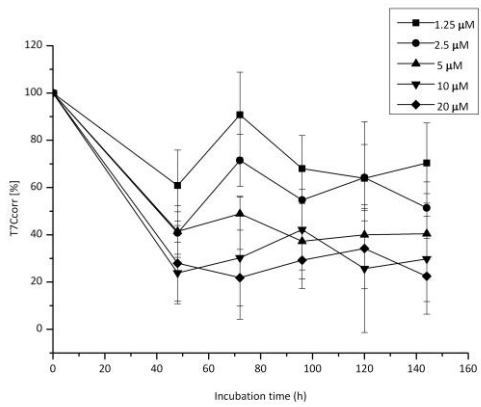
9 Appendix: Time- and concentration-dependent cytotoxicity diagram



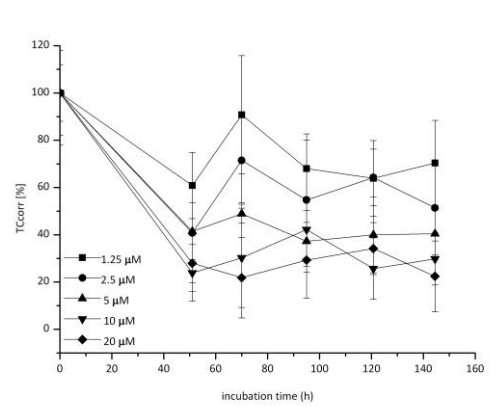
1d-Co



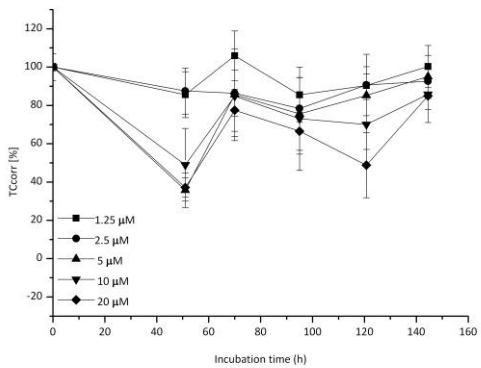
1d'-Co



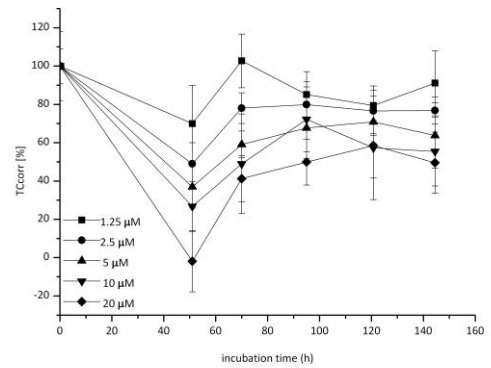
1e-Co



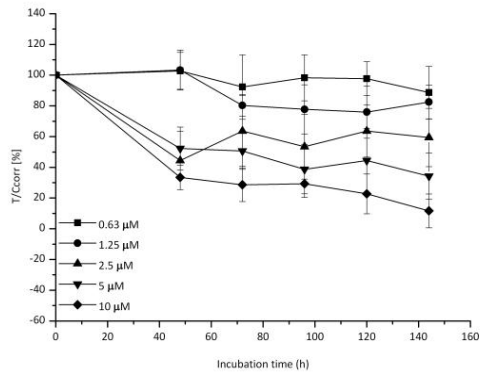
1e'-Co



2a



2c



cisplatin

Curriculum Vitae

For reasons of data protection,
the curriculum vitae is not included in the online version

References

- 1 Jemal, A.; Siegel, R.; Ward, E.; Hao, Y.; Xu, J.; Murray, T.; Thun, M.J. Cancer Statistics, 2008. *CA Cancer J Clin* **2008**, 58, 71–96.
- 2 World cancer Report 2011, IARC, 2011.
- 3 Airley, R. Cancer chemotherapy: basic science to the clinic. *Wiley-Blackwell*, **2009**, 67-111.
- 4 Batzler, W. U.; Giersiepen, K.; Hentschel, S.; Hausmann, G. et al. in Krebs in Deutschland 2003–2004. Häufigkeiten und Trends. Robert-Koch-Institut and Gesellschaft der epidemiologischen Krebsregister in Deutschland e.V. (Hrsg.), 6. Überarbeitete Auflage, Berlin, **2008**.
- 5 Becker, N.; Holzmeier, S. Cancer Epidemiology German Cancer Research Center Heidelberg, **2010**. http://www.dkfz.de/en/krebsatlas/total/organ_e.html; last request: 11.08.2012
- 6 Kamangar, F.; Dores, G.M.; Anderson, W.F. Patterns of cancer incidence, mortality, and prevalence across five continents: defining priorities to reduce cancer disparities in different geographic regions of the world. *J. Clin. Oncol* **2006**, 24, 2137–50.
- 7 DeSantis, C. et al. Breast cancer. Facts and figures, **2010**. <http://www.cancer.org/acs/groups/content/@nho/documents/document/f861009final90809pdf.pdf>; last request: 09.08.2012.
- 8 Ali, S.; Buluwela, L.; Coombes, R.C. Antiestrogens and their therapeutic applications in breast cancer and other diseases *Annu. Rev. Med.* **2011**, 62, 217–32.
- 9 Jordan, V. C. Antiestrogens and selective estrogen receptor modulators as multifunctional medicines. 1. Receptor interactions. *J. Med. Chem.* **2003**, 46, 883-908.
- 10 Singh, M. N.; Stringfellow, H. F.; Paraskevaidis, E.; Martin-Hirsch, P. L.; Martin, F. L. Tamoxifen: Important considerations of a multi-functional compound with organ-specific properties. *Cancer Treatment Reviews* **2007**, 33 (2), 91-100.
- 11 Winer, E. P.; Hudis, C.; Burstein, H. J.; Wolff, A. C.; Pritchard, K. I.; Ingle, J. N.; Chlebowski, R. T.; Gelber, R.; Edge, S. B.; Gralow, J.; Cobleigh, M. A.; Mamounas, E. P.; Goldstein, L. J.; Whelan, T. J.; Powles, T. J.; Bryant, J.; Perkins,

C.; Perotti, J.; Braun, S.; Langer, A. S.; Browman, G. P.; Somerfeld, M. R. American society of clinical oncology technology assessment on the use of aromatase inhibitors as adjuvant therapy for post-menopausal women with hormone receptor-positive breast cancer: status report 2004. *J Clin Oncol*. **2005**, 23, 619-629.

¹² Jensen, E.V.; Jordan, V.C. The estrogen receptor: a model for molecular medicine. *Clin. Cancer Res*. **2003**, 9, 1980-1989.

¹³ Walter, P.; Green, S.; Greene, G. Cloning of the human estrogen receptor cDNA. *Proc Natl Acad Sci USA* **1985**, 82, 7889–93.

¹⁴ Green, S.; Walter, P.; Kumar, V. Human oestrogen receptor cDNA: sequence. *Nature* **1986**, 320, 134–9.

¹⁵ Tremblay, G.B.; Tremblay, A.; Copeland, N.G. Cloning, chromosomal localization, and functional analysis of the murine estrogen receptor beta. *Mol Endocrinol* **1997**, 11, 353–65.

¹⁶ Enmark, E.; Peltö-Huikko, M.; Grandien, K. Human estrogen receptor beta-gene structure, chromosomal localization, and expression pattern. *J Clin Endocrinol Metab* **1997**, 82, 4258–65.

¹⁷ Komesaroff, P. A.; Sudhir, K., Estrogens and human cardiovascular physiology. *Reprod Fertil Dev* **2001**, 13, (4), 261-72.

¹⁸ Lee, C. H.; Edwards, A. M., Stimulation of DNA synthesis and c-fos mRNA expression in primary rat hepatocytes by estrogens. *Carcinogenesis* **2001**, 22, (9), 1473-81.

¹⁹ Qu, Q.; Perala-Heape, M.; Kapanen, A.; Dahllund, J.; Salo, J.; Vaananen, H. K.; Harkonen, P., Estrogen enhances differentiation of osteoblasts in mouse bone marrow culture. *Bone* **1998**, 22, (3), 201-9.

²⁰ Mangelsdorf, F.J.; Thummel, C.; Beato, M.; Herrlich, P.; Schutz, G.; Umesono, K.; Blumberg, B.; Kastner, P.; Mark, M.; Chambon P.; Evans, R. The nuclear receptor superfamily: The second decade. *Cell* **1995**, 83, 835–839.

²¹ Gustafsson, J. A., Estrogen receptor beta: a new dimension in estrogen mechanism of action. *J Endocrinol* **1999**, 163, (3), 379-83.

²² Leygue, E.; Dotzlaw, H.; Watson, P.H.; Murphy, L.C. Altered estrogen receptor alpha and beta messenger RNA expression during human breast tumorigenesis. *Cancer Res* **1998**, 58, 3197–201.

- ²³ Lazennec, G.; Bresson, D.; Lucas, A.; Chauveau, C.; Vignon, F., ER beta inhibits proliferation and invasion of breast cancer cells. *Endocrinology* **2001**, 142, (9), 4120-30.
- ²⁴ Pearce, S.T.; V. Craig Jordan, V.C. The biological role of estrogen receptors α and β in cancer. *Critical Reviews in Oncology/Hematology* **2004**, 50, 3–22.
- ²⁵ Mosselman, S.; Polman, J.; Kijkema, R. Identification and characterization of a novel human estrogen receptor. *FEBS Lett* **1996**, 392, 49-53.
- ²⁶ Fuqua, S.A.W.; Schiff, R. The biology of estrogen receptors, in Harris, J.R.; Lippman, M.E.; Morrow, M. *Diseases of the Breast* Philadelphia, PA, Lippincott Williams & Wilkins, **2004**, 3rd ed., 585-602.
- ²⁷ Kong, E. H.; Pike, A. C. W.; Hubbard, R. E. Structure and mechanism of the oestrogen receptor *Biochem. Soc. Trans.* **2003**, 31, 56-59.
- ²⁸ Menasce, L.P.; White, G.R.; Harrison, C.J.; Boyle, J.M. *Genomics* **1993**, 17, 263–265.
- ²⁹ Ruff, M.; Gangloff, M.; Wurtz, J.; Moras, M.D. Estrogen receptor transcription and transactivation: Structure-function relationship in DNA- and ligand-binding domains of estrogen receptors *Breast Cancer Res.* **2000**, 2, 353–359.
- ³⁰ Bai, Z.; Gust, R. Breast Cancer, Estrogen Receptor and Ligands *Arch. Pharm. Chem. Life Sci.* **2009**, 342, 133 – 149.
- ³¹ Muramatsu, M.; Inoue, S. Estrogen receptors: how do they control reproductive and nonreproductive functions? *Biochem. Biophys. Res. Commun.* **2000**, 270, 1–10.
- ³² Pace, P.; Taylor, J.; Suntharalingam, S.; Coombes, R.C.; Ali, S. Human estrogen receptor beta binds DNA in a manner similar to and dimerizes with estrogen receptor alpha. *J Biol Chem.* **1997**, 272(41), 25832-8.
- ³³ Osborne, C.K.; Schiff, R. Estrogen-Receptor Biology: Continuing Progress and Therapeutic Implications *J Clin Oncol* **2005**, 23, 1616-1622.
- ³⁴ Kushner, P.J.; Agard, D.A.; Greene, G.L.; Estrogen receptor pathways to AP-1. *J Steroid Biochem Mol Biol* **2000**, 74, 311-317.
- ³⁵ Edwards, D. P. Regulation of signal transduction pathways by estrogen and progesterone. *Annu. Rev. Physiol.* **2005**, 67, 335–376.

- ³⁶ Horard, B.; Vanacker, J.M. Estrogen receptor-related receptors: orphan receptors desperately seeking a ligand. *Journal of Molecular Endocrinology* **2003**, 31, 349–357.
- ³⁷ Dorssers, L.C.J.; van der Flier, S.; Brinkman, A.; van Agthoven, T.; Veldscholte, J.; Berns, E.M.J.J.; Klijn, J.G.M.; Beex, L.V.A.M.; Foekens, J.A. Tamoxifen Resistance in Breast Cancer: Elucidating Mechanisms *Drugs* **2001**, 61 (12), 1721-1733.
- ³⁸ McDonnell, D.P.; Clemm D.L.; Herman, T.; Goldman, M.E.; Pike, J.W. Analysis of estrogen receptor function in vitro reveals three distinct classes of antiestrogens. *Mol Endocrinol* **1995**, 9, 659-669.
- ³⁹ Ruff, M.; Gangloff, M.; Wurtz, J.; Moras, M. D. Estrogen receptor transcription and transactivation: structure-function relationship in DNA- and ligand-binding domains of estrogen receptors *Breast Cancer Res.* **2000**, 2, 353–359.
- ⁴⁰ Danielian, P. S.; White, R.; Lees, J.A.; Parker, M.G. Identification of a conserved region required for hormone dependent transcriptional activation by steroid hormone receptors. *EMBO J.* **1992**, 11, 1025–1033.
- ⁴¹ Moras, D.; Gronemeyer, H. The nuclear receptor ligand-binding domain: structure and function. *Curr. Opin. Cell Biol.* **1998**, 10, 384–391.
- ⁴² Katzenellenbogen, J.A.; Muthyala, R.; Katzenellenbogen, B.S. Nature of the ligand-binding pocket of estrogen receptor α and β : The search for subtype-selective ligands and implications for the prediction of estrogenic activity. *Pure Appl. Chem.* **2003**, 75 (11–12), 2397–2403.
- ⁴³ Shiau, A.K.; Barstad, D.; Loria, P.M.; Cheng, L. et al. The structural basis of estrogen receptor/coactivator recognition and the antagonism of this interaction by tamoxifen. *Cell* **1998**, 95, 927-937.
- ⁴⁴ Rosbenberg, B.; Van Camp, L.; Krigas, T. Inhibition of cell division in *Escherichia coli* by electrolysis products from a platinum electrode. *Nature*, **1965**, 205, 698-699.
- ⁴⁵ Jung, Y.; Lippard, S.J. Direct cellular responses to platinum-induced DNA damage. *Chem. Rev.* **2007**, 107(5), 1387-407.
- ⁴⁶ Ott, I.; Gust, R. Non Platinum Metal Complexes as Anti-cancer Drugs *Arch. Pharm. Chem. Life Sci.* **2007**, 340, 117-126.

- ⁴⁷ Corry, A.J. Novel Ferrocenyl benzoyl peptide esters as anti-cancer agents and Ferrocenoyl self assembled monolayers as anion sensors. **2009**, thesis 1-223.
- ⁴⁸ Gasser, G.; Ott, I.; Metzler-Nolte, N. Organometallic Anticancer Compounds *J. Med. Chem.* **2011**, 54, 3–25.
- ⁴⁹ Bruijninx P.C.A.; Sadler P.J. New trends for metal complexes with anticancer activity. *Curr. Opin. Chem. Biol.* **2008**, 12, 197-206.
- ⁵⁰ Thompson K.H.; Orvig C. Metal complexes in medicinal chemistry: new vistas and challenges in drug design. *Dalton Trans.* **2006**, 6, 761-764.
- ⁵¹ Ware, D.C.; Palmer, B.D.; Wilson, W.R.; Denny, W.A. Hypoxia-selective anti-tumor agents. 7. Metal-complexes of aliphatic mustards as a new class of hypoxia-selective cytotoxins – Synthesis and evaluation of cobalt(III) complexes of bidentate mustards. *J. Med. Chem* **1993**, 36, 1839-1846.
- ⁵² Ware, D. C.; Palmer, H. R.; Brothers, P. J.; Rickard, C. E. *Bis-tropolonato derivatives of Cobalt(III) complexes of bidentate aliphatic nitrogen mustards as potential hypoxia-selective cytotoxins* *J. Inorg. Biochem.* **1997**, 68, 215–224.
- ⁵³ Ahn, G. O.; Ware, D. C.; Denny, W. A.; Wilson, W. R. Optimization of the auxiliary ligand shell of cobalt(III)(8-hydroxyquinoline) complexes as model hypoxia-selective radiation-activated prodrugs. *Radiat. Res.* **2004**, 162, 315–325.
- ⁵⁴ Ahn, G.O.; Botting, K.J.; Patterson, A.V.; Ware, D.C. Radiolytic and cellular reduction of a novel hypoxia-activated cobalt(III) prodrug of a chloromethylbenzindoline DNA minor groove alkylator. *Biochem. Pharmacol.* **2006**, 71, 1683-1694.
- ⁵⁵ Gust, R.; Ott, I.; Posselt, D.; Sommer, K.; Development of cobalt(3,4 diarylsalen)complexes as tumor therapeutics. *J. Med. Chem.* **2004**, 47, 5837-5846.
- ⁵⁶ Hall, I.H.; Lackey, C.B.; Kistler, T.D.; Durham, R.W.; Jouad, E.M.; Khan, M.; Thanh, X.; Djebbar-Sid, S.; Benali-Baitich, O; Bouet, G. M. Cytotoxicity of copper and cobalt complexes of furfural semicarbazone and thiosemicarbazone derivatives in murine and human tumor cell lines. *Pharmazie*, **2000**, 55, 937-941.
- ⁵⁷ Hall, I. H.; Lackey, C. B.; Kistler, T. D.; Durham, R.W.; Russell J. M.; Grimes, R. N. Antitumor activity of mono- and dimetallic transition metal carborane complexes of Ta, Fe, Co, Mo, or W. *Anticancer Res.*, **2000**, 20, 2345-2354.
- ⁵⁸ Hall, M.D.; Failes, T.W.; Yamamoto, N.; Hambley, T.W. Bioreductive activation and drug chaperoning in cobalt pharmaceuticals. *Dalton Trans.* **2007**, 3983-3990.

- ⁵⁹ Ott, I.; Abraham, A.; Schumacher, P.; Shorafa, H.; Gastl, G.; R. Gust, R.; Kircher, B. Synergistic and additive antiproliferative effects on human leukemia cell lines induced by combining acetylenehexacarbonyldicobalt complexes with the tyrosine kinase inhibitor imatinib. *J. Inorg. Biochem.* **2006**, 100, 1903-1906.
- ⁶⁰ Ott, I.; Gust, R. Stability, protein binding and thiol interaction studies on [2-acetoxy-(2-propyl)benzoate]hexacarbonyldicobalt. *BioMetals* **2005**, 18, 171-177.
- ⁶¹ Omae, I. Three characteristic reactions of organocobalt compounds in organic synthesis. *Appl Organomet Chem* **2007**, 21, 318-344.
- ⁶² Teobald, B.J. The Nicholas reaction: the use of dicobalt hexacarbonyl-stabilised propargylic cations in synthesis. *Tetrahedron*, **2002**, 58, 4133-4170.
- ⁶³ Hyama, T.; Nishide, K.; Saimoto, H. et al. *Chem Abstr* **1987**, 107.
- ⁶⁴ Jung, M.; Kerr, D.E.; Senter, P.D. Bioorganometallic chemistry: synthesis and antitumor activity of cobalt carbonyl complexes. *Arch Pharm* **1997**, 330 (6), 173-176.
- ⁶⁵ Ott, I.; Kircher, B.; Dembinski, R.; Gust, R. Alkyne hexacarbonyl dicobalt complexes chemistry and drug development. *Expert Opin. Ther. Patents* **2008**, 18 (3), 327-337.
- ⁶⁶ Sergeant, C. D.; Ott, I.; Sniady, A.; Meneni, S.; Gust, R.; Rheingold, A. L.; Dembinski, R. Metallo-nucleosides: synthesis and biological evaluation of hexacarbonyl dicobalt 5-alkynyl-2'-deoxyuridines. *Org. Biomol. Chem.* **2008**, 6, 73-80.
- ⁶⁷ Neukamm, M.A.; Pinto, A.; Metzler-Nolte, N. Synthesis and cytotoxicity of a cobaltcarbonyl-alkyne enkephalin bioconjugate. *Chem. Commun.* **2008**, 232-234.
- ⁶⁸ Schlenk, M.; Ott, I.; Gust, R. Cobalt-alkyne complexes with imidazoline ligands as estrogenic carriers: synthesis and pharmacological investigations. *J. Med. Chem.* **2008**, 51, 7318-7322.
- ⁶⁹ Osella, D.; Galeotti, F.; Cavigliolo, G.; Nervi, C.; Hardcastle, K. I.; Vessières, A.; Jaouen, G. The hexacarbonyl(ethyne)dicobalt unit: an androgen tag. *Helv. Chim. Acta* **2002**, 85, 2918-2925.
- ⁷⁰ Vessières, A.; Top, S.; Vaillant, C.; Osella, D.; Mornon, J.-P.; Jaouen, G. Carbonylmetallcluster-modifizierte Östradiole als Suizidsubstrate zur Untersuchung

von Rezeptorproteinen: Anwendung beim Östradiol-Rezeptor. *Angew. Chem.* **1992**, 104, 790-792.

⁷¹ Osella, D.; Cavigliolo, G.; Vincenti, M.; Vessières, A.; Laios, I.; Leclercq, G.; Napoletano, E.; Fiaschi, R.; Jaouen, G. The first organometallic derivative of 11 β -ethynylestradiol, a potential highaffinity marker for the estrogen receptor. *J. Organomet. Chem.* **2000**, 596, 242-247.

⁷² Zeise, W.C. Cover [(C₂H₄)PtCl₃]-, the Anion of Zeise's Salt, K[(C₂H₄)PtCl₃]xH₂O. *Organometallics* **2001**, 20, 2-6.

⁷³ Love, R. A.; Koetzle, T. F.; Williams, G. J. B.; Andrews, L. C.; Bau, R. *Inorg. Chem.* **1975**, 14, 2653.

⁷⁴ Kubas, G.J. Metal–dihydrogen and π -bond coordination: the consummate extension of the Dewar–Chatt–Duncanson model for metal–olefin bonding. *Journal of Organometallic Chemistry* **2001**, 635, 37-68.

⁷⁵ Hahn, C. Enhancing electrophilic alkene activation by increasing the positive net charge in transition-metal complexes and application in homogeneous catalysis. *Chemistry*. **2004**, 10 (23), 5888-99.

⁷⁶ De Pascali, S.A.; Migoni, D.; Papadia, P.; Muscella, A.; Marsigliante, S.; Ciccarese, A.; Fanizzi, F.P.; New water-soluble platinum(II) phenanthroline complexes tested as cisplatin analogues: First-time comparison of cytotoxic activity between analogous four- and five-coordinate species. *Dalton Trans.* **2006**, 42, 5077-5087.

⁷⁷ Tan, Y.L.K.; Pigeon, P.; Hillard, E.A. Top, S.; Plamont, M.A.; Vessières, A.; Michael J. McGlinchey, M.J.; Müller-Bunz, H.; Jaouen, G. Synthesis, oxidation chemistry and cytotoxicity studies on ferrocene derivatives of diethylstilbestrol *Dalton Trans.* **2009**, 10871-10881.

⁷⁸ Jaouen, G.; Vessières, A.; Butler, I.S. *Acc. Chem. Res.* **1993**, 26, 361.

⁷⁹ Graham, C. 1-Hydrocarbyloxyphenyl-1,2-diphenylalkene derivatives. *European Patent Application.* **1980**.

⁸⁰ Milas, L; Mason, K.A.; Crane, C.H.; Liao, Z. Masferrer J Improvement of radiotherapy or chemoradiotherapy by targeting COX-2 enzyme. *Oncology (Williston Park).* **2003**, 17 (5), 15-24.

⁸¹ Friedel, C.; Crafts, J. M. Sur une nouvelle methode generale de synthese d'hydrocarbures, d'acetones, etc. *Comptes rendus hebdomadaires des seances de*

l'Academie des sciences **1877**, 84, 1450-1454. Pearson, D. E.; Buehler, C. A. Friedel-Crafts acylations with little or no catalyst. *Synthesis* **1972**, 10, 533–542.

⁸² Lubczyk, V.; Bachmann, H.; Gust, R. Investigations on Estrogen Receptor Binding. The Estrogenic, Antiestrogenic, and Cytotoxic Properties of C2-Alkyl-Substituted 1,1-Bis(4- hydroxyphenyl)-2-phenylethenes. *J. Med. Chem.* **2002**, 45, (24), 5358-5364.

⁸³ Carey, F. A.; Sundberg, R. J. *Advanced organic chemistry*, 5th edition part B: reactions and synthesis **2007**, 8.

⁸⁴ Valliant, J.F.; Schaffer, P.; Stephenson, K.A.; Britten, J.F. Synthesis of boroxifen, a nido-carborane analogue of tamoxifen. *J. Org. Chem.* **2002**, 67, 383-387.

⁸⁵ Peter, G. M. Wuts, Theodora W. Greene *Greene's Protective Groups in Organic Synthesis*, 4th Edition **2006**

⁸⁶ Wedemeyer, E.F. Ein und mehrwertige Phenole, Spaltung von Phenolethern. Houben-Weyl, Methoden der Organischen Chemie, Phenole. Teil 1, 6/1c. Stuttgart: *Thieme* **1976**, 340-358.

⁸⁷ Suzuki, A. New application of organoboron compounds in organic synthesis. *Pure and applied chemistry*, **1986**, 37, 231-282.

⁸⁸ Jung, M. E.; Lyster, M. A. Quantitative dealkylation of alkyl ethers via treatment with trimethylsilyl iodide. A new method of ether hydrolysis. *J. Org. Chem.* **1977**, 42 (23), 3761-3764.

⁸⁹ Weissman S. A.; Zewge, D. Recent avances in ether dealkylation. *Tetrahedron* **2005**, 61, 7833-7863.

⁹⁰ Shaterian, H. R.; Shahrekipoor, F.; Ghashang, M. Silica supported perchloric acid (HClO₄-SiO₂): A highly efficient and reusable catalyst for the protection of hydroxyl groups using HMDS under mild and ambient conditions. *Journal of Molecular Catalysis A: Chemical* **2007**, 272, 142-151.

⁹¹ Khan, A.T.; Parvin, T.; Choudhury, L.H. Silica supported perchloric acid (HClO₄-SiO₂): A versatile catalyst for the tetrahydropyranylation, thioacetalization and oxathioacetalization. *Synthesis* **2006**, 15, 2497-2502.

⁹² Frye, S.V.; Eliel, E.L. Prevention of chelation by an oxygen function through protection with a triisopropyl silyl group. *Tetrahedron Lett.* **1986**, 27, 3223-3226.

⁹³ Schweizer, E.E.; Nelson, M.; Stallings, W. Dehydrative ring closure of some α -pyrazolyl ketones. Anomalous closure of 1-phenyl-1-[3-methyl-5-(2-

naphthyl)pyrazolyl]acetophenone to 2-methyl-4,5-diphenylbenzo[g]pyrazolo[5,1-a]isoquinoline. *J. Org. Chem.* **1980**, 45 (23), 4795–4797.

⁹⁴ Greenfield, H.; Sternberg, H.W.; Friedel, R.A.; Wotiz, J.H.; Markby, R.; Wender, I. Acetylenic Dicobalt Hexacarbonyls. Organometallic Compounds derived from alkynes and dicobalt octacarbonyl. *Organometallic Compounds from Alkynes and Dicobalt Octacarbonyl* **1956**, 75, 120-124.

⁹⁵ Ott, I.; Koch, T.; Shorafa, H.; Bai, Z.; Poeckel, D.; Steinhilber, D.; Gust, R. Synthesis, cytotoxicity, cellular uptake on eicosanoid metabolism of cobalt-alkyne modified fructoses in comparison to auranofin and cytotoxic COX inhibitor Co-ASS. *Org. Biomol. Chem.* **2005**, 3, 2282-2286.

⁹⁶ Schmid, K.; Jung, M.; Keilitz, R.; Schnurr, B.; Gust, R. Acetylenehexacarbonyldicobalt complexes, a novel class of antitumor drugs. *Inorganica Chimica Acta* **2000**, 306, 6-16.

⁹⁷ Soule, H. D.; Vasquez, J.; Long, A.; Albert, S.; Brennan, M.: *J. Natl. Cancer Inst.*, **1973**, 51, 1409-1413.

⁹⁸ Benton, F.L.; Dillon, T.E. The Cleavage of Ethers with Boron Bromide. I. Some Common Ethers. *J. Am. Chem. Soc.* **1942**, 64, 1128-1129.

⁹⁹ Robertson, D.W.; Katzenellenbogen, J.A. Synthesis of the *E* and *Z* isomers of the antiestrogen tamoxifen and its metabolite, hydroxytamoxifen, in tritium-labeled form. *J. Org. Chem.* **1982**, 47, 2387-2393.

¹⁰⁰ Pink, J. J.; Wu, S. Q.; Wolf, D. M.; Bilimoria, M. M.; Jordan, V. C. A novel 80 kDa human estrogen receptor containing a duplication of exons 6 and 7. *Nucleic Acids Res.* **1996**, 24, 962-969.

¹⁰¹ Irving, W.; Sternberg, H.W.; Friedel, R.A.; Metlin, S.J.; Markby, R.E. The Chemistry and Catalytic Properties of Cobalt and Iron Carbonyls. **1962**, 22.

¹⁰² Meieranz, S. Synthese und pharmakologische Testung von NSAR-Zeise-komplexen. Dissertation Freie Universität **2011**

¹⁰³ Schwieger, S.; Wagner, C.; Bruhn, C.; Schmidt, H.; Steinborn, D. Synthesis and Structures of Zeise-type Complexes with Vinylsilane Ligands and Quantum Chemical Analysis of the Platinum Vinylsilane Bonding. *Z. Anorg. Allg. Chem.* **2005**, 631, 2696-2704.

- ¹⁰⁴ Gauthier, S.; Mailhot, J.; Labrie, F. New highly stereoselective synthesis of (Z)-4-hydroxytamoxifen and (Z)-4-hydroxytoremifene via McMurry reaction. *J. Org. Chem.* **1996**, 61, 3890-3893.
- ¹⁰⁵ Robertson, D.; Katzenellenbogen, J. A.; Long, D. J.; Rorke, E. A.; Katzenellenbogen, B. S. Tamoxifen antiestrogen. A comparison of activity, pharmacokinetics, and metabolic activation of the *cis* and *trans* isomers of tamoxifen. *Journal of steroid biochemistry* **1982**, 16, 1-13.
- ¹⁰⁶ Hesse, M.; Meier, H.; Zeeh, B. Spektroskopische Methoden in der organischen Chemie. *Thiem Verlag* **2005**, 7. Auflage.
- ¹⁰⁷ Burdall, S. E.; Hanby, A. M.; Lansdown, M. R.; Speirs, V. Breast cancer cell lines: friend or foe? *Breast Cancer Res.* **2003**, 5, 89-95.
- ¹⁰⁸ Whang-Peng, J.; Lee, E.C.; Kao-Shan, C.S.R.; Seibert, K.; Lippman, M. Cytogenetic Studies of Human Breast Cancer Lines: MCF-7 and Derived Variant Subline. *NCI J Natl Cancer Inst* **1983**, 71(4), 687-695.
- ¹⁰⁹ Seibert, K.; Shafie, S. M.; Triche, T. J.; Whang-Peng, J. J.; O'Brien, S. J.; Toney, J. H.; Huff, K. K.; Lippman, M. E. Clonal Variation of MCF-7 Breast Cancer Cells in Vitro and in Athymic Nude Mice *Cancer research* **1983**, 43, 2223-2239.
- ¹¹⁰ Soule, H. D.; Vasquez, J.; Long, A.; Albert, S.; Brennan, M., A human cell line from a pleural effusion derived from a breast carcinoma. *NCI J Natl Cancer Inst* **1973**, 51, (5), 1409-16.
- ¹¹¹ Watanabe, T.; Inoue, S.; Ogawa, S.; Ishii, Y.; Hiroi, H.; Ikeda, K.; Orimo, A.; Muramatsu, M.: Agonistic effect of tamoxifen is dependent on cell type, ERE-promoter context, and estrogen receptor subtype. *Biochem. Biophys. Res. Commun.* **1997**, 236, 140-145.
- ¹¹² Girault, I.; Andrieu, C.; Tozlu, S.; Spyrtos, F.; Bieche, I.; Lidereau, R., Altered expression pattern of alternatively spliced estrogen receptor beta transcripts in breast carcinoma. *Cancer Lett* **2004**, 215, (1), 101-12.
- ¹¹³ Treeck, O.; Juhasz-Boess, I.; Lattrich, C.; Horn, F.; Goerse, R.; Ortmann, O., Effects of exon-deleted estrogen receptor β transcript variants on growth, apoptosis and gene expression of human breast cancer cell lines. *Breast Cancer Research and Treatment* **2008**, 110, (3), 507-520.

¹¹⁴ Liu, X.H.; Rose, D.P. Differential Expression and Regulation of Cyclooxygenase-1 and -2 in Two Human Breast Cancer Cell Lines *Cancer Res.* **1996**, *56*, 5125-5127.

¹¹⁵ Dettmann, S.; Szymanowitz, K.; Wellner, A.; Schiedel, A.; Müller, C. E.; Gust, G. 2-Phenyl-1-[4-(2-piperidine-1-yl-ethoxy)benzyl]-1*H*-benzimidazoles as ligands for the estrogen receptor: Synthesis and pharmacological evaluation *Bioorganic & Medicinal Chemistry* **2010**, *18*(14), 4905–4916.

¹¹⁶ Poten, J.; Saksela, E. Two established in vitro cell lines from human mesenchymal tumours. *NCI J Natl Cancer Inst* **1967**, *2*, 434-447.

¹¹⁷ Bernhardt, G.; Reile, H.; Birnböck, H.; Spruss, T.; Schönenberger, H. Standardized kinetic microassay to quantify differential chemosensitivity on the basis of proliferative activity. *J. Cancer Res. Clin. Oncol.* **1992**, *118*, 35-43.

¹¹⁸ Reile, H.; Birnböck, H.; Bernhardt, G.; Spruss, T.; Schönenberger, H. Computerized determination of growth kinetic curves and doubling times from cells in microculture. *Anal. Biochem.* **1990**, *187*, 262-267.

¹¹⁹ Maia, P. I.; Nguyen, H.H.; Ponader, D.; Hagenbach, A.; Bergemann, S.; Gust, G.; Deflon, V. M.; Abram, U. Neutral gold complexes with tridentate SNS thiosemicarbazide ligands. *Inorg. Chem.* **2012**, *51*, 1604-1613.

¹²⁰ de Wet, R. J.; Wood, K. V.; de Luca, M.; Helinsky, D. R.; Subramani, S.: Firefly luciferase gene: structure and expression in mammalian cells. *Mol. Cell. Biol.*, **1987**, *7*, 725-737.

¹²¹ Promega Corporation: Luciferase Assay System *Technical Bulletin No. 281*. <http://www.promega.com/~media/Files/Resources/Protocols/Technical%20Bulletins/0/Luciferase%20Assay%20System%20Protocol.pdf>

¹²² Hoffmann, K. H. Leuchtende Tiere: Chemie und biologische Bedeutung. *Biologie in unserer Zeit* **1981**, *11*, (4), 97-106.

¹²³ Hafner, F.; Holler, E.; von Angerer, E.: Effect of growth factors on estrogen receptor mediated gene expression. *J. Steroid Biochem. Molec. Biol.*, **1996**, *58*, 385-393.

¹²⁴ von Angerer, E.; Biberger, C. 1-Benzyl-2-phenylindole- and 1,2-diphenylindole-based antiestrogens. Estimation of agonist and antagonist activities in transfection assays. *J. Steroid Biochem. Molec. Biol.*, **1998**, *64*, 277-285.

- ¹²⁵ Bradford, M.M. A rapid and sensitive method for the quantitation of microgram quantities of protein utilizing the principle of protein-dye binding. *Anal. Biochem.*, **1976**, 72, 248-254.
- ¹²⁶ Gust, R.; Lubczyk, V. Structure activity relationship studies on C2 side chain substituted 1,1-bis-(4-methoxyphenyl)-2-phenylalkenes and 1,1,2-tris(4-methoxyphenyl)alkenes. *Journal of Steroid Biochemistry & Molecular Biology* **2003**, 87, 75-83.
- ¹²⁷ Sanoh, S.; Kitamura, S.; Sugihara, K.; Fujimoto, N.; Ohta, S.: Estrogenic Activity of Stilbene Derivatives. *J. Health Sci.* **2003**, 49 (5), 359-367.
- ¹²⁸ Mitlak, B.H.; Cohen, F.J. Selective estrogen receptor modulators. A look ahead. *Drugs* **1999**, 57, 653-663.
- ¹²⁹ Meegan M. J., Lloyd, D. G..Advances in the science of estrogen receptor modulation. *Curr. Med. Chem.* **2003**, 10, 181-210.
- ¹³⁰ Agouridas, V.; Laios, I.; Cleeren, A.; Kizilian, E.; Magnier, E.; Blazejewski, J.-C; Leclercq, G.Loss of antagonistic activity of tamoxifen by replacement of one N-methyl of its side chain by fluorinated residues. *Bioorg Med Chem*, **2006**, 14 (22), 7531-7538.
- ¹³¹ Robertson, D.W.; Katzenellenbogen, J.A.; Hayes, J.R.; Katzenellenbogen, B.S..Antiestrogen basicity-activity relationships: a comparison of the estrogen receptor binding and antiuterotrophic potencies of several analogs of (Z)-1,2-diphenyl-1-[4-[2-(dimethylamino)ethoxy]phenyl]-1-butene (Tamoxifen, Nolvadex) having altered basicity. *J. Med. Chem*, **1982**, 25 (2), 167-171.
- ¹³² Wu, Y.L.; Yang, X.; Ren, Z.; McDonnell, D.P.; Norris, J.D.; Willson, T.M.; Greene, G.L. Structural basis for an unexpected mode of SERM-mediated ER antagonism. *Molecular Cell*, **2005**, 18 (4), 413-424.
- ¹³³ Crawly; Gramely, C. 1-Hydroxycarbyloxyphenyl-1,2-diphenylalkene derivatives. *European Patent Application* **1980**, EP 0019377.
- ¹³⁴ Schaefer, A.; Wellner, A.; Strauss, M.; Wolber, G.; Gust, R. Development of 2,3,5-Triaryl-1H-pyrroles as Estrogen Receptor α Selective Ligands *Chem Med Chem* **2011**, 6, 2055-2062.
- ¹³⁵ Liu, W.; Zhou, J.; Bendsdorf, K.; Zhang, H.; Liu, H.; Wang, Y.; Qian, H.; Zhang, Y.; Wellner, A.; Rubner, G.; Huang, W.; Guo, C.; Gust, R. Investigations on cyto-

toxicity and anti-inflammatory potency of licofelone derivatives. *European Journal of Medicinal Chemistry* **2011**, 46, 907-913.

¹³⁶ Liu, W.; Bendsdorf, K.; Proetto, M.; Hagenbach, A.; Abram, U.; Gust, R. Synthesis, characterization, and in vitro studies of bis[1,3-diethyl-4,5-diarylimidazol-2-ylidene]gold(I/III) complexes. *J. Med. Chem.* **2012**, 55, 3713-3724.

¹³⁷ Schottenfeld, D.; Beebe-Donk, J. Chronic inflammation: a common and important factor in the pathogenesis of neoplasia. *Cancer journal of clinicians* **2006**, 56, 69-83.

¹³⁸ <http://chemistry.gravitywaves.com>

¹³⁹ Fu, J.Y.; Masferrer, J.L.; Seibert, K.; Raz, A.; Needleman, P. The induction and suppression of prostaglandin H₂ synthase (cyclooxygenase) in human monocytes. *J Biol Chem.* **1990**, 265, 16737-16740.

¹⁴⁰ Steinmeyer, J. Pharmacological basis for the therapy of pain and inflammation with nonsteroidal anti-inflammatory drugs. *Arthritis Res* **2000**, 2, 379-385.

¹⁴¹ Rubner, G.; Bendsdorf, K.; Wellner, A.; Kircher, B.; Bergemann, S.; Ott, I.; Gust, R. Synthesis and biological activities of transition metal complexes based on acetylsalicylic acid as neo-anticancer agents *J. Med. Chem.* **2010**, 53, 6889-6898.

¹⁴² <http://www.caymanchem.com/app/template/Product.vm/catalog/560131>

¹⁴³ Liu, W.; Bendsdorf, K.; Proetto, M.; Abram, U.; Hagenbach, A.; Gust, R. NHC Gold Halide complexes derived from 4,5-diarylimidazoles: synthesis, structural analysis, and pharmacological investigations as potential antitumor agents *J. Med. Chem.* **2011**, 54, 8605-8615.

¹⁴⁴ Wiglenda, T.; Ott, I.; Kircher, B.; Schumacher, P.; Schuster, D.; Langer, T.; Gust, R. Synthesis and pharmacological evaluation of 1Himidazoles as ligands for the estrogen receptor and cytotoxic inhibitors of the cyclooxygenase. *J. Med. Chem.* **2005**, 48, 6516-6521.

¹⁴⁵ Rubner, G.; Bendsdorf, K.; Wellner, A.; Kircher, B.; Bergemann, S.; Ott, I.; Gust, R. Synthesis and biological activities of transition metal complexes based on acetylsalicylic acid as neo-anticancer agents. *J. Med. Chem.* **2010**, 53 (19), 6889-6898.

¹⁴⁶ Bradford, M.M. A rapid and sensitive method for the quantitation of microgram quantities of protein utilizing the principle of protein–dye binding. *Anal. Biochem.* **1976**, 72, 248–254.

Abbreviations

$^1\text{H-NMR}$	Hydrogen nuclear magnetic resonance
abs.	absolute
A_x	Absorbance at x nm
AlCl_3	Aluminium chloride
BBr_3	Boron tribromide
d	doublet
Dd	double doublet
CDCl_3	Chloroform deuterio
DMF	<i>N,N</i> -Dimethylformamide
$\text{DMSO}(d_6)$	Dimethylsulfoxide (Hexadeutero)
DNA	Deoxyribonucleic acid
ELISA	enzyme-linked immune absorbant assay
Eq.	Equation
ER	Estrogen receptor
ESI	Electrospray-Ionization
Etl	Ethidium bromide
EtOH	Ethanol
EtSH	Ethenethiol
FCS	Fetal calf serum
Fig.	Figure
h	hour(s)
H-bond	Hydrogen-bond
HMDS	1,1,1,3,3,3-Hexamethyldisilazane
HSA	Human serum albumin

IC₅₀	Half maximal inhibitory concentration
J	Coupling constants
KHMDS	Potassium bis(trimethylsilyl)amide
LBD	Ligand Binding Domain
Luc	Luciferase
m	multiplet
m/z	Mass-to-charge ratio
min	minute(s)
MS	Mass spectrometry
obs.	observed
PBS	Phosphate buffered saline
s	singlet
t	triplet
<i>t</i>-BuOK	Potassium tertbutoxide
TMS	Tetramethylsilane
UV	Ultraviolet
δ	Chemical shift